Development of Novel Anti-Trypanosomal Compounds via Computational, *In Vitro* and *In Vivo* Methods

By

Nikoletta Adler

Thesis submitted to the University of Dublin in
candidature or the Degree of Research Masters

Supervisors: Dr. Andrew Knox & Professor Derek Nolan
School of Biochemistry & Immunology,
Trinity College, Dublin

2018

Declaration

I declare this thesis has not been submitted as an exercise for a degree at this or any other university and it is my own work, with the following exceptions:

- The design and synthesis of all vinyl sulfone dipeptides was carried out by Dr. Paul Evans and his group, School of Chemistry and Chemical Biology, University College Dublin.
- The intracellular locatisation of the cysteine protease inhibitor target was conducted in conjunction with Laura Martin (Chapter 3).
- The functional-class fingerprint (FCFP4) similarity searching and 3D flexible alignment to prioritise drugs that have the potential to act as anti-trypanocidal molecules and pass the BBB was carried out by Dr. Andrew Knox, School of Biological Sciences, Dublin Institute of Technology (Chapter 4).

I agree to deposit this thesis in the University's open access institutional repository or allow the library to do so on my behalf, subject to Irish Copyright Legislation and Trinity College Library conditions of use and acknowledgement.

_____

Name: Nikoletta Adler

Year: 2018

Abstract

Human African Trypanosomiasis is a neglected parasitic disease caused by *Trypanosoma brucei*, which if left untreated eventually leads to coma and death. With no successful vaccine to date, treatment relies on chemotherapy. The currently used 5 parenteral drugs (melarsoprol, pentamidine, suramin, eflornithine, nifurtimox) all have non-negligible toxicity and are complex to use, requiring close monitoring. Additionally, there is emergence of parasite resistance to these drugs, in particular to melarsoprol, the only effective drug for the late, CNS invasive stage of both human infective *T. brucei* subspecies. Thus, there is a need to develop more tolerable and efficacious treatments. This study investigated the efficacy of various new therapeutic leads as anti-trypanosomal agents, including some repurposed and already FDA-approved.

First, a series of vinyl sulfones (40 compounds) from traditional drug discovery pipelines were evaluated for their ability to disrupt the life cycle of trypanosomes in a whole-cell screen of *T. b. brucei* via a standard Alamar Blue assay. Out of the series tested, 13 compounds were identified with nanomolar activity, making them more potent than the original K777 vinyl sulfone, a promising therapeutic lead against the similar protozoan disease American Trypanosomiais. Additionally, through fluorescence imaging, this study showed that the cysteine protease inhibitor subcellular localisation was in the lysozyme as expected, but surprisingly it was present in nucleus and kinetoplast as well.

Further new leads were identified through drug repurposing methods including: a) similarity searches between databases of anti-trypanocidal compounds vs drugs with blood-brain barrier passing capabilities, and b) identifying compounds that modulate the activity of a conserved parasite target, in this case ergosterol, between parasites of similar biology and genomic sequences (*T. brucei*, *T. cruzi*, *Leishmania*). For the first time, the study demonstrated that the antifungals amphotericin B (AmpB) and SPK-843 as well as, fingolimod (FTY720), the first FDA-approved oral agent for the management of relapsing forms of multiple sclerosis, its phosphorylated derivative FTY720P, and endogenous structural mimics sphingosine and sphingosine-1-phosphateare (S1P) were able to kill *T. b. brucei in vitro* at low and submicromolar concentrations. Specifically, SPK-843, which was tested because of its structural similarity to AmpB, induced parasite death more rapidly and with a greater efficacy than AmpB. The mode of action following AmpB treatment involved membrane permeabilisation as demonstrated by the entry of fluorescent propidium iodide into the cells, possibly via formation of pore-inducing

AmpB-ergosterol complexes. Channel formation upon AmpB binding ergosterol was expected as it has been shown in *Leishmania* and fungal studies. In contrast, there was no membrane disruption detected following SPK-843 treatment. It is proposed here that SPK-843 was able to induce trypansome cell death by simply binding ergosterol, a signaling molecule in BSF rypanosomes, vital to their growth and survival.

Interestingly, when the potencies of FTY720, FTY720P, sphingosine and SIP were compared in the different life cycle stages of the parasite all 4 compounds showed higher efficacy against bloodstream form than in procyclic form *T. b. brucei*. The potency matched those of early stage treatments, suramine and pentamidine. However, FTY720 killed *T. brucei* faster than FYY720P, with sub-micromolar IC_{50} occurring after 8 h and 24 h exposure, respectively. Pharmacological time-course studies revealed that FTY720 was irreversible at sub-micromolar concentrations (IC_{50} ~0.32 μM) and the mode of killing of FTY720 and FTY720P is partly due to membrane disruption and a secondary mechanism of cell division disruption, including failure to undergo cytokinesis, which is apparent from the presence of cells with atypical DNA content observed with fluorescent imaging. Significantly, in trial infections of mice harbouring an acute strain of *T. b. brucei*, oral administration of fingolimod and intravenous injection of SPK-843 dosed over 5 days was sufficient to clear infection below detectable levels and the lives of the animals were extended by several days. AmpB in its lipid formulation (AmBisome®) did not impede infection.

Taken together the results presented in this thesis indicate that lead vinyl sulfones, amphotericin B, SPK-843, and fingolimod present new chemical starting entities for development of anti-trypanosomal agents. The Drugs for Neglected Diseases Initiative (DNDi) highlighted in their Target Product Profile (TPP) that an ideal candidate would have the potential to be used as a treatment for both stages of the disease. Importantly, fingolimod is known to readily penetrate the CNS and may provide the most promise for future treatment of both haemolymphatic and meningoencephalitic stages of trypanosomiasis. For future work, it would be essential to undertake further *in vivo* experiments using a chronic model of trypanosomiais with longer treatment periods to improve fingolimod efficacy in an animal model and to clear infection completely. Also, further pharmacodynamics investigations of vinyl sulfones and *in vitro* studies investigating the potential to increase efficacy of SPK-843 and ampothericin B when used in combination with current HAT drugs are warranted.

List of Publications

Doherty W, **Adler N**, Knox A, Nolan D, McGouran J, Nikalje A, Lokwani D, Sarkate A & Evans P (2017) Synthesis and Evaluation of 1,2,3-Triazole-Containing Vinyl and Allyl Sulfones as Anti-Trypanosomal Agents. *Eur J Org Chem* 2017, 175–185.

Doherty W, James J, Evans P, Martin L, **Adler N**, Nolan D & Knox A (2014) Preparation, anti-trypanosomal activity and localisation of a series of dipeptide-based vinyl sulfones. *Org. Biomol. Chem.* 12, 7561–71.

Acknowledgements

Firstly, I would like to thank my supervisor Dr. Andrew Knox for giving me the chance to undertake the Masters experience and grow both personally and professionally. For all the deeps chats, guidance and motivation, unique ideas and approaches to life.

I would like to thank Professor Derek Nolan for his continuous kind support, guidance, advice, patience, and belief in me. Thank you for helping me with statistics, the continuous writing support and general insight.

A massive thanks to Jenni, Natalie, Ryan and Andy Cheung who were with me from the beginning to the end. For listening to all my woes and helping me find my way when I got lost. Thank you guys for all the support, for all the science and personal chats over coffee and everywhere else, and for the amazing adventures. I wouldn't have come this far without you guys.

There are so many other people to thank, here we go! Thank you to Paul B, Darren, Nidhi for their good banter on the fun side of the partition. For the older generation: Jer, Neil, Rob, Laura B for their support and advice ot navigate science life. For the fascinating hallway chats with Dr. Paul Voorheis, Dr. Vinnie Kelly and Dr. James Murray. For everyone from the 5th floor who made science life so much better, who brought sunshine into any room they went to: Nadine, Ji Yoon, Laura O, Aisling, Peter, Roisin, Katie, Emma, Aoife, Simon, Ray, Louise, Jess, and the newbie Gavin D. I could not have done this by myself and I am so blessed to have met so many wonderful and engaging people that I know I can count on for many years to come.

Special thanks to Helen T. from Graduates office for her understanding, her incredible amount of help, and giving me a second chance to redeem myself.

And last but not least, my deepest thanks to my family: my sisters Szilvi and Kati and my parents Maria and Frank for supporting me in every way they could and not giving up on me even at the hardest of times when I was at my lowest point.

Table of Contents

List of Figures & Tables

Abbreviations

1N1K	1 nucleus and 1 kinetoplast
1N2K	1 nucleus and 2 kinetoplasts
2N2K	2 nuclei and 2 kinetoplasts
3-KDS	Ketodihydrosphingosine
AAT	African animal trypanosomiasis
AmpB	Ampothericin B
ASM	Acid sphingomyelinase
ATP	Adenosine triphosphate
BBB	Blood-brain barrier
BLAST	Basic Local Alignment Search Tool
BSF	Blood stream form
CADD	Computer-aided drug design
CL	Cardiolipin
CNS	Central nervous system
CoMFA	Comparative molecular field analysis
CoMSIA	Comparative molecular similarity index analysis
DAPI	4′,6-diamidino-2-phenylindole
DHS1P	Dihydrosphingosine 1-phosphate
DRC	Democratic Republic of the Congo
DMEM	Dulbeccos Modified Eagle Medium
DMSO	Dimethyl sulfoxide
DNDi	Drugs for Neglected Diseases Initiative
EC_{50}	Half maximal effective concentration
ECM	Extracellular matrix
EPC	Ethanolamine phosphorylceramide
FBS	Fetal bovine serum
FDA	Food and Drug Administration

FCFP4	Feature-connectivity bit string fingerprint search
HAT	Human African Trypanosomiasis
HAPT1	High-affinity pentamidine transporter
HEK293T	Human embryonic kidney cells
HL-60	Human acute myeloblastic leukemia cell line
i.v.	Intravenous injection
IPC	Inositol phosphorylceramide
IC_{50}	Half maximal inhibitory concentration
LAPT1	Low-affinity pentamidine transporter
LAMB	Liposomal ampothericin B
LBDD	Ligand-based drug design
NECT	Nifurtimox-eflornithine combination therapy
NCE	New chemical entity
N/K	Nucleus/kinetoplast
NME	New molecular entity
NMR	Nuclear Magnetic Resonance
NMRI	Naval Medical Research Institute
NTR	Nitroreductase
NSM	Neutral sphingomyelinases
MEM	Medium essential medium
MOE	Molecular Operating Environment
PBS	Phosphate buffered saline
PC	Phosphotidylcholine
PCF	Procyclic form
PE	Phosphatidylethanolamine
PFA	Paraformaldehyde
PI	Propidium iodide
PI	Phosphatidylinositol
PS	Phosphatidylserine
PSG	Phosphate-buffered-saline-glucose

QSAR	Quantitative structure–activity relationship
RPMI	Roswell Park Memorial Institute medium
RNAi	RNA interference
SD	Standard deviation
SEM	Standard error of the mean
S1P	Sphingosine-1-phosphate
S1P1	S1P receptor type 1
S1PL	Sphingosine-1-phosphate lyase
SBDD	Structure-based drug design
SPL	Sphingosine lyase
SPHK	Sphingosine kinase
SPT	Serine palmitoyltransferase
STED	Stimulated emission depletion microscopy
SM	sphingomyelin
T. b. brucei	*Trypansoma brucei brucei*
TbCatB	*Trypansoma brucei* cathepsin B-like
TbSPHK	*Trypansoma brucei* sphingosine kinase
TbSLS	*Trypansoma brucei* sphingolipid synhtase
TPH	Tropical and Public Health Institute
TPP	Target product profile
VS	Vinyl sulfone
VSG	Variable surface glycoproteins
WHO	World Health Organization

CHAPTER 1. General Introduction

1.1 Introduction - Trypanosomiasis

African sleeping sickness (African trypanosomiasis, human African trypanosomiasis – HAT) is a neglected parasitic disease endemic in over 36 countries in sub-Saharan Africa (Renslo & McKerrow 2006). It is caused by the flagellate kinetoplastid protozoan parasite, *Trypanosoma brucei* (Figure 1.1), which resides extracellularly in the blood and tissue fluids of the mammalian host and is transmitted by the tsetse fly. There are two forms of HAT: one form is gambiense HAT, caused by *Trypanosoma brucei gambiense,* which is widespread in central and western Africa and presents itself as a chronic infection in humans (95% of current cases). The other form rhodesiense HAT, caused by *Trypanosoma brucei rhodesiense,* is restricted to east and east central Africa, accounting for the remainder of cases (5%) and produces an acute infection (Renslo & McKerrow 2006; Frearson et al. 2010; Organization 2013).

The colloquial term for African sleeping sickness refers to the most serious phase of the disease – the neurological phase - which occurs when the parasite penetrates the central nervous system causing a sense of confusion, changes in behavior, poor coordination, and a disturbed sleep cycle. If left untreated the disease eventually leads to coma and death. Sleeping sickness has a devastating impact on human health and prosperity. In 1995, a World Health Organization (WHO) Expert Committee estimated that 60 million people were at risk with an estimated 300,000 new cases per year in Africa, and fewer than 30,000 cases diagnosed and treated. Over the next couple decades these numbers started dropping and encouragingly in 2014 only 3,796 cases were reported with less than 15,000 estimated cases. While the number of cases has declined, there are concerns that drug resistance will impact this position (Vincent et al. 2010; Baker et al. 2013), especially since there is no vaccine available for trypanosomiasis treatment relies only on chemotherapies. An additional problem is that these affected regions are also highly prone to malnutrition in part due to the inability to raise live-stock, as cattle and numerous domestic animals also act as reservoirs for trypanosomes (e.g. *T. brucei brucei, T. congolense, T. simiae*). Their infection leads to nagana, a wasting form of anaemia in animals, significantly lowering milk and meat yields. In fact, nagana now costs livestock producers and consumers an estimated $1.34 billion annually with total agricultural losses reaching $4.5 billion per year (Kristjanson et al. 1999).

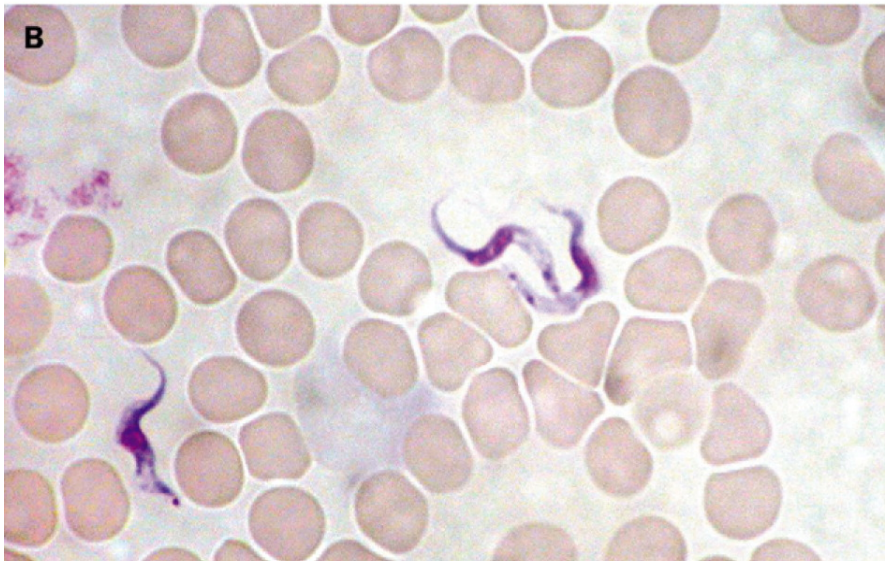

Figure 1.1 Blood smear with *T. brucei* trypomastigotes. Taken from Barrett et al. (2003). DOI: 10.1016/S0140-6736(03)14694-6

1.1.1 Epidemiology

The transmission cycle of the parasite is important in understanding the epidemiology of HAT. Human African trypanosomiasis is transmitted only in sub-Saharan Africa, where there are suitable habitats for the tsetse fly vector. The 31 species and subspecies of *Glossina* can be classified into three distinct groups based on habitat: fusca (forest), morsitans (savannah), and palpalis group (riverine and forest) (Jordan 1976). The wide range of environmental requirements results in discontinuous distribution of the vector across the African tsetse belt. In Western and Central Africa the *T. b. gambiense* subspecies are most likely injected by the *Glossina palpalis* group (also called *G. fuscipes*), flies inhabiting hot humid forests. Whereas, *T. b. rhodesiense* is most likely ingested by *G. morsitans* in the savannah, *G. pallipides* at the forest edge or *G. fuscipes* in riverine and marshland areas of Eastern and Southern Africa. Most often however, the different species of tsetse flies co-exist in the same areas (Buguet et al. 2001). The interrelationships among the host, vector and parasite are complex, and the geographical distribution of HAT is highly focal (Organization 2013).

1.1.2 Disease severity & control strategies

Although, infection with either *T. b. rhodesiense* or *T. b. gambiense* is termed "sleeping sickness", biologically, clinically, therapeutically, geographically and, most importantly, epidemiologically, these parasites present as distinct entities and cause, in effect, separate diseases (Ekwanzala et al. 1996). Appreciation of the differences is critical to understanding the options for HAT control. Important, although, *T. rhodesiense* and *T. gambiense* cause separate diseases, these parasites are morphologically similar and they can only be distinguished through biological, biochemical and molecular biological means (Gibson et al. 1999). African sleeping sickness symptoms are characterized by an initial heamolymphatic stage, in which the infection is generalised. The first manifestation is at the site of the tsetse fly's bite, a local skin reaction called trypanosomal chancre. It is typically accompanied by regional lymphadenopathy (less common in the chronic Gambian sleeping sickness), other early symptoms are usually more inconspicuous: lymphadenopathy, especially in the posterior triangle of the neck (Winterbottom's sign, see Figure 1.2), hepatosplenomegaly, and a faint rash (Stich et al. 2002). Gambian sleeping sickness has a long asymptomatic stage, which is eventually succeeded by a subacute febrile illness followed by late-stage chronic meningoencephalitis; death might occur several years after onset of the disease (Welburn et al. 2001). In the acute Rhodesian sleeping sickness, symptoms during the heamolymphatic stage of infection can already be severe: around one tenth of patients without rapid access to treatment will die, often due to myocardial involvement. Overall disease progression is much more rapid as well, with >80% of deaths occurring within six months of the onset of illness (Odiit et al. 1997).

These clinical differences are reflected in the methods adopted to control the disease. The control of Gambian sleeping sickness relies on case identification (principally using the card agglutination test (Magnus et al. 1978) and chemotherapy of the largely asymptomatic human reservoir. Rhodesiense HAT is different, in that it is a zoonosis, meaning a "disease or infection naturally transmitted between vertebrate animals and humans" (WHO 1959). It is believed that the transmission cycle of *T. b. rhodesiense* mainly involves transmission between non-human reservoirs, with occasional animal-tsetse-human transfer. This is because rapid onset of severe symptoms in infected patients means they are less likely to be in tsetse fly-infected environment thus they can't serve as reservoirs of infection for the vector (WHO 2013). Wild animals and domestic livestock acting as reservoirs of infection, combined with the acuteness of the

disease, thus means Rhodesian sleeping sickness demands a much more aggressive response: previously, with epidemics the large-scale removal of human populations at risk; in recent times, large-scale tsetse control operations (Lancien 1991), together with medical interventions (Welburn et al. 2001).

Figure 1.2 Winterbottom's sign. Enlarged cervical lymph nodes is a characteristic sign for infection with *T. b. gambiense*. Image taken with permission from BMJ Best Practice, Franco JR.

1.1.3 African animal trypanosomiasis

The third subspecies of the *Trypanosoma brucei* genus is *T. brucei brucei,* which infects cattle and game, where it causes the disease 'nagana' or African animal trypanosomiasis (AAT), thereby restricting agricultural development and significantly contributing to poverty in afflicted areas. Other species also contributing to this disease are *Trypanosoma congolense* (3 types: savannah, forest, kilifi), *T. vivax, T. simiae* and *T.* godfrey (Auty et al. 2015). In wild animals, these parasites cause relatively mild infections while in domestic animals they cause a severe, often fatal, infection. All domestic animals can be affected by nagana and the symptoms are fever, listlessness, emaciation, hair loss, discharge from the eyes, oedema, anaemia, and paralysis. As the illness progresses the animals weaken more and more and eventually become unfit for work, hence the name of the disease "N'gana" which is a Zulu word that means "powerless/useless". Because of nagana, stock farming is very difficult within the tsetse belt (Steverding 2008).

1.1.4 Control of tsetse fly

In general, the prevention of HAT includes reducing bites from tsetse flies, early diagnosis and treatment of cases. While individual protection against bites may be useful in some instances, they can penetrate lightweight clothing and repellents are not common in many endemic areas. Thus, community level vector control and screen and treat programs, which involve the detection of human cases for subsequent treatment, are typically employed together (Keating et al. 2015). Several techniques are recommended for the control of tsetse fly populations: sequential aerial insecticide spraying to target adult flies during the first spray and tsetse flies as they emerge from pupal stages in the ground during subsequent sprays; ground spraying to target pupae and resting flies; the use of odour-baited or visual-baited (e.g. black or blue cloth) insecticide treated traps and targets; sterile insect release; and insecticide treatment of cattle (ICT) (Welburn et al., 2009). A total of 13 Sleeping Sickness National Control Programs are developing vector control activities (out of 24 countries reporting HAT cases) (Franco et al., 2014), although in some countries institutions other than national control programs are also engaged in vector control activities (Keating et al. 2015).

1.2 Tryapnosome brucei cell biology

1.2.1 The Trypanosome cell architecture

Structurally, the trypanosome cell is elongated and has a highly polarized microtubule cytoskeleton, which defines the cell shape and remains intact throughout the cell cycle (Figure 1.3). The trypanosome cell's single-copy organelles (i.e. the flagellar pocket, flagellum, kinetoplast, mitochondrion and nucleus) are precisely positioned within the cytoskeletal corset and are concentrated between the posterior end and the centre of the cell. The most posterior structure is the mouth of the flagellar pocket, an invagination at the exit point for the flagellum of the parasite, where all exo- and endocytosis occurs.

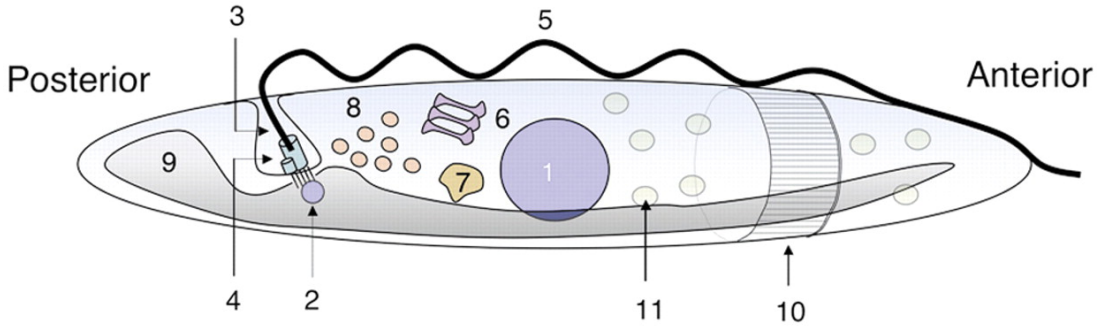

1. Nucleus
2. Kinetoplast
3. Flagellar pocket
4. Basal body and probasal body
5. Axoneme and paraflagellar rod
6. Golgi
7. Lysosome
8. Endosomes
9. Mitochondrion
10. Microtubule cytoskeleton
11. Glycosomes

Figure 1.3 Trypanosome cell architecture. A simplified representation of trypanosome cell architecture depicting the location of the major structural and intracellular features. Taken from Matthews (2005).

1.2.2 The Trypanosome cell cycle

The cell division cycle in *Trypanosoma brucei* broadly follows that of the typical eukaryotic cell, however, it possesses unique features and complexities (see Figure 1.4). *Trypanosoma brucei* has a single nucleus and a single kinetoplast – a disk like structure containing the mitochondrial genome. Each of these organelles has a distinct S phase, which is followed by a segregation period, prior to cell division. The segregation of the two genomes takes place in a specific temporal order by interaction with microtubule-based structures, the spindle for nuclear DNA and the flagellum basal bodies for the kinetoplast DNA (Ploubidou et al. 1999). The order of these events (kinetoplast segregation, basal body duplication, flagellar axoneme growth, mitosis and cytokinesis) in the cell cycle of *T. brucei* is known with a reasonable level of accuracy and is depicted in Figure 1.4. These events are driven by the activation and inactivation of cyclin dependent kinases and are monitored by specific signalling 'checkpoints' (Skibbens and Heiter, 1998; Mendenhall and Hodge, 1998). Co-ordination of cell cycle events is necessary for cell survival and therefore it is essential that these events occur correctly, both sequentially and temporally (Ploubidou et al. 1999). A cell in G1 phase has 1 nucleus and 1 kinetoplast (1N1K cell), while a cell in G2/M phase will have 1 nucleus and 2 kinetoplasts (1N2K) and a cell that has undergone mitosis but has not yet undergone cytokinesis will have 2 nuclei and 2 kinetoplasts (2N2K). Any other NK configuration is abnormal (Jones et al. 2014). A block in mitosis, for example, due to depletion of cytokinesis regulatory proteins, inhibits cytokinesis but not successive rounds of nuclear DNA synthesis or kinetoplast replication and segregation, which results in the appearance of multi-nucleate cells and non-viable progeny (Hammarton 2007).

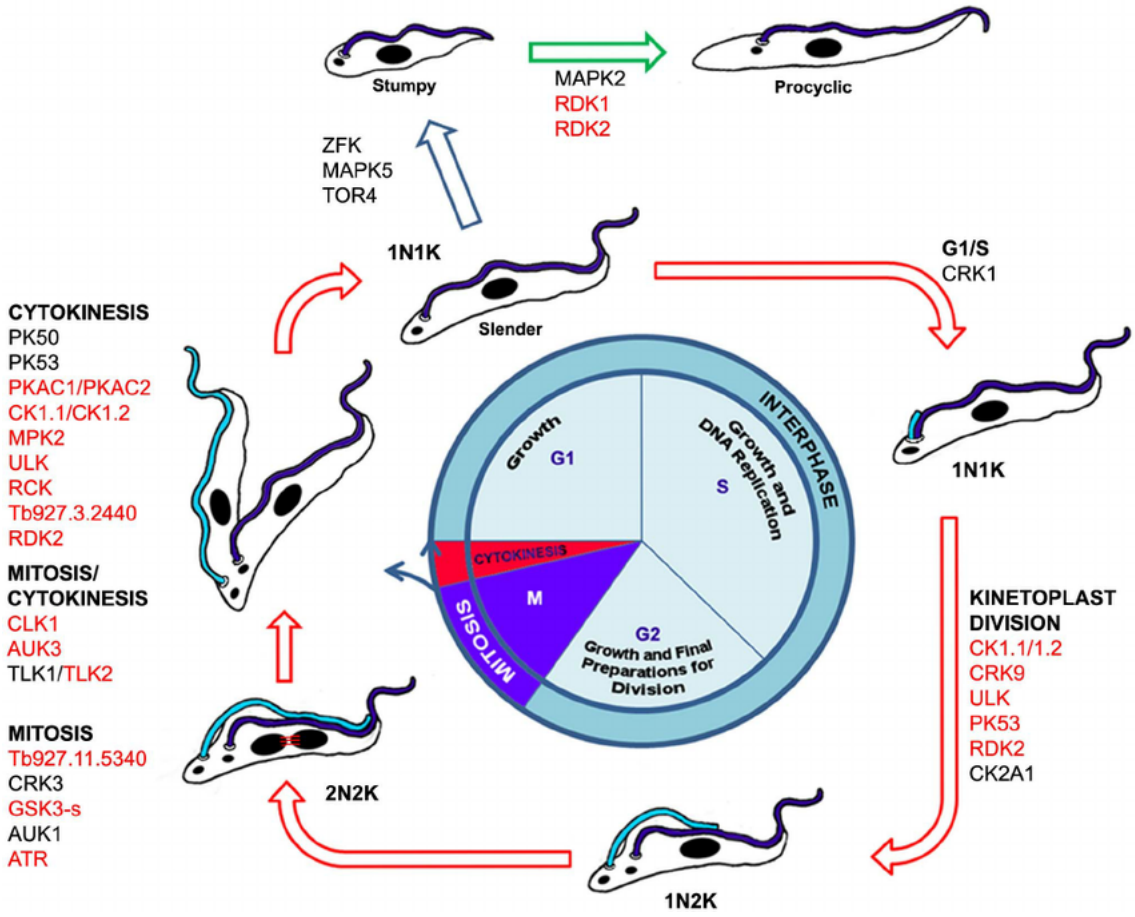

Figure 1.4 Schematic representation of the BSF trypanosome cell cycle and differentiation from BSF to procyclic (insect) form. G1 cells possess a single kinetoplast and nucleus (termed 1K1N) as well as an attached flagellum. As the cell cycle progresses, a new basal body forms and nucleates a new flagellum. The nucleus is still in S phase when kinetoplast DNA shows an elongated morphology. In G2 phase, segregation of basal bodies leads to the separation of attached kinetoplast and these cells are termed 2K1N. When cells enter nuclear M phase, chromosome segregation occurs. When nuclear division is complete and these cells are termed 2K2N. Next, cleavage furrow ingression occurs between the two flagella. At the end of the cell cycle, two daughter cells are formed, and each cell inherits a single kinetoplast, nucleus and flagellum. Protein kinases implicated in cell cycle control and differentiation are indicated. Image taken from Jones et al (2014).

1.2.3 The Trypanosome lifecycle

T. brucei has a complex life cycle, whereby the parasite differentiates multiple times through a series of morphologically and biochemically distinct life cycle stages in each host; vector and mammal, see Figure 1.5. Some life cycle stages, such as the short stumpy bloodstream form (BSF) and the metacyclic form in the tsetse salivary glands are cell cycle arrested, while others, such as the long slender BSF, the insect procyclic form (PCF) and the insect epimastigote form are proliferative (Jones et al. 2014). In both the vector and host the parasite is present as proliferative and non-diving forms, and it is the transfer between hosts that results in differentiation of the parasite to a form suited to their new environment. The slender form trypanosomes are well adapted to the rich blood-glucose environment in their mammalian host and opportunistically multiply by longitudinal binary fission, facilitating new epidemic waves. In contrast, following the vector's bloodmeal, stumpy forms quickly adapt to the loss of glucose, undergoing changes that lead to proliferative procyclic trypomastigotes in the midgut of the fly (Matthews 1999). One central feature of this differentiation is extensive restructuring of external cell surface proteins and glycoconjugates (Morgan et al 2002). Notably, altering plasma membrane composition and organisation is the mechanism, which allows the parasite to escape the immune defences of the host (Pays 1999).

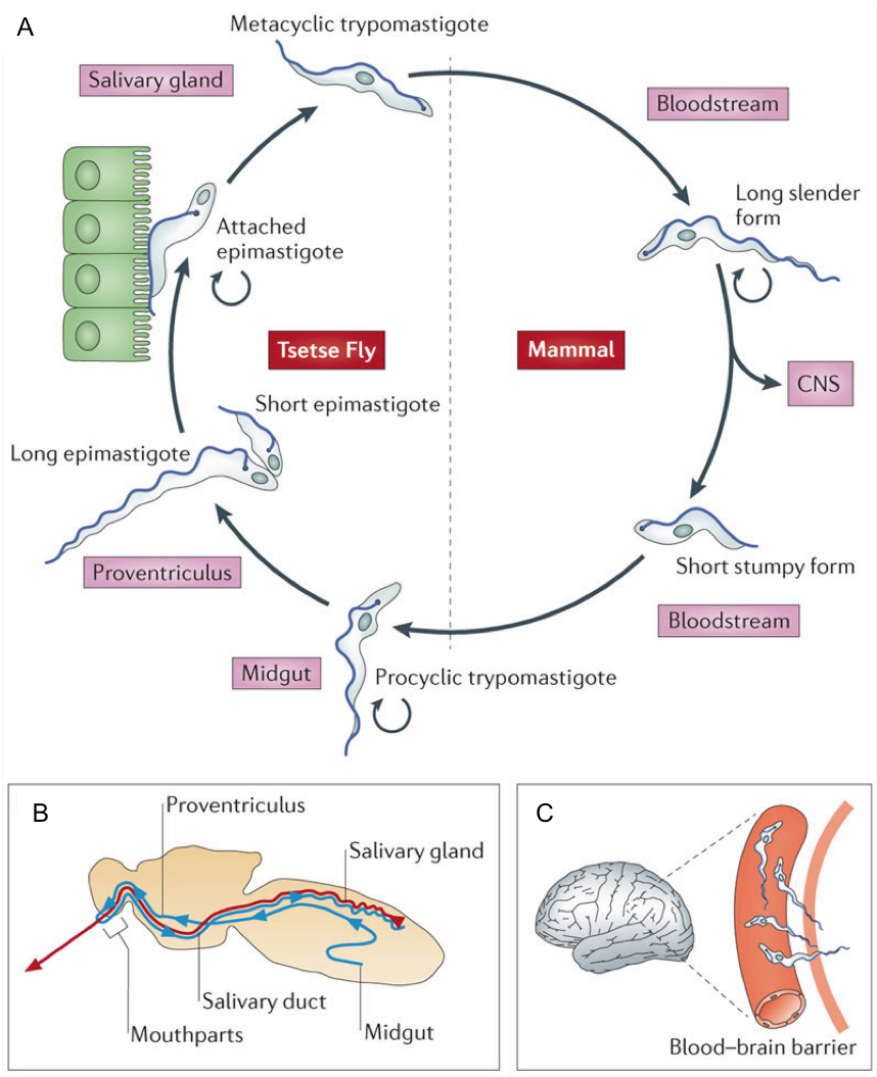

Figure 1.5 The life cycle of *Trypanosoma brucei* in mammalian and insect host. (A) Infection of a mammalian host commences when a tsetse fly bite delivers growth-arrested metacyclic trypomastigotes to the mammalian bloodstream, where parasites then differentiate into proliferating long slender forms that establish and maintain a bloodstream infection. Parasites eventually penetrate blood vessel endothelium and invade the CNS (late stage of the disease), see (C). When an infected mammalian host is bitten by a tsetse fly, parasites are taken up with the blood meal into the midgut, where short stumpy forms quickly differentiate into procyclic trypomastigotes. Midgut procyclic trypomastigotes then migrate and ultimately reach the salivary gland, where they attach to the salivary gland epithelium, see (B). Attached epimastigotes replicate and ultimately complete the life cycle by generating metacyclic trypomastigotes that are free in the salivary gland lumen and are uniquely adapted to survive in the mammalian host. The dividing forms that replicate via binary fission are indicated with a circular arrow. Images taken from Langousis & Hill (2014).

1.2.4 Host immune system evasion

BSF African trypanosomes have evolved two key strategies to prevent killing by the host immune response and, thus, maintain a long-term infection in the mammalian host. Both are based on the variant surface glycoprotein (VSG), a densely packed coat of a single protein, which covers the entire extracellular surface of the cell (Vickerman 1978, Schwede et al. 2015). The first approach to host immune evasion is antigenic variation through which individual cells switch the identity of the expressed VSG at a low frequency. Upon interaction with the host immune response, if the VSG is novel, the trypanosome proliferates, maintaining the infection; if it doesn't switch, or if the new VSG is not novel, it will be exterminated. In the second approach, the VSG acts as a protective barrier, shielding the cell from innate and adaptive immune factors until there is an overwhelming titre of antibodies recognising the expressed VSG.

The VSG coat is not a static entity that simply expands as the cell grows through the addition of new membrane and VSG. There is rapid endocytosis and recycling of the plasma membrane and VSG (Manna et al. 2014) that processes the equivalent to the entire cell surface every 12 minutes (Engstler et al. 2004). The flagellar pocket is the site of endocytosis where antibody removal from the surface of the parasite occurs (Overath & Engstler 2004). The flagellar pocket constitutes a highly differentiated region of the trypanosomatid surface that facilitates the endocytic process. Endocytic vesicles pinch off from the flagellar pocket membrane and after endocytosis and processing in the endosomes, the VSG is recycled back to the plasma membrane, whereas the antibodies are delivered to the lysosome and degraded (Engstler et al., 2007; Engstler et al., 2004). The rate of endocytosis is ~10-fold higher in the mammalian BSF than in the insect procyclic form, attributed to the dual role of the acquisition of nutrients in addition to the high rate of plasma membrane turnover (i.e. internalization and re-emergence) linked to the removal of surface-bound antibody (Morgan et al 2002).

Overall, *T. brucei's* antigenicity elicits an efficient antibody response from the host, which limits the number of parasites, however, due to the continuous variation of the VSG, some parasites escape the antibody response, provoking new waves of parasitemia and establishing persistent infection (Buguet et al. 2001). It is the almost unlimited capacity for antigenic variation of the surface glycoproteins on *Trypanosoma brucei* that has been the major hurdle for producing a successful vaccine to date, and thus, chemotherapies are employed.

1.3 Current treatments & problems

1.3.1 Current therapeutic treatments for HAT

African trypanosomiasis is considered a lethal disease in the absence of treatment, although individual cases of possible spontaneous infection clearance have been reported (Checchi et al. 2008). Therapeutic strategies and treatment choice is determined by drug efficacy against parasite subspecies, drug toxicity and ability of drug to cross the blood-brain barrier (haemolymphatic vs. neurological disease stage). Current treatments consist of 5 parenteral drugs, which all have non-negligible toxicity and are complex to use, requiring close monitoring (Brun et al. 2010), see Table 1.1. Suramin is used for first-stage *T. b. rhodesiense*, pentamidine for first-stage *T. b. gambiense*, melarsoprol for the second stage of both forms of the disease and eflornithine (α-difluoromethylornithine, DFMO), which is only effective in the second stage of the gambiense sleeping sickness. Melarsoprol was introduced in the mid-20th century and is currently the only effective drug against the late stage of human African trypanosomiasis caused by both subspecies (Garcia-Salcedo et al. 2016). However, there are several issues concerning melarsoprol, an arsenical derivative, including that it causes post-treatment reactive encephalopathy in 5–10% of melarsoprol-treated cases and is associated with up to 70% mortality (Pardridge 2005). While melarsoprol treatment failure rate is typically less than 10%, areas in the Democratic Republic of the Congo (DRC) have reported rates as high as 58.8%, due to drug resistance, host factors, or both (Moore & Richer 2001; Ngoyi et al. 2010). Eflornithine was the last drug to be introduced to treat human African trypanosomiasis 50 years ago. The drug crosses the blood-brain barrier (BBB), but lacks effectiveness against *T. b. rhodesiense*.

Nifurtimox, an oral drug developed initially for Chagas disease and not specifically registered for HAT, is used in melarsoprol relapse cases, which are now occurring with a frequency of approximately 30%. More recently, co-administering a combination of Nifurtimox and Eflornithine: 7 days eflornithine (2 infusions/day) and 10 days oral nifurtimox – NECT – has been developed by the Drugs for Neglected Diseases Initiative (DNDi (Checkley et al. 2007)). Médicins Sans Frontières (MSF), Epicentre, Swiss Tropical and Public Health Institute (TPH), and the National Trypanosomiasis Programmes of the Republic of the Congo and the DRC, has reduced the number of eflornithine infusions needed, concomitant with a higher cure rate than eflornithine alone and less adverse events. Management of patients with any of these drugs requires

highly-trained staff, and numerous issues preventing patient treatment arise due to high toxicity of these drugs, prolonged treatment periods, high cost in many cases and the emergence of parasite resistance to these drugs. Thus, there has been a recent resurgence to develop newer, more tolerable and efficacious treatments.

1.3.2 Mechanism of action of current therapeutic treatments for HAT

Firstly, **pentamidine** is a water-soluble, positively-charged, aromatic diamidine used to treat the initial stages of the Gambiense infection due to its selective toxicity for trypanosome parasites, accumulating in these organisms, while generally avoiding the host cells (Babokhov et al. 2013). Pentamidine uptake in *Trypanosome brucei brucei* is mediated by at least three distinct transporters: P2 adenosine/adenine transporter, low-capacity high-affinity pentamidine transporter (HAPT1) and a high-capacity low-affinity pentamidine transporter (LAPT1) (Koning 2001). Many studies have focused on the mechanism of pentamidine action; however, none appears to conclusively define the target. It is a cidal drug.

Suramin is a drug that is utilized against the first stage of *T. b. rhodesiense* infection. Suramin most likely enters trypanosomes by way of receptor-mediated endocytosis and acts upon *T. b. rhodesiense* by inhibiting the glycosomal enzymes involved in glycolysis, the bloodstream form's only source of energy (Babokhov et al. 2013). Suramin also inhibits other trypanosomal enzymes, these are enzymes of the pentose phosphate pathway, such as 6-phosphogluconate dehydrogenase. The main advantages of suramin are that it is highly effective against *T. b. rhodesiense* and there have been no drug resistances reported in the field. The lack of resistance could be in part due to suramin's inhibition of multiple enzymes and metabolic pathways.

Mechanisms of action for second stage treatments are the following. The organic arsenical drug **melarsoprol**, introduced in 1949, was the most commonly used treatment against HAT until the introduction of the nifurtimox–eflornithine combination treatment in 2009. The specific trypanocidal mechanisms of melarsoprol are currently unknown, but the effects of the drug upon trypanosomes have been observed. Parasites exposed to even a low dose of melarsoprol lyse rapidly. Scientists postulate that this lysis occurs due to interruption of glycolysis and the redox metabolism of trypanosomes.

Eflornithine has a trypanostatic effect upon *T. b. gambiense* parasites, irreversibly inhibiting trypanosome's polyamine biosynthesis, by binding to the catalytic site on the enzyme (Vincent et al. 2010). This depletion of essential polyamines results in reduced trypanosomal proliferation in BSF by blocking cell division. Eventually, the trypanosomes are transformed into the short stumpy forms, which can be cleared by the body's immune defences. In addition, levels of S-adenosyl methionine become increased within the trypanosome, disturbing proper methylation of proteins, nucleic acids and lipids.

Lastly, the mechanism of **nifurtimox** is unknown, but is thought to rely on generation of free radicals as a by-product of nitrofuran reduction. These free radicals then interact with the trypanosomal membrane and the associated DNA and proteins. This mode of action attacks processes such as the trypanosomal redox metabolism, creating reduced oxygen metabolites. Another mode of action for nifurtimox involves the type I nitroreductase (NTR) pathway, which reduces nifurtimox into open-chain nitrile products with cytotoxic properties (Hall et al. 2011).

1.3.3 Origin of drug resistance in trypanosomes

Besides most current HAT treatments having high toxicity, the situation has worsened by the development of resistance to almost all current treatments. *T. brucei* have evolved numerous ways to overcome the toxicity of drugs: by reducing the drug concentration that can access the target or, alternatively, by modifying the target molecule (see Table 1.1). Thus, drug resistance might involve mutations causing the loss of their uptake system (for a recent review, see Garcia-Salcedo et al. 2016). Most resistance mechanisms developed by *T. brucei* are related with a decreased uptake or increased efflux of the drug due to mutations or altered expression of membrane transporters.

Melarsoprol and pentamidine's method of parasite killing differs, yet it is well established that they both enter the cell using the same transporter. Recently aquaglyceroporin 2, a member of a family of surface channel proteins involved in the transport of water and small non-charged solutes, has been identified as the transporter responsible for resistance to high concentrations of pentamidine and melarsoprol (Alsford et al. 2012; Baker et al. 2012). A recent study on *T. b. gambiense* demonstrated

that rearrangements of the *aquaglyceroporin 2/3* locus accompanied by *aquaglyceroporin 2* gene loss also occurs in the field (in Africa, where African's are treated), and that *T. b. gambiense* carrying such mutations correlates with a resistance to pentamidine and melarsoprol (Graf et al. 2013). Meanwhile, eflornithine's entry into trypanosomes is also transporter-mediated. Several groups have identified the amino acid transporter TbAAT6 as responsible for eflornithine uptake, showing that its loss is associated to drug resistance (Vincent et al. 2010; Baker et al. 2011; Schumann Burkard et al. 2011). To overcome the drug resistance occurring in *T. brucei* new solutions need to be developed for the use of current drugs or to replace these chemotherapies with new drug candidates. Ideally such new treatments should be fast-acting cidal agents that cure the disease in as few doses as possible.

Table 1.1 Current HAT treatments & resistance mechanism corresponding to membrane transporters

	T. b. gambiense	***T. b. rhodesiense***
Current front-line therapies	Early stage: pentamidine Late stage: melarsoprol, eflornithine monotherapy a and NECT (nifurtimox-eflornithine combination therapy)	Early stage: suramin Late stage: melarsoprol
Transporters associated to resistance	Aquaglyceroporin 2 – loss of gene (pentamidine and melarsoprol) TbAAT6 – loss of gene (eflornithine) ABC transporters – overexpression of gene (nifurtimox)	

Modified from Garcia-Salcedo et al. (2016)

1.3.4 Target Product Profile of new therapeutic candidates for HAT

The international DNDi (www.dndi.org), an independent, nonprofit, product development partnership organization dedicated to the development of new treatments for a number of diseases, including sleeping sickness, has developed a target product profile (TPP) for drug research and development for the treatment of HAT. The initiative proposed a dual strategy based on discussion with various HAT players and experts. The first priority is to develop a safe, effective, and practical stage 2 HAT drug to replace current first-line treatments, and to improve and simplify the current case management. Ideally, TPP includes: a new treatment for adults and children effective against both stages of the disease and both parasite sub-species, non-toxic, have at least 95% efficacy at 18 months post end of dosing follow-up examination, effective in melarsoprol refractory patients, cidal, multitarget, be safe for pregnant and breastfeeding women, easy to use (short-course or once a day), oral, require no monitoring, affordable, and adapted to tropical climates.

The second priority that they proposed was for a very simple stage 1 treatment, to be used at the local health centre level, which in turn could lead to increased access to treatment and coverage of HAT. Depending on the availability of a simple diagnostic, such a drug would allow for mass screening + treatment campaigns in endemic areas, thus preventing disease progression to stage 2 and reducing disease transmission.

As mentioned already, current drugs are a far cry from even a minimal target profile developed for a new chemical entity (NCE). Developing an NCE with an optimal TPP is expected to allow greater feasibility of use in the field, greater roll out and access to treatment and sustainability of control and elimination efforts against HAT.

1.4 Developments and outlook: new trypanosomal leads and clinical drug candidates

1.4.1 Overcoming melarsoprol resistance

The loss of function of surface transporters responsible for drug uptake is a common mechanism of drug resistance in African trypanosomes (Munday et al. 2015). Approaches that can overcome typical mechanisms of resistance in *T. brucei* include the use of inhibitors for efflux pumps and drug carriers for both active and passive targeting (Garcia-Salcedo et al. 2016). Cyclodextrins are cyclic oligosaccharides, with a hydrophilic outer surface and a hydrophobic interior cavity (Garcia-Salcedo et al. 2016). Cyclodextrins can form water-soluble inclusion complexes with many poorly soluble lipophilic compounds, and have been used to enhance drug solubility and reduce drug toxicity (Zhang & Ma 2013). Melarsoprol has been successfully occluded within β-cyclodextrin and randomly methylated-β-cyclodextrin (Rodgers et al. 2011). It was demonstrated that these compounds retained trypanocidal activities *in vitro* and cured the late stage of the disease in a murine model. The entrance route of melarsoprol-cyclodextrin complexes is likely via endocytosis rather than via specific transporters, as for free melarsoprol. Therefore, although it has not been tested, it is quite possible that the melarsoprol-cyclodextrin formulation could circumvent melarsoprol resistance.

Another option may be specific cell-surface targeting, as it has been shown to be an effective strategy to overcome drug resistance associated with the loss of function of surface transporters responsible for drug uptake in *T. brucei*. PEGylated PLGA nanoparticles were coupled to a single-domain heavy-chain antibody fragment (nanobody) that specifically recognizes the surface of the parasite (Stijlemans et al. 2004). Nanoparticles were loaded with pentamidine, the first-line drug for *T. b. gambiense* acute infection. An *in vitro* and *in vivo* effectiveness assay demonstrated that the formulation was able to significantly reduce the effective drug concentration (Arias et al. 2015). Moreover, in the same year Unciti-Broceta et al. created an improved version of this nanocarrier, which not only reduced the curative dose 100-fold, but impeded drug resistance as a result of mutations in aquaglyceroporin 2 (Unciti-Broceta et al. 2015).

1.4.2 Trypanocidal agents: proteasome inhibitor

Treatment of HAT and other parasitic diseases are under threat from drug resistance, and not only is understanding the mechanisms of resistance a high a priority, but also the development of new drug targets. An interesting and seemingly effective new approach is to target the proteasome of the causative agents of sleeping sickness, along with Chagas disease, leishmaniasis. Last year in 2016, researchers working at the Genomics Institute of the Novartis Research Foundation described a selective inhibitor of the kinetoplastid proteasome (GNF6702) with unprecedented *in vivo* efficacy, which cleared parasites from mice in all three models of infection (Khare et al. 2016). These parasites have similar biology and genomic sequence, suggesting that all three diseases could be cured with drug(s) modulating the activity of a conserved parasite target (El-Sayed et al. 2005). They tested 3 million compounds in proliferation assays on all three parasites, followed by prioritizing of active compounds (EC_{50} < 10 μM) with a clear window of selectivity (> 5-fold) with respect to growth inhibition of mammalian cells. They identified azabenzoxazole GNF5343, as a hit in screens of *L. donovani* and *T. brucei* cultures, and potent anti-*T. cruzi* activity in secondary assays. Optimization of GNF5343 involved the design and synthesis of ~ 3,000 compounds that focused on improving bioavailability and potency, which resulted in identifying GNF6702, (see Figure 1.6 for chemical evolution from first potent hit; Khare et al. 2016). GNF6702 inhibited the kinetoplastid proteasome through a non-competitive mechanism, did not inhibit the mammalian proteasome or growth of mammalian cells, and was well tolerated in mice. When tested for the treatment of parasite clearance in a mouse model of stage II sleeping sickness, GNF6702 given for seven days caused a sustained clearance of parasites (days 42 and 92 post-infection) with no detectable parasites in the brain at termination of the experiment. In comparison, mice treated with diminazene aceturate, a stage I drug that poorly crosses the blood-brain barrier, exhibited parasites in their brains at termination. Their data provide genetic and chemical validation of the parasite proteasome as a promising therapeutic target for treatment of kinetoplastid infections, and underscore the possibility of developing a single class of drugs for these neglected diseases (Khare et al. 2016).

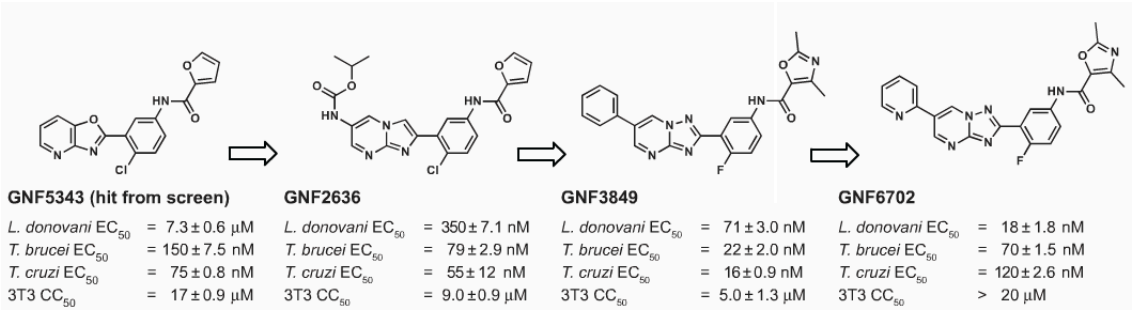

Figure 1.6 Chemical evolution of GNF6702 from the phenotypic hit GNF5343. Image taken from Khare et al. (2016).

1.4.3 Trypanosomal drug candidates in clinical trials

There are two relatively new drug candidates in clinical trials for treating second stage HAT: oxaborole and fexinidazole. After oxaborole was found to be active against HAT parasites, a two-year compound optimization followed with an examination of over 1,000 compounds, from which benzoxaborole **SCYX-7158** was selected as a promising pre-clinical candidate for gambiense HAT in late 2009. In pre-clinical studies, SCYX-7158 was shown to be safe and efficacious in treating the second stage of the disease in murine models against both subspecies, when administered orally in a single dose (Jacobs et al. 2011). In 2012, SCYX-7158 became DND*i*'s first new chemical entity resulting from its own lead optimization programme, to enter clinical development. When tested in healthy volunteers, SCYX-7158 was found to have an unusually long half-life. Clinical trials in diseased patients are still ongoing.

The other drug candidate in clinical trials, **fexinidazole** is the most advanced oral candidate under development for HAT. Originally developed as an antimicrobial by Hoechst, fexinidazole was shown to be active against trypanosomes in the 1980s (Raether & Seidenath 1983; Jennings & Urquhart 1983), but never made it to clinical testing. Since then, it has been shown that in mammals fexinidazole is rapidly absorbed and metabolized to fexinidazole-sulfoxide and fexinidazole-sulfone (Mäser et al. 2012) and all three compounds cross the blood-brain barrier and possess trypanocidal activity against both drug-sensitive and drug-resistant *T. brucei spp.* isolates (Kaiser et al. 2011). Fexinidazole cleared both *T. b. rhodesiense* and *T. b. gambiense* in acute mouse models of trypanosomiasis (Torreele et al. 2010).. Furthermore, its preclinical profile indicates the potential of fexinidazole to become safe, efficacious, affordable, oral treatment with a

suitable shelf life in tropical conditions (Torreele et al. 2010); meeting most of DNDi's TPP criteria. Two additional complementary clinical trials with fexinidazole were completed in 2016 and follow up of patients was scheduled to be completed in 2017 (DNDi portfolio). However promising these two clinical drug candidates might be, due to potential parasite drug resistance it is important to develop additional drug leads.

1.5 Drug discovery:

1.5.1 Traditional drug discovery route

New drugs have traditionally been discovered by highthroughput screening naturally occurring compounds for biological activity or *in vitro* (in bacterial viral cultures, tissue cultures), or live animals, (see Figure 1.7, Wheelis 2002). Once a compound with biological activity was discovered (a.k.a hit identification), it would be chemically modified in various ways in the hopes that one of the variants would have increased activity. Further modification of the lead compound is then tested in pre-clinical studies to determine their effectiveness as drug candidates, then to be further tested in clinical trials. From hightroughput screening of large sets of compounds to the production of a completely new drug is a very lengthy process.

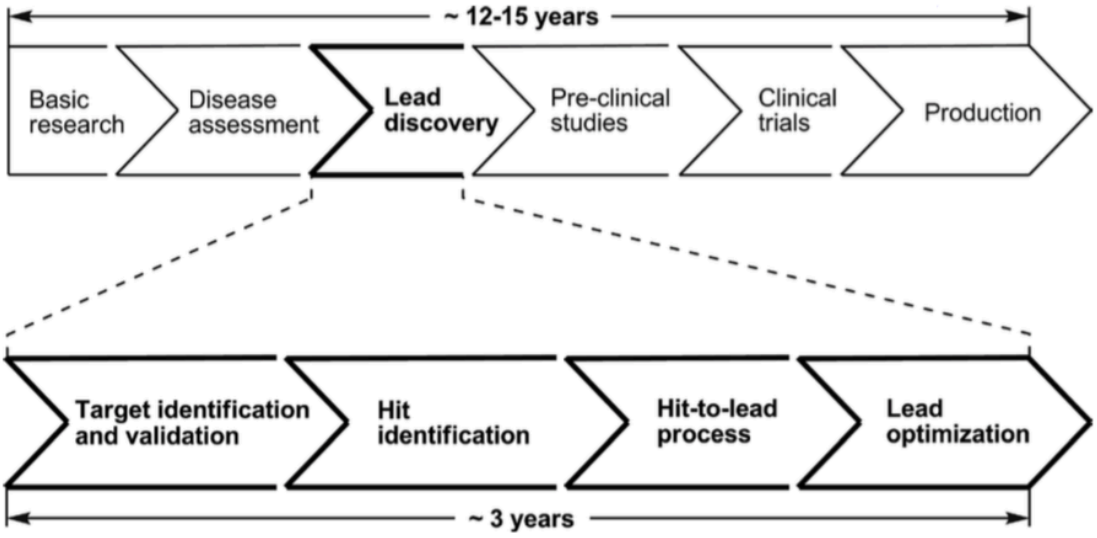

Figure 1.7 Schematic representation of drug discovery pipeline. Image taken from Minovski & Novič (2017).

1.5.2 Computer-aided drug design

Now, there are new approaches that work in the opposite direction. They generally rely on identifying likely targets first, followed by finding molecules that are complementary in shape and charge to the biomolecular target with which they interact and therefore will bind to it and affect their functioning. Since the initiation of the human genome project and functional genomics, there has been a continual increase in the number of new therapeutic targets available for drug design (Moitessier et al. 2008).

In particular, computer-aided drug design (CADD) offers an *in silico* addition to standard medicinal chemistry programs for studying the structure and predicting the biological activity of drug candidates. Now, screening of large libraries is being used in combination with or in parallel to computational approaches (Moitessier et al. 2008). In practice, identifying hits with subsequent optimisation to leads *in silico* rather than via library generation and physical screening is both faster and more economical (Moitessier et al. 2008; Huang et al. 2010). There are two major strands of CADD, namely structure-based drug design (SBDD) and ligand-based drug design (LBDD) (Huang et al. 2010). Both structure-based and ligand-based techniques can be applied in the initial drug discovery process and aid the discovery of a hit compound which serves as the starting basis for further modification to improve pharmacokinetics, solubility, selectivity, potency or stability, see Figure 1.7 (Huang et al. 2010).

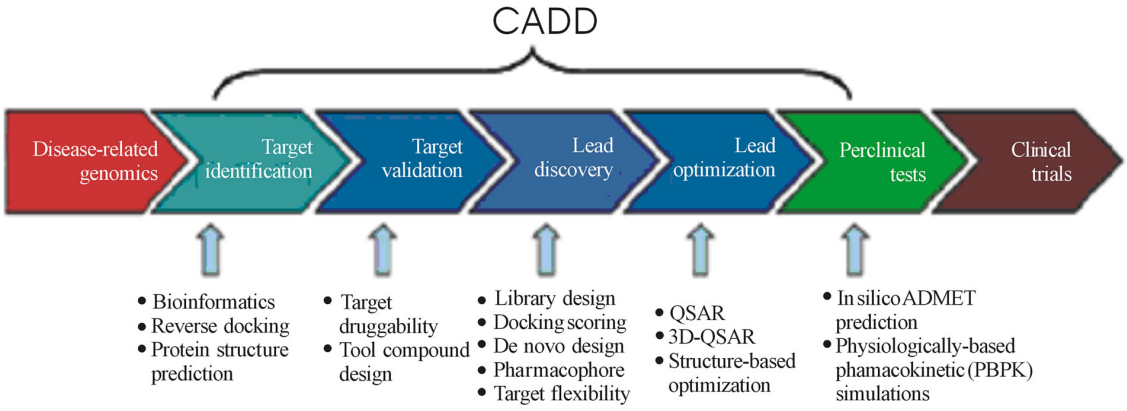

Figure 1.8 Position of *in silico* methods in the drug discovery cycle. Image taken from Kore et al. (2012).

1.5.1 Structure based drug design (SBDD)

Structure-based drug design relies on three-dimensional knowledge of a protein structure and its intrinsic active site(s), which enables investigation of the interaction, binding energy and steric relationship between ligand and receptor (Huang et al. 2010). A priority before investigating receptor–ligand relationship is to obtain the target structure. Protein structure determination is generally carried out by X-ray crystallography and/or Nuclear Magnetic Resonance spectroscopy (NMR) (Martí-Renom et al. 2000). The solved protein structures can be readily found at Protein Data Bank (www.rcsb.org/). However, if the structure of the protein drug target is not available (has not been solved or are difficult to isolate), protein structure can be predicted by computational methods like threading and homology modeling (Huang et al. 2010; Aparoy et al. 2012). Two commonly used methods in SBDD are molecular docking approaches and de novo ligand (antagonists, agonists, inhibitors, etc. of a target) design (Leelananda & Lindert 2016). Molecular dynamics simulations are frequently used in SBDD to give insights into not only how ligands bind with target proteins, but also the pathways of interaction and to account for target flexibility. This is especially important when drug targets are membrane proteins where membrane permeability is considered to be important for drugs to be useful.

1.5.2 Ligand based drug design (LBDD)

When the target protein structure is unknown or cannot be accurately predicted by modeling techniques, ligand-based drug design can be utilised to generate alternative hypotheses for hit identification and also for 'scaffold hoping'. The method relies on knowledge of molecules that bind to the biological target of interest and may be used to derive, for example, a pharmacophore model, which defines the minimum necessary structural characteristics a molecule must possess in order to bind to the target (Merz Jr et al. 2010). Alternatively, other methods using statistical approaches to correlate ligand activity to structural information may be used (Singer & Purcell 1967), such as a) Quantitative structure–activity relationship (QSAR), b) comparative molecular field analysis (CoMFA), and c) comparative molecular similarity index analysis (CoMSIA) (Huang et al. 2010).

In the early 1900s Paul Ehrlich suggested the term *pharmacophore* refer to the molecular framework that carries (*phoros*) the features that are essential for the biological activity of a drug (*pharmacon*). Pharmacophore mapping/modeling involves three processes: (i) finding the features required for a particular biological activity (ii) determining the molecular conformation required (i.e. the bioactive conformation); and (iii) developing a superposition or alignment rule for the series of compounds (Aparoy et al. 2012). The process of pharmacophore based virtual screening involves the following successive computational steps: drug target selection, database preparation, pharmacophore model generation, 3D screening (Güner et al. 2004; Sun 2008; Kim et al. 2010; Melagraki & Afantitis 2011; Caporuscio & Tafi 2011). Automated pharmacophore mapping is now supported by programs, such as Catalyst, LigandScout (Wolber & Langer 2005), Phase, MOE and others. The types of interaction sites most often recognized by pharmacophore software include hydrogen bond acceptor (A), hydrogen bond donor (D), hydrophobic (H), negative ionic/ionizable (N), aromatic rings (R) and positive ionic/ionizable (P) (Aparoy et al. 2012).

Figure 1.9 Main methods used in rational drug design: structure and ligand-based drug design and where they fit in the drug discovery pipeline. SBDD involves approaches where the structural knowledge of the drug target is already known. LBDD uses strategies where knowledge of existing ligands of a drug target is employed. Figure taken from Leelananda & Lindert (2016).

1.6 Aims of the current study

The aim of the current study was to investigate different strategies for lead compound discovery against trypanosomiasis. A series of compound hits from both traditional (semi-rational; cysteine protease inhibitors) and computer-aided drug discovery (rational; repurposed drugs) pipelines were tested for anti-trypanosomal properties using a series of *in vitro* and *in vivo* assays.

CHAPTER 2. Materials & Methods

2.1 Materials

Series of sulfone vinyl compounds were received from Paul Evans – Chemistry Group (UCD, Ireland). FTY720 (2-amino-2-[2-(4-octylphenyl)ethyl]-1,3-propanediol, hydrochloride), FTY720P (2-amino-2[2-(4-octylphenyl)ethyl]-1,3-propanediol, mono dihydrogen phosphate ester), D-erythro-Sphingosine (2S-amino-4E-octadecene-1,3R-diol) and Sphingosine-1-Phosphate (2S-amino-1-(dihydrogen phosphate)-4E-octadecene-1,3R-diol) were all purchased from Cayman Chemical Company (Ann Arbor, MI, USA). AmBisome (Gilead, Paris, France), SPK-843 (Bioseutica Group), Pentamidine Isethionate, Suramin sodium salt, 2-(Difluoromethyl) ornithine hydrochloride hydrate, Nifurtimox. All other reagents were of standard laboratory grade and purchased from commercial suppliers.

2.2 Preparation of buffers and solutions

All reagents were weighed out on a Mettler College Model analytical balance for weights less than 5 g, and reagents over 5 g were weighed using a Mettler model KTT loading balance (Model R20). All aqueous solutions were made using distilled deionized water from a Millipore Direct-Q3 Water Purification System, unless otherwise stated. Unless specified, all solutions were titrated at room temperature as necessary, using 12 M HCl or 5 M NaOH and the hydrogen ion concentration of solutions was measured using an Amagrass glass electrode connected to an EDT RE357 pH meter. The pH meter was calibrated daily using standard buffer solutions of pH 4, 7, and 10 (Sigma-Aldrich). All chemical and working stock solutions were prepared and stored as recommended by the relevant manufacturers.

2.3 Buffers

Phosphate-buffered saline (PBS): KH_2PO (3 mM), Na_2HPO_4 (16 mM), NaCl (136 mM), KCl (3 mM), pH 7.4

Phosphate-buffered saline glucose (PSG): KH_2PO (1.5 mM), Na_2HPO_4 (8 mM), NaCl (137 mM), KCl (2.7 mM), glucose (5 mM), pH 7.5

2.4 General Cell Culture

2.4.1 *In vitro* culturing conditions

Monomorphic bloodstream forms (BSFs) of *T. brucei brucei* MITat1.1 strain were maintained in complete, antibiotic-free HMI-9 medium (Gibco) supplemented with 10 % heat-inactivated fetal bovine serum (FBS) (BioSera) as described elsewhere (Hirumi & Hirumi 1989). Trypanosomes were subcultured at the appropriate dilutions (1:10) every 24 h in fresh HMI-9 medium to ensure log growth phase. Procyclic cells (PCFs) (strain 29.13) were maintained in log phase growth in SDM-79 (Gibco/Invitrogen) containing 10% FBS as described previously (Brun 1979). HL-60, a human acute myeloblastic leukemia cell line, was kindly provided by Prof. Luke O'Neill (School of Biochemistry and Immunology, TBSI, TCD, Ireland) and was maintained in RPMI-1640 (Sigma-Aldrich) medium supplemented with 10 % FBS, 100 units/mL penicillin and 0.1 mg/mL streptomycin (Sigma-Aldrich), and 2 mM L-glutamine (Sigma-Aldrich). All cultures were maintained in a humidified atmosphere containing 5 % CO_2 at 37 °C (BSF *T. b. brucei* and HL-60 cells), or at 27 °C (PCF *T. b. brucei*).

2.4.2 Cell counting

The density of cultured cells was enumerated using an Improved Neubaur haemocytometer, with a silvered stage (Gelman-Hawksley, Lancing, Susse, UK) and a light microscope (Olympus CK2).

2.4.3 Preparation of cell stocks for liquid nitrogen

Glycerol stocks for storage of trypanosome cell lines in liquid nitrogen were prepared by mixing an equal volume of cell cultures with growth medium that was supplemented with 30 % glycerol (Sigma-Aldrich). These samples were cooled to -80 °C in a Mr. Frosty Freezing™ Container (Thermo Scientific) containing 100 % isopropyl alcohol, and left overnight before transferring to liquid nitrogen for long-term storage.

2.5 Dissolving compounds

2.5.1 For *in vitro* testing

For all *in vitro* studies, compounds were dissolved as follows: Vinyl sulfone compounds were received in a powder form and they were reconstituted to 10 mM in sterile DMSO, then stored at 4 °C. FTY720 was dissolved in ethanol:water (1:1 ratio), FTY720P in DMSO/50 mM HCL followed by methanol. The following compounds were dissolved in water: AmBisome, SPK-843, Pentamidine Isethionate, Suramin sodium salt, 2-(Difluoromethyl) ornithine hydrochloride hydrate. Sphingosine 1-phosphate was dissolved in 0.3 M NaOH. D-erythro-Sphingosine, Nifurtimox and all control compounds were dissolved in DMSO. Subsequent dilution of all compounds in HMI-9 medium was carried out whereby the maximum concentration of all solvents was 0.5 %.

2.5.2 For *in vivo* testing

For *in vivo* studies, FTY720 was dissolved in sterile phosphate-buffered saline glucose (PSG), SPK-843 in 10 % intralipid emulsion, AmBisome in 5 % Glucose solution.

2.6 Viability Assays

2.6.1 Cysteine protease inhibitors (Alamar Blue)

The effect of our cysteine protease inhibitors (compounds 13-53, see Appendix A1) on parasite growth and HL-60 cells was determined using the Alamar Blue assay, essentially as described by Räz *et al*. Briefly, *T. b. brucei* cells (strain MITat1.1) and HL-60 cells were seeded in 96-well plates at a density of 2×10^5 cells/mL in 100 μL of their appropriate media (HMI9 or RMPI) in the presence of 5 μL of a series of concentrations of predicted inhibitors (5 μM to 500 nM) or DMSO alone. A further 30 μL of media was added to each well. After 6-8 h for *T. b. brucei* and 30–32 h for HL-60 cells, 15 μL of Alamar Blue (Invitrogen) was added to the cells and incubation continued so that the total incubation time was 24 or 48 h, respectively. Absorbances at 540 and 595 nm were measured using SpectraMax M3 microplate reader (Molecular Devices), and EC_{50} values were calculated using the GraphPad Prism 6 software.

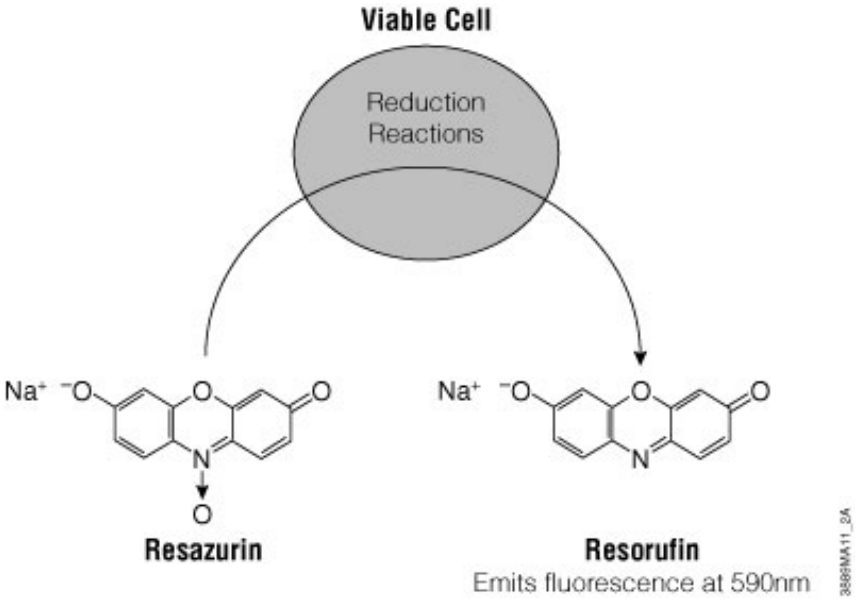

Figure 2.1 Alamar Blue assay explained. Conversion of resazurin to resorufin by viable cells results in a fluorescent product. The fluorescent resorufin is proportional to the number of metabolically active, viable cells present in a population. Image taken from Promega Protocols and Application Guide: Cell Viability.

2.6.2 Fingolimod (Alamar Blue)

The effect of FTY720, FTY720P, D-Sphingosine (SIP), and Sphingosine 1-Phosphate (SIPP) on parasite grown was also determined using Alamar Blue assay. Both *T. b. brucei* BSFs and PCFs parasites were maintained in log phase growth, counted and diluted in their appropriate media (HMI9 or SDM79) to 2 x 10^4 cells/mL or 2 x 10^5 cells/mL, respectively. 100 µL of cells from diluted stock were added to 96-well plates (Corning) with each well containing 30 µL of HMI9 or SDM79 media. 5 µL of serially diluted compound (300 µM→0.3 nM) were subsequently added to each well. After 42 h incubation period, 15 µL of Alamar Blue (Invitrogen) was added to each well and incubated for a further 6 h. To assess cell viability, fluorescence was read on a SpectraMax M3 plate reader (Molecular Devices, Sunnyvale, CA, USA) after the total incubation period of 48 h at an excitation wavelength of 540 nm and emission of 590 nm. GraphPad Prism v5.0 (San Diego, CA) was used to generate sigmoidal dose-response curves for the determination of IC_{50} values, and also in the construction of all graphs.

2.6.3 Propidium Iodide (measurement of cell permeabilisation)

A fluorescence assay using propidium iodide (PI) was set up to assess for cell death caused by cell permeabilisation. Trypanosomes were only permeable to propidium iodide (PI) if plasma membrane integrity was disrupted, resulting in staining of both nuclei and kinetoplasts, and fluorescence then detectable by a plate reader. Propidium iodide (PI) binds to nucleic acids by intercalating between the bases and once bound, PIs fluorescence is enhanced 20- to 30-fold, the fluorescence excitation maximum is shifted ~30–40 nm to the red, and the fluorescence emission maximum is shifted ~15 nm to the blue. This assay was performed using a slightly modified version of the protocol described by Gould et al (Gould et al. 2008). Briefly, 80 μL of serum-free HMI-9 medium containing 12.5 μg/mL propidium iodide and 1 μM (final) of test compound (SPK-843, AmpB, FTY720P) was added to a well of a 96-well plate; a well containing 80 μL of medium with propidium iodide only was set up as a control and digitonin (50 μM final) was used as a positive control. 40 μL of medium containing blood-stream-form trypanosomes was added to each well to give a final cell density of 2 x 10^7 cells/well. Fluorescence was monitored over time using a SpectraMax M3 plate reader (Molecular Devices, Sunnyvale, CA, USA) at 37 °C with excitation and emission filters at 544 and 620 nm, respectively. Percentage permeabilisation was calculated by normalising compound fluorescence values to the defined parameters of 0% as the digitonin values and 100% as the vehicle values at each time point.

2.6.4 ATP Assay – Time of kill (Measurement of ATP content)

CellTiter-Glo® luminescent cell viability assay (Promega) was used to detect compound mediated killing of *T. brucei brucei in vitro* over time via measurement of parasite ATP content as a real-time indicator of cell viability. Firstly, *T. b. brucei* (BSFs) in log phase of growth were counted and diluted to 2 x 10^5 cells/mL in complete HMI-9 medium. 95 μL of cells from diluted stock were then added to each well of 96-well opaque bottom plates (Corning). 5 μL of serially diluted compound (10 μM→ 10 pM for FTY720, FTY720P, pentamidine and 33 μM -> 1 nM) were subsequently added to each well. At selected time-points, 50 μL of Cell-Titer Glo reagent was added to relevant wells, the plates were mixed on an orbital shaker for 2 min. After 10 min incubation in the dark at 37 °C to ensure full parasite lysis, luminescence was read on a SpectraMax M3 plate reader (Molecular Devices, Sunnyvale, CA, USA) at 37 °C.

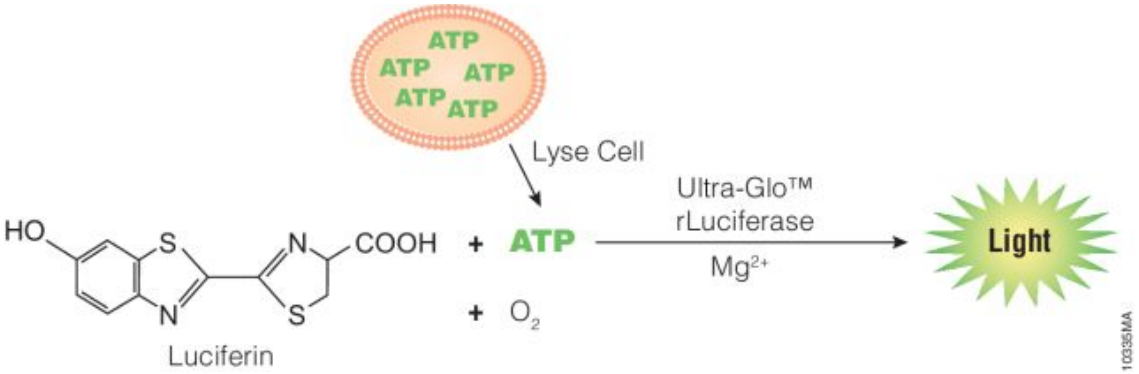

Figure 2.2 CellTiter-Glo viability assay explained. Luciferase reaction: mono-oxygenation of luciferin is catalysed by luciferase in the presence of Mg^{2+}, ATP (from the lysed cells) and molecular oxygen. The luminescence signal resulting form this reaction can be measured by a plate reader and is directly proportional to the number of cells in the well. Image taken from Promega technical bulletin: CellTiter-Glo Luminescence cell viability assay.

2.7 Fluoresence Microscopy - Immunocytochemistry

2.7.1 Cell fixation

Paraformaldehyde solutions of 4 % and 6 % were prepared and stored at -20 °C. Paraformaldehyde powder was added to 5 volumes of distilled deionised water and titrated with NaOH (5 M) until fully dissolved. 10 volumes of PBS was added to the fixative and the pH was adjusted to 7.4. The final volume was adjusted with distilled water as required. Bloodstream or procyclic form trypanosomes were harvested from culture, washed twice with phosphate-buffered saline glucose (PSG buffer) and resuspended in phosphate-buffered saline (PBS) at a concentration of 2 x 10^6 - 10^7 cells/mL. An equal volume of 6 % PFA solution was added. Bloodstream form cells were incubated for 10 min, and procyclic forms for 20 min at room temperature. Following this incubation step the fixed cells were washed once with PBS buffer and resuspended at 2 x 10^6 - 10^7 cells/mL in PBS containing sodium azide (15 mM). Samples were stored at 4 °C.

2.7.2 Immunofluorescence and Confocal microscopy

Microscope coverslips were prepared by washing with poly-L-lysine solution (10%). The coverslips were allowed to dry, then they were washed with 70 % ethanol and, again,

allowed to fully dry. Fixed cells were washed once with sterile deionised water before addition of 10 μL onto coverslips. Cells were allowed to settle for 20 min at room temperature. The coverslips were mounted onto slides with Pro-Long Gold anti-fade reagent (Molecular Probes) containing 4′,6-diamidino-2-phenylindole (DAPI) to visualize the nucleus and kinetoplast, unless stated otherwise. Coverlsips were sealed and samples were visualized using Leica SP8 gated STED microscope or Zeiss Axiovert 100 fluorescence microscope.

2.7.3 Organelle targeting /lysosime imaging

Cysteine protease inhibitor was assessed for lysosomal targeting. *T. b. brucei* were treated with compound 7 and incubated at 37 °C for 24 h, then incubated with lysotracker. Cells were fixed for 10 min at 37 °C with 4 % (w/v) paraformaldehyde final concentration. Following fixation, cells were washed once in PBS buffer containing sodium azide (15 mM) and once in water, before allowing the cells to settle on poly-L-lysine coated coverslips. The coverslips were mounted onto slides with Pro-Long Gold anti-fade reagent (Molecular Probes) containing 4′,6-diamidino-2-phenylindole (DAPI) - to visualize the nucleus and kinetoplast - and finally sealed. Samples were visualized using Leica SP8 gated STED microscope.

2.8 Drug reversibility assay (drug washout)

T. b. brucei parasites were assessed for their ability to recover from transient exposure to FTY720, FTY720P, SPK-843, and pentamidine. Cells were seeded in clear 96-well V-bottom plates at a density of 2 x 10^4 cells/well and incubated with a range of concentrations of FTY720 (30 μM- 0.03 nM final). One plate was prepared for each time point and spun at 650 x g at the appropriate time for 5 min to sediment the parasites. The supernatant was removed and 100 μL of warmed HMI-9 medium was added to each well. The washing process was repeated two more times and following addition of the final 100 μL, 50 μL was transferred to new flat-bottom culture plates containing 80 μL of pre-warmed media per well. All plates were incubated for 72 h and 10% Alamar Blue (Invitrogen) was subsequently added for an additional 4 h period prior to determining IC_{50} values.

2.9 Morphology and Cell Cycle Analysis

T. b. brucei at 5 x 10^5 cells/mL were incubated in HMI-9 medium in a humidified incubator at 37 °C and 5 % CO_2 in the presence or absence of FTY720 and FTY720P. At time-points of 3 h and 8 h respectively, cells were fixed in 3 % paraformaldehyde (PFA) for 10-15 min. Fixed cells were washed twice in PBS by centrifugation at 2700 rpm for 10 min and resuspended at 1-2 x 10^8 cells/50 μL. Cells were spread on slides, dried and washed once in water and further allowed to dry. Finally, cells were mounted in Pro-Long Gold anti-fade reagent containing 4′,6-diamidino-2-phenylindole (DAPI) (Molecular Probes) and examined using a Zeiss Axiovert 100 fluorescence microscope equipped with an AxioCam HRc camera. All images were captured and processed using Zeiss AxioVision v4.8 software. For cell cycle analysis, >100 cells were analysed in two separate experiments and cells were manually assigned to the following categories: 1N1K (1 nucleus + 1 kinetoplast; G1-phase), 1N2K (1 nucleus + 2 kinetoplasts; early S-phase), 2N2K (2 nuclei + 2 kinetoplasts; cleavage furrow with ongoing cytokinesis), 2N1K (2 nuclei + 1 kinetoplast; Aberrant cells blocked in late mitosis), 2N2K† (2 nuclei + 2 kinetoplast; Aberrant cells blocked in late mitosis) and MultiNuc (aberrant cells with > 2 nuclei + 2 kinetoplasts).

2.10 Ethics Statement

The work described in this study involved the use of laboratory rats obtained from the BioResources unit, which is the licensed facility at Trinity College Dublin. The work was approved by the Bio Resources Ethics Review committee at Trinity College Dublin and was performed under a certificate A licence issued by the Minister for Health and Children under the Cruelty to Animals Act as amended by European Community Directive 86/609/EC. All animals were maintained and all procedures were conducted in the BioResources Unit.

2.11 *In vivo* experiments

10 week old adult female NMRI mice (Harlan Laboratories, The Netherlands) weighing between 25 and 30 kg at the beginning of the study were housed under standard conditions (Bio Resources Unit (BRU), TCD) with food pellets and water *ad libitum*. 22 female NMRI mice were infected intraperitoneally (i.p.) on Day 0 with 1 x 10^4 BSF *T. b. brucei* monomorphic strain Lister 427 in Phosphate-buffered-Saline-Glucose (PSG) and the infection was allowed to progress for an additional 72 h prior to initiating treatment. Two groups of mice (four per group) received treatment with FTY720 (1 mg/kg; p.o.), or control vehicle (PSG) for 5 consecutive days. Two groups of mice (four per group) received treatment with SPK-843 (5 mg/kg; i.v.) and AmBisome® (5mg/kg; i.v.), while two control groups (three per group) were treated only with vehicle (10% intralipid emulsion; SPK-843 (i.v.) and 5% Glucose solution; AmBisome® (i.v.)) for 5 consecutive days. At the indicated days post-infection, 2 μL of peripheral blood was obtained by cheek bleed and diluted 1:200 into phosphate saline glucose buffer and parasites were enumerated on a haemocytometer. The limit of detection using this method was ≥10^6 cells. Moribund mice or those with parasitemias >10^8 cells/mL were euthanized in accordance with our animal care protocol. Survival was monitored daily throughout the course of infection.

2.12 Statistics

Data were expressed as mean ± standard error of the mean (SEM), or standard deviation (SD), where indicated. Student's unpaired t test was used to determine statistical significance between groups for each timepoint. A value of $p < 0.05$ was considered statistically significant.

CHAPTER 3. Results: Investigating anti-trypanosomal properties of a series of cysteine protease inhibitors

3.1 Introduction

3.1.1 Cysteine proteases

From a pharmaceutical point of view, due to recent progress in the understanding of the physiological roles of these enzymes, cysteine proteases may present viable drug targets for not just major diseases such as atherosclerosis, cancer, rheumatoid arthritis, but also for a wide variety of parasitic infections (Lecaille et al. 2002; Turk et al. 2012). Interest in cysteine proteases as targets derive from the recognition that they are critical to the life cycle or pathogenicity - immunoevasion, enzyme activation, virulence, tissue and cellular invasion - of many parasites (Sajid & McKerrow 2002).

Proteases are categorized based on their catalytic mechanism used during the hydrolytic process or their substrate specificities. Five major known protease classes ranked by the mechanism of peptide hydrolysis are: serine, cysteine, aspartic, threonine, and metallo-proteases (Lecaille et al. 2002). In particular, cysteine proteases comprise a group of papain-related enzymes (Turk et al. 2001): these papain-like cysteine proteases are the largest subfamily among the cysteine protease class (clan CA, family C1). They are widely expressed throughout the animal and plant kingdoms, and have also been identified in viruses and bacteria (Lecaille et al. 2002). Cysteine proteases have unique reactive-site properties and an uneven tissue-specific expression pattern. In living organisms, their activity is a delicate balance of expression, targeting, inhibition by protein inhibitors and degradation. The specificity of their substrate binding sites, small-molecule inhibitor repertoire and crystal structures are providing new tools for research and development (Turk et al. 2012). Here, the focus was on parasitic, *T. brucei*, cysteine proteases and recent development in inhibitor design for parasitic indications.

3.1.2 Cysteine proteases: cathepsins

Mammalian papain-like cysteine proteases are also known as thiol-dependent cathepsins (Lecaille et al. 2002), as these proteases share a common catalytic mechanism that involves a nucleophilic cysteine thiol. The name cathepsin was originally proposed for proteases that were active in a slightly acidic environment (Willstätter & Bamann 1929). Now, under the term cathepsin there are the serine proteases cathepsins A and G, the aspartic proteases cathepsins D and E, and the lysosomal cysteine cathepsins. To date, there are 11 human cysteine cathepsins: cathepsins B, C, F, H, K (O2), L, O, S, V (or L2),

X (or Z) and W, existing at the sequence level as confirmed by a bioinformatic analysis of the draft sequence of the human genome (Rossi et al. 2004). From herein papain-like cathepsins refers to lysosomal cysteine proteases.

3.1.3 *Trypanosoma brucei* cysteine proteases

Cysteine proteases are important for growth and survival of kinetoplastid parasites, as illustrated in Figure 3.1. For example in relation to immunity, parasitic cysteine proteases facilitate degradation of some nuclear factors mediating host cell activation, thus, offering an explanation for reduced or lack of response from the host immune system following parasitic infection (Dunny & Evans 2011). Kinetoplastid parasites express two C1 proteases related to mammalian cathepsins B and L, and are, therefore often referred to as cathepsin B- and L-like proteases (Caffrey & Steverding 2009). Over the years, there has been little consistency with the naming of kinetoplastid cathepsin L-like cysteine proteases. The terms, 'brucipain' and 'Trypanopapain-Tb' (Caffrey et al. 2000) have been used for the cathepsin L-like proteases of *Trypanosoma brucei* species. In addition, 'rhodesain' emerged in an attempt to differentiate the *rhodesiense* sub-species enzyme from that of brucipain, of the *brucei* sub-species (Caffrey et al. 2001; Lecaille et al. 2002), while other researchers use rhodesain, brucipain and trypanopain interchangeably to describe cathepsin L-like proteases in all species of *T. brucei* (Mackey et al. 2008). Likewise, no rigorous nomenclature has been applied to the kinetoplastid cathepsin B-like peptidases (Caffrey & Steverding 2009). Currently, the designations CATB with the first letter of the genus followed by the first letter of the species is employed to indicate the source organism of the protease: TbCatB for Cathepsin B-like protease in *Trypanosoma brucei* (Watts et al. 2010; Caffrey & Steverding 2009). Brucipain is the more abundant cysteine protease in *T. brucei* (Ettari et al. 2016).

.

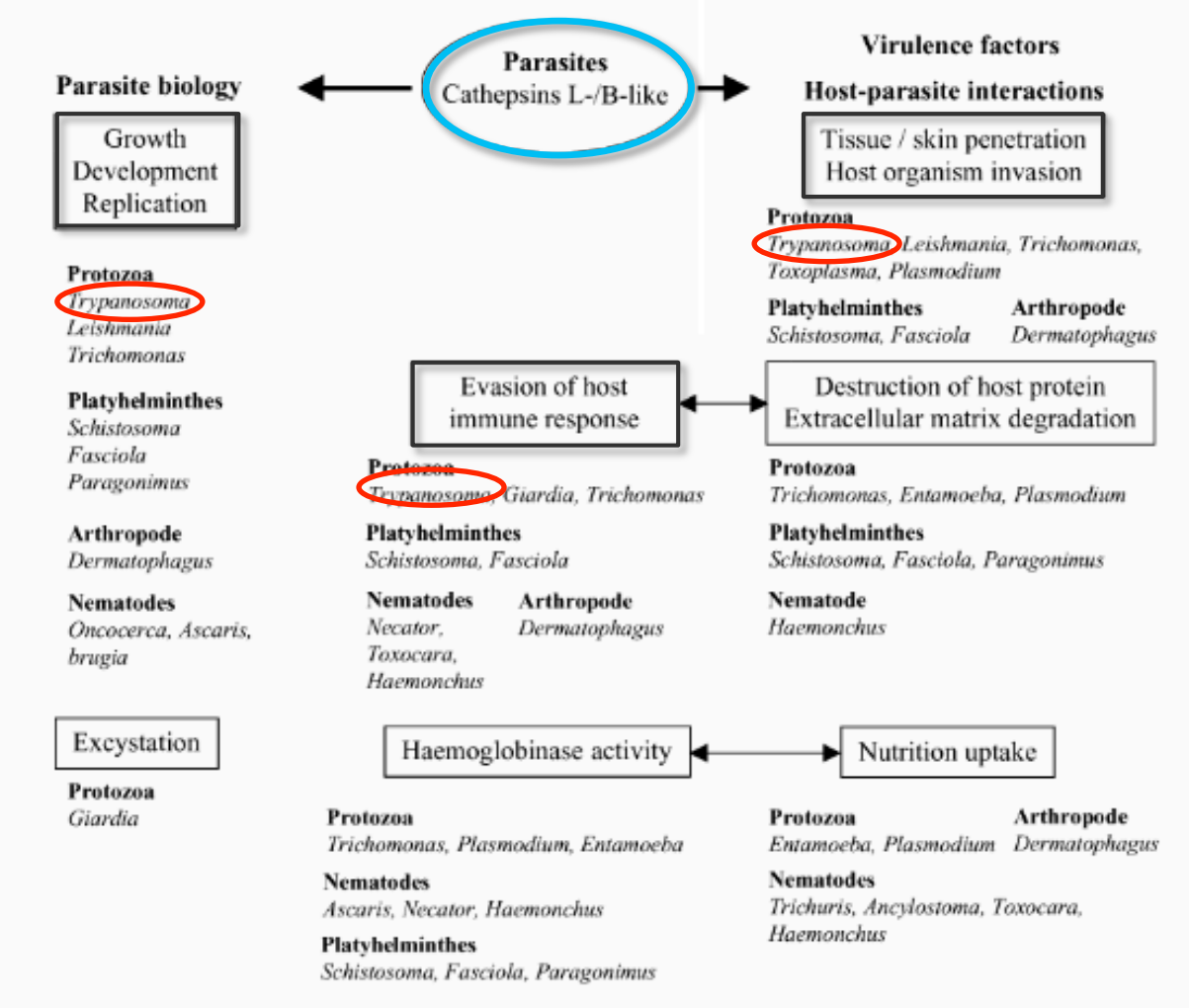

Figure 3.1 Physiological roles of parasitic papain-like cysteine proteases. Taken from Lecaille et al. (2002), with slight modifications to highlight the roles of Cathepsins L & B-like for the *Trypanosoma* genus.

3.1.4 Cysteine protease structure and specificity

All papain-like cysteine proteases have common features: they consist of a signal peptide, a propetide, and a catalytic domain, in which the latter represents the mature proteolytically active enzyme (Lecaille et al. 2002). Catalysis can be initiated either within a polypeptide chain (endoprotease activity) or from amino or carboxyl ends (exopeptidase activity) (Sajid & McKerrow 2002). The amino acid sequences of brucipain, the target of cysteine proteases in *T. brucei*, when compared to mammalian proteinases are most related to cathepsin L (approximately 45% identity) (Mottram et al. 1989; Campetella et al. 1992; Eakin et al. 1992). Distinct from the trypanosomatid protease is, however, an additional 11-13 kDa C-terminus extension separated from the mature catalytic domain by a poly-proline (brucipain) tract (Caffrey et al 2000). The catalytic mechanism of parasitic cysteine proteases is typical of most papain-like proteinases (Lecaille et al. 2002; Otto & Schirmeister 1997; Steverding & Caffrey 2006) and is highly conserved and consists of three residues: cysteine, histidine and aspargine (Dunny & Evans 2011). Hydrolysis of substrates by the mature parasite protease proceeds essentially as for mammalian cathepsins through a catalytic diad of cysteine and histidine, which are located on opposite sides of the enzyme's active site cleft (Drenth et al. 1968; Storer & Ménard 1994), see Figure 3.2.

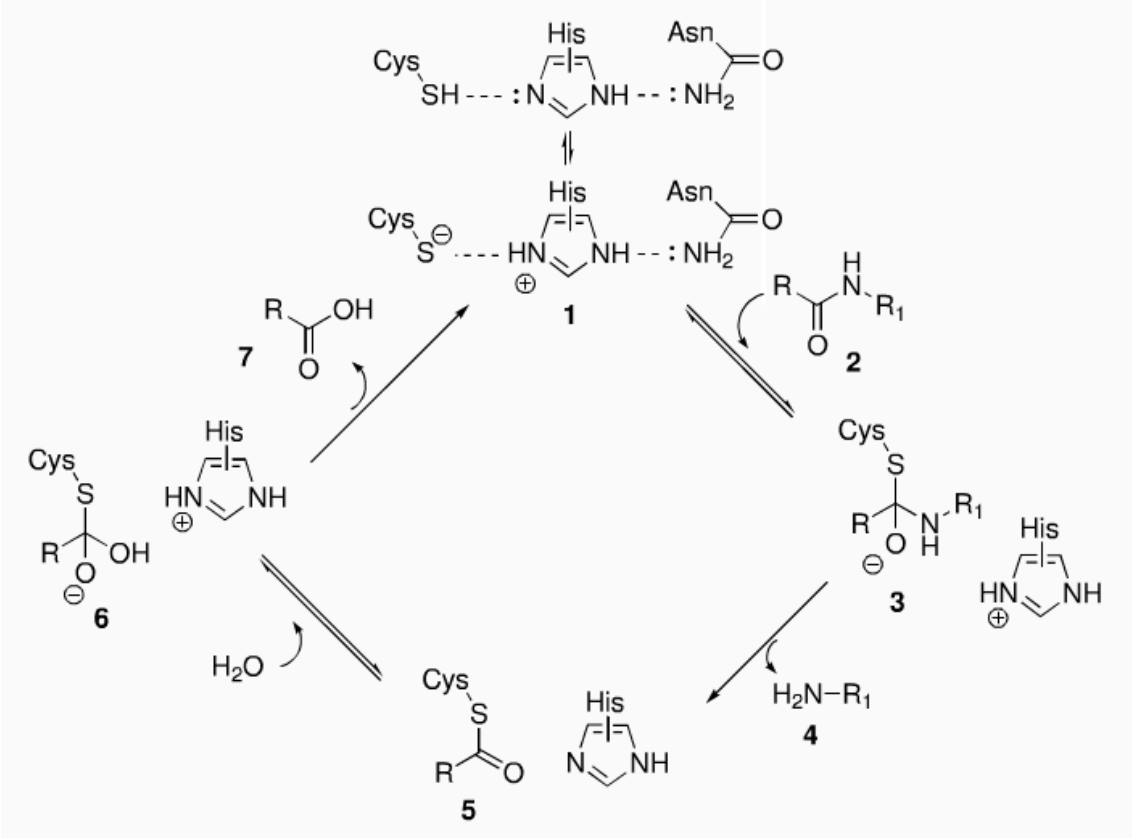

Figure 3.2 Scheme of catalytic mechanism of proteolysis by papain-like cysteine proteases. The catalytic mechanism of parasitic cysteine proteases is typical of most papain-like proteinases. In the catalytic active site the imidazole group of the histidine polarizes the thiol group of cysteine and enables deprotonation resulting in a thiolate/imidazolium ion pair **1,** which is stabilized by a hydrogen bond with asparagine. Subsequent to recognising and binding a digestible peptide, the nucleophilic ion pair **1** attacks the carbonyl of the scissile bond of the bound substrate **2**. This results in a tetrahedral intermediate **3**, which collapses to form the acyl enzyme **5**, leaving the imidazolium ion sufficiently acidic to protonoate the nitrogen of the leaving group **4**. Hydrolysis of the acyl enzyme **5** with water produces a second tetrahedral intermediate **6,** which collapses to generate the free enzyme and the cleaved substrate **7**, as the acid. Image taken from Dunny & Evans (2011).

3.1.5 Optimum function of cysteine proteases is dependent on pH

Parasite cysteine proteases function in a broader chemical environment than the homologous host enzymes. With the exception of cathepsin S (Kirschke et al. 1986; Kirschke et al. 1989), human cathepsins have an acidic pH optimum that allows full activity within the lysosomal compartment (Barrett & Kirschke 1981), where the lysosomal pH has been estimated to be as low as pH 4.0 (Turk et al. 1995). Most mammalian cathepsins are rapidly inactivated at neutral pH, an adaptive change that might represent protective mechanism against accidental leakage from the lysosomes into the cytosol (Turk et al. 1993). While parasite cathepsins are also active at low pH, in contrast to the vertebrate proteases, many parasitic cysteine protease are most active at neutral or slightly alkaline pH (Sajid & McKerrow 2002; Caffrey et al. 2001; Eakin et al. 1992). Neutral or alkaline pH optima are in accordance with the extracellular activity observed for these proteases: involved in nutrition, tissue and cell invasion and immunoevasion (Sajid & McKerrow 2002).

3.1.6 Cysteine protease chemotypes

The design and synthesis of cysteine protease inhibitors has been extensively reviewed in recent years (Demuth 1990; Grzonka et al. 2001; Otto & Schirmeister 1997; Leung-Toung et al. 2006; Leung-Toung et al. 2002; Yamashita & Dodds 2000). Lecaille *et al.* (2002) provided an excellent review on the chemotypes synthesized: diacyl bis hydrazides, diamino pyrrolidinone, aldehydes, acyclic and cyclic ketones, nitriles, epoxysuccinyl analogs, β-lactams, and vinyl sulfones. Cysteine protease inhibitors have, for example, been shown to kill *T. cruzi* (Ashall et al. 1990; Harth et al. 1993; de Cazzulo & Martínez 1994), *T. congolense* (MBAWA et al. 1992), and *Trichomonas vaginalis* (Irvine & North 1997) and to halt the development of *Schistosoma mansoni* (Wasilewski et al. 1996), *Plasmodium vinckei* (Rosenthal et al. 1993), and *P. falciparum* (Rosenthal et al. 1989; Rockett et al. 1990). Only recently have cysteine protease inhibitors been developed into drugs through the dramatic increase in the understanding of papain-like cysteine proteases as pharmaceutically valid targets (Lecaille et al. 2002).

3.1.7 Vinyl sulfones as inhibitors of cysteine proteases

In particular, peptidyl vinyl sulfones (VS) were first introduced by Hanzlik and co-workers as a group of compounds which inhibit the cysteine protease papain (Hanzlik & Thompson 1984; Dunny et al. 2013). Vinyl sulfones (α-β unsatured sulfones) are functional groups with strong electrophilic activity due to the electron poor nature of the double bond, which enable it to react with sulfur-based nucleophiles (particularly under basic conditions). Covalent bonds can thus be formed between the vinylic group and the catalytically active cysteine residue within the binding pocket of the protease inhibiting its function, as depicted in Figure 3.3 (Doherty et al. 2014; Dunny et al. 2013). This capacity can thus make irreversible reactions with cysteine proteases, inhibiting their function. The irreversibility of vinyl sulfones cysteine protease binding was explored by Palmer *et al.* in 1995 and they showed that mammalian cathepsin B was completely inactivated with no recovery of enzymatic activity following purification. They also showed selectivity for cysteine proteases over serine proteases, with a library of synthesized peptidyl vinyl sulfones that contained "functional scaffolds", combining inhibitor–protease complementarity in terms of binding with enzymatic deactivation (Palmer et al. 1995). Vinyl sulfones also have other desirable attributes, including stable inactivation of the target enzyme, and relative inertness in the absence of the protease target active site (Palmer et al. 1995; Brömme et al. 1996). Only recently has attention been focused on investigating vinyl sulfones against *Trypanosoma brucei* species and other parasitic diseases.

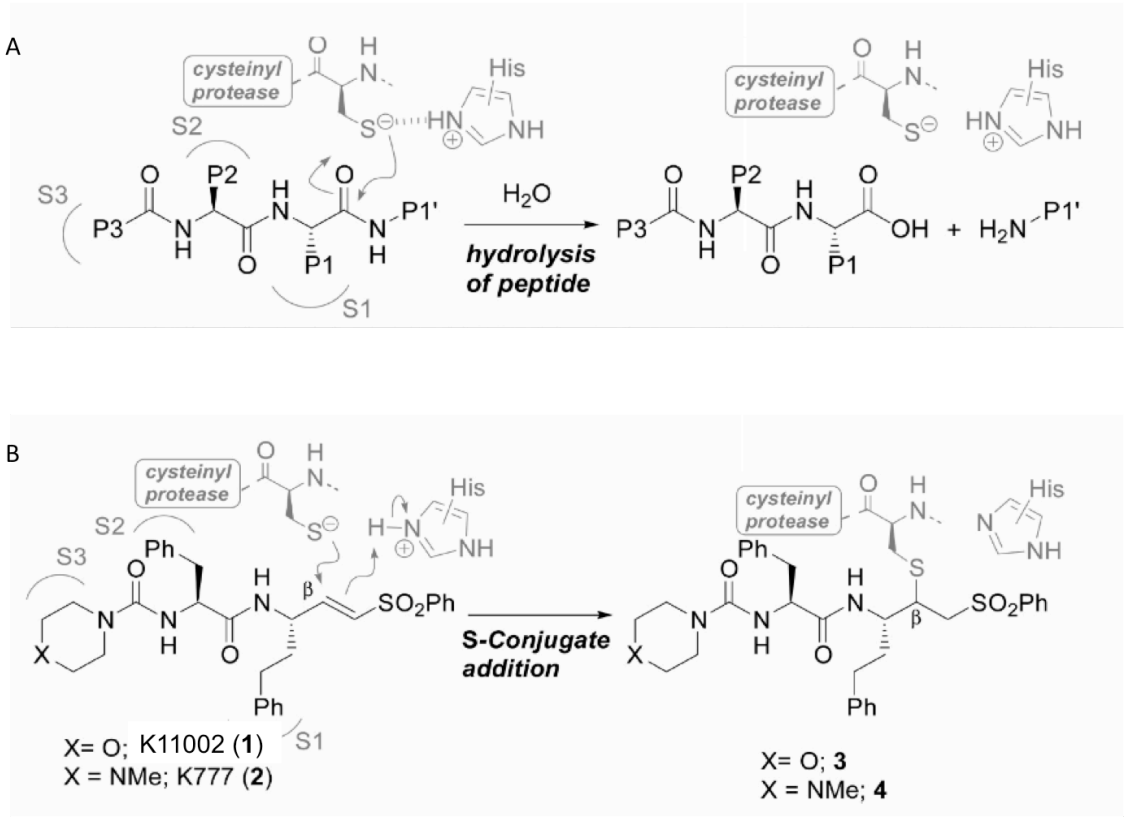

Figure 3.3 Cysteine protease-based peptide hydrolysis and the mechanism-based cysteine protease inhibition by vinyl sulfone. (A) Schematic representation of peptide bond hydrolysis relying on the nucleophilic cysteine residue within the active site of the cysteine protease. (B) The chemical structures of benchmark peptidic vinyl sulfone inhibitors (1) K11002 (Mu-Leu-Hph-VSPh) (2) K777 (*N*-Mpip-Phe-Hph-VSPh) and their interaction with parasitic cysteine proteases. Interactions with the moieties located at P1, P1', P2 and P3 are how these inhibitors usually exploit the S1, S1', S2 and S3 subsites on the enzyme. Images taken from Dunny et al (2013).

3.1.8 Vinyl sulfone inhibitors specific to parasitic diseases

Rosenthal and colleagues (1996) initially demonstrated that a peptidyl vinyl sulfone (morpholine-leucine-homophenylalanine-vinyl sulfone-phenyl, Mu-Leu-Hph-VSPh) was a potent inhibitor of falcipain, the major cysteine protease found in *Plasmodium falciparum*. When administered in a murine model of malaria, this VS compound markedly delayed the progression of malaria and cured about 40% of mice when they were treated orally twice a day for four days (Olson et al. 1999).

McKerrow et al. (1998) reported that dipeptide vinyl sulfone K777 (a.k.a K11777, *N*-Mpip-Phe-Hph-VSPh) when administered in a murine model of Chagas' disease (American sleeping sickness) rescued mice from lethal *Trypanosoma cruz*i infection as a result of the inhibition of the major cysteine protease, cruzain. Simultaneously Roush, McKerrow and co-workers designed, synthesized and screened a range of vinyl sulfones, sulfonamides and sulfonate ester K777 analogues as cruzain inhibitors (Roush et al. 1998; Roush et al. 2001; Brinen et al. 2000). Enzyme inhibition studies indicated that members of the sulfonamide family were potent, irreversible cysteine protease inhibitors and in certain cases active in tissue culture *T. cruzi* assays (Roush et al. 2001). It was subsequently demonstrated that K777, protected Beagle dogs from cardiac damage during *T. cruzi* infection (Barr et al. 2005). Results of a preclinical trial demonstrated K777 to be non-mutagenic, well tolerated, and efficacious in models of acute and chronic Chagas' disease in both mice and dogs (Kerr et al. 2009). Since 2007, FDA approval has been sought to allow K777 to enter phase I trials in humans (Kerr et al. 2009).

3.1.9 Investigations of vinyl sulfones against *T. brucei* cysteine protease

Troeberg et al reported investigations on the effects of various irreversible cysteine protease inhibitors, including vinyl sulfones, peptidyl chloromethylketones, diazomethylketones, and fluoromethylketones, on the major *T. b. brucei* lysosomal cysteine protease, brucipain, and cultured BSF (Troeberg et al. 1999). Methylpiperazine urea-Phe-homoPhe VS was identified as the most effective trypanocidal agent, killing 50% of test populations at a working concentration of 0.11 μM. Since then, only one example of a lysine–vinyl sulfone and one example of an arginine–vinyl sulfone based (K777 analogue) cysteine protease inhibitors have been reported against Trypanosomes (Troeberg et al. 1999; Chen et al. 2010). While very recently, it was shown by Steverding (2015) that the anti-HAT drug eflornithine had increased trypanocidal effect (syngergistic effect) when used in combination with K777 against *T. b. brucei* cultured *in vitro*.

As mentioned, dipeptide vinyl sulfones are an efficacious, biologically active scaffold upon which irreversible inhibitor design can be based (Potashman & Duggan 2009; Singh et al. 2011). These compounds, at least in part (Choy et al., 2013; Engel et al., 1998), mediate biological effects via disruption of lysosomal parasitic cysteinyl protease activity (McKerrow, Engel & Caffrey, 1999) and several X-ray crystal structures are available indicating how the thiophilic vinyl sulfone entity forms a covalent bond with the catalytically active cysteine residue within the binding pocket of the protease (see Figure 3.3) (Kerr et al. 2010).

3.2 Results

3.2.1 1st generation of vinyl sulfone cysteine protease inhibitors against *T. b. brucei*

As the first approach to investigate the efficacy of various new therapeutic leads as anti-trypanosomal agents, a traditional drug discovery route was explored. Dr Paul Evans and his group in UCD reported the design, synthesis of a small library of lysine-containing dipeptide vinyl sulfones and the anti-trypanosomal properties of these compounds were investigated in a previous collaboration with our lab (Dunny et al. 2013). The design of the first series of compounds was inspired by the benchmark vinyl sulfone K777 developed by McKerrow and colleagues as a potential treatment for American sleeping sickness (Engel, Doyle, Hsieh, *et al.*, 1998; Barr, Warner, Kornreic, *et al.*, 2005; Doyle, Zhou, Engel, *et al.*, 2007). Trypanosomal activity was evaluated and peptidomimetics based on the known lead compound K777 was carried out, with the aim of improving the efficacy for the vinyl sulfones as trypanocidal agents. The biological evaluation of this library against *T. b. brucei* led to identification of the lysine-based compound, lysine sulfonamide (compound 29: trans-5S-(2′S-Benzyloxycarbonylamino-3′phenylpropanamido)-7-(phenylsulfonyl)hept-6-en-1-(1-naphthalene)-sulfonamide), see Figure 3.4. This lysine sulfonamide showed a higher trypanocidal activity *in vitro* compared to the benchmark K777 with IC_{50} values of 0.07 μM and 5.56 μM, respectively. Computational binding predictions also supported the i*n vitro* efficacy results (Dunny et al, 2013). Significantly, very low selectivity towards mammalian cell line HL-60 was reported (typically 2 orders of magnitude higher than the EC_{50} values recorded, Figure 3.4).

A

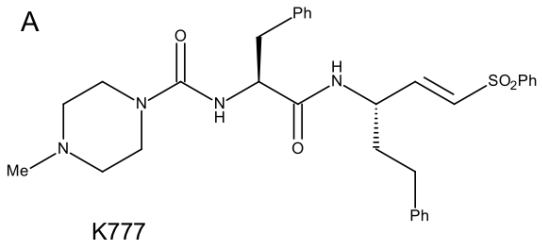

K777

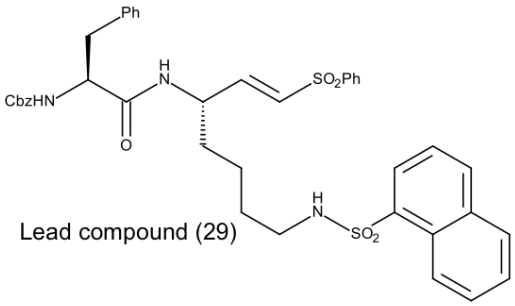

Lead compound (29)

B

Compound	*T.b.b* EC_{50} (μM)	Selectivity vs HL-60
K777	5.56	>9.9
Lead compound (29)	0.07	>785.7

Figure 3.4 K777 and lead compound (29). **(A)** Chemical structure of benchmark K777 and new lead compound 29, **(B)** table showing activity against *T. b. brucei* and selectivity compared to HL-60 cell line. Figure adapted from Dunny *et al.* (2013).

3.2.2 Testing further generation of vinyl sulfones

To investigate if additional structural changes to the leading lysine-containing vinyl sulfones K777 and derivative 29 could increase trypanocidal activity, further generations of compounds were designed and synthesized by Dr Paul Evans and his group (Centre of Synthesis and Chemical Biology, UCD). The aim was to explore substrate-cysteinyl protease complementarity by determining the chemical group responsible for evoking parasite killing. Thus, a further series of vinyl sulfone derivatives 13-53 (see chemical structures in Appendix A1) were evaluated for their ability to disrupt the life cycle of trypanosomes in a whole-cell screen of *T. b. brucei* via using a standard Alamar Blue assay. The efficacy of the series was compared to compound 29 (also called derivative 20 here), which previously showed higher activity than benchmark K777 (Dunny et al. 2013), and a bulk of the cysteine protease inhibitors here were thus derived from compound 29. Parasites were exposed to a sufficiently wide compound concentration range (10 μM - 1 nM) and the effective concentration that killed 50% of trypanosome population was determined after 24 h drug treatment (IC_{50}). As expected, a dose-dependent effect on trypanosome viability was observed (Figure 3.5), with IC_{50} values ranging from 0.09 μM to > 10 μM (Table 3.1). Interestingly, the most active compound was derivative 25 with an IC_{50} of 0.093 μM, which compared favourably to compound 29, with an IC_{50} of 0.07 μM in previous publication (Dunny et al, 2013) and of IC_{50} of 0.7 μM when retested here as "derivative 20". Significantly, a further twelve derivatives 21, 24, 26-30, 32-34, 36, 37 all showed submicormolar IC_{50} values. The most potent vinyl sulfone derivatives (ones with submicromolar efficacies) were structurally the most similar to compound 29, with different inhibitor residues at P3 (position 3) in contact with the subsite binding pocket S3 of the cysteine protease enzyme.

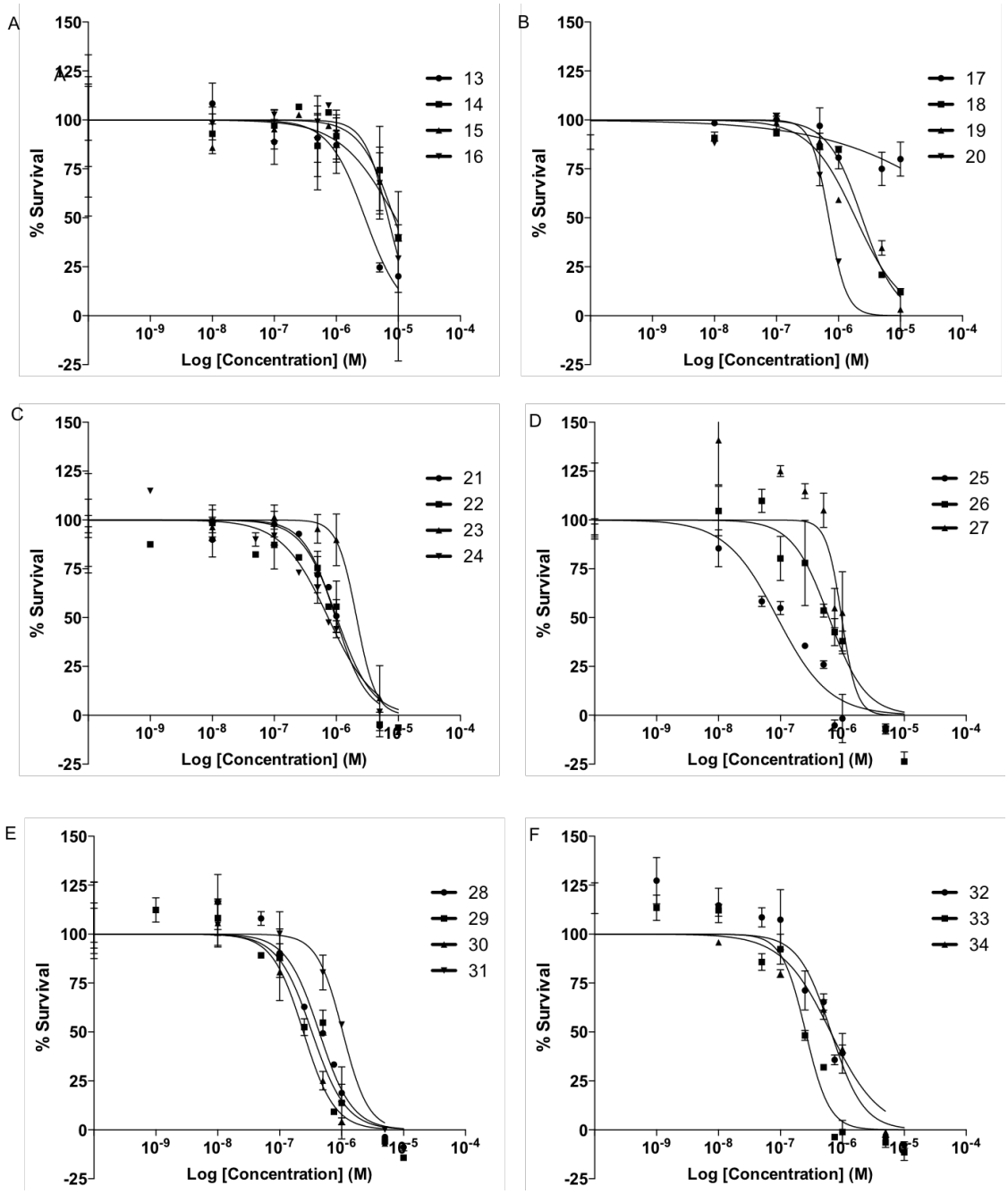
A
% Survival
Log [Concentration] (M)
13
14
15
16
B
% Survival
Log [Concentration] (M)
17
18
19
20
C
% Survival
Log [Concentration] (M)
21
22
23
24
D
% Survival
Log [Concentration] (M)
25
26
27
E
% Survival
Log [Concentration] (M)
28
29
30
31
F
% Survival
Log [Concentration] (M)
32
33
34

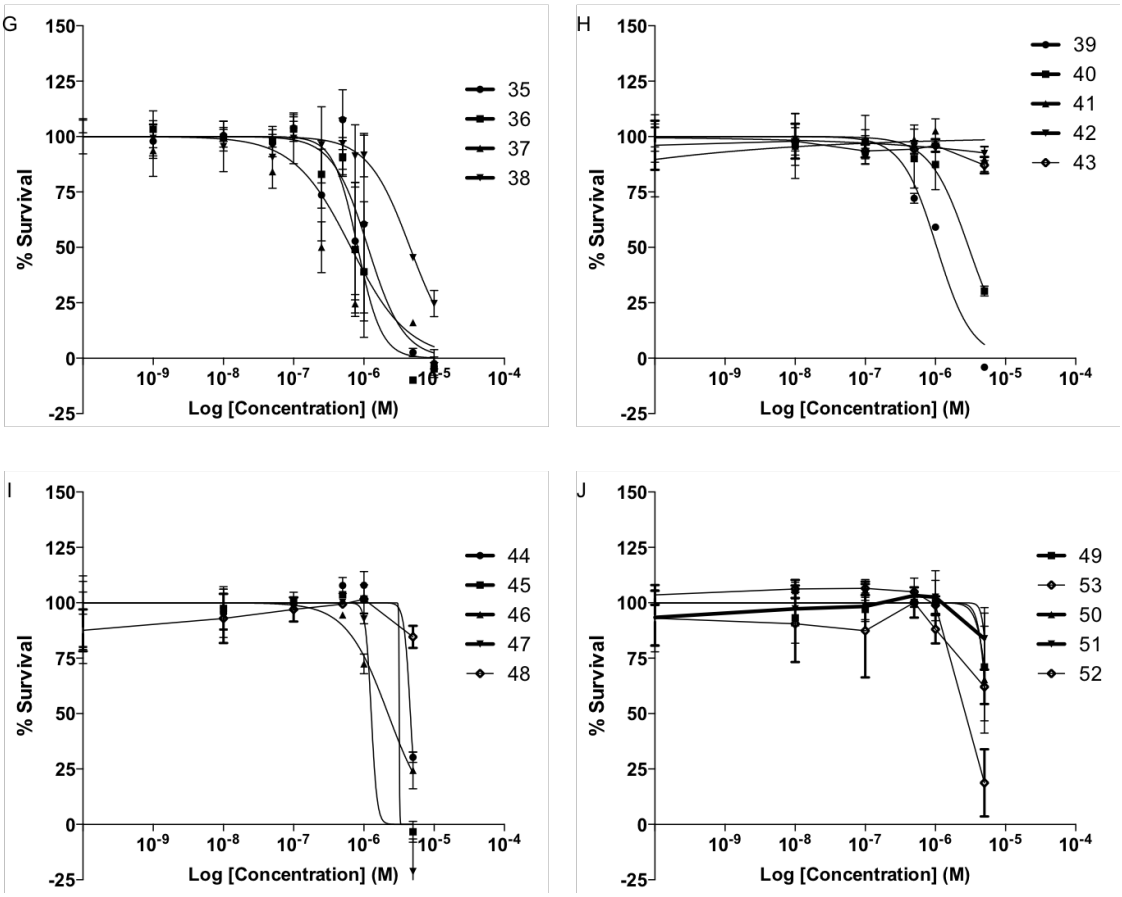

3.5 Response of *T. b. brucei* to a secondary series of vinyl sulfone compounds. The percentage of viable *T. b. brucei* bloodstream form (2×10^5 cells/mL) was determined with Alamar blue viability assay following a 24 h exposure to media containing serial dilutions of **(A-J)** a series of vinyl sulfones: entries 13-53. Percentage inhibition of the fluorescent signal was compared to controls minus inhibitor, with DMSO vehicle only. Error bars represent mean ±SEM of three independent experiments performed in triplicate wells. Dose-response curves were determined using GraphPad Prism software version 6.

Table 3.1. IC_{50} values of vinyl sulfone cysteine protease inhibitors against *T. b. brucei*

Entry	IC_{50} value (μM)[a]	SE log IC_{50}[b]
20 (Comp. 29)	0.7	0.104
13	2.635	0.138
14	8.547	0.093
15	9.031	0.190
16	6.855	0.043
17	>10	0.673
18	2.40	0.069
19	1.89	0.078
21	0.974	0.062
22	1.017	0.053
23	2.124	0.080
24	0.739	0.034
25	0.093	0.123
26	0.61	0.081
27	0.977	0.080
28	0.434	0.067
29	0.329	0.065
30	0.242	0.066
31	1.041	0.043
32	0.658	0.054
33	0.256	0.052
34	0.65	0.058
35	1.147	0.087
36	0.816	0.033
37	0.655	0.100
38	4.543	0.058
39	1.049	0.047
40	2.99	0.051
41	>10	ND
42	>10	ND
43	>10	ND
44	~4.6	ND
45	~3.191	ND
46	2.2	0.058
47	~1.27	ND
48	8.56	ND
49	6.11	ND
50	~5.47	ND
51	~5.782	ND
52	8.414	0.240
53	3.477	0.200

[a] Response of *T. b. brucei* (2×10^5 cells/mL) to exposure of varying concentrations of each compound determined by non-linear regression analysis of curve-fitting.[b] Standard errors (SE) were calculated based on the average of triplicate values from three independent experiments (ND = not determined).

Next, ten of the most active vinyl sulfones were investigated for their activity against a human cell line. Compounds 24-28, 29-34 were evaluated for their ability to kill human embryonic kidney cells (HEK293T) in a whole-cell screen via a standard Alamar Blue assay. Testing was done at a sufficiently wide concentration range (35 μM - 48 nM) to determine the effective concentration that killed 50% of mammalian cell population within the 46-48 h drug exposure (IC_{50}). The compounds exhibited a >2-fold selective inhibition of parasite versus mammalian cell (HEK293T cell line) proliferation *in vitro* (Table 3.2 & Figure 3.6). Across the compounds tested, none of them showed a significant effect on HEK293T cells and thus show their selective inhibition towards trypanosomal cysteine protease.

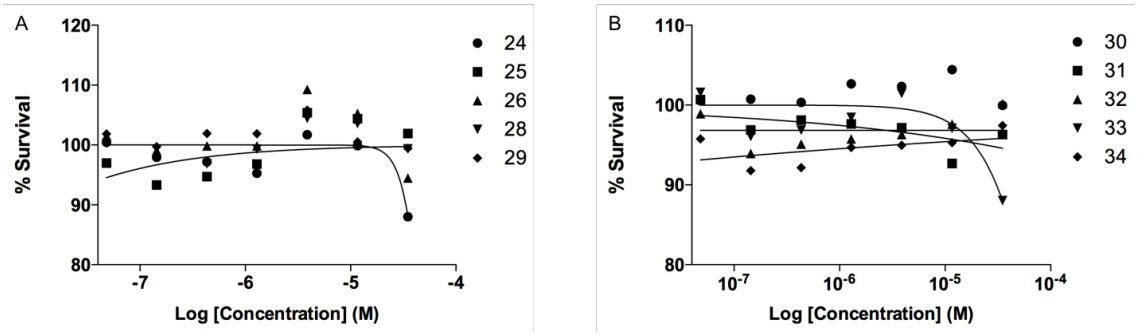

3.6 Response of HEK293T to secondary series of vinyl sulfone compounds. The percentage of viable HEK293T (2.3×10^5 cells/mL) was determined with Alamar blue viability assay following a 46 – 48 h exposure to media containing serial dilutions of a series of vinyl sulfones: (A) derivatives 24-26, (B) derivatives 28-30. Percentage inhibition of the fluorescent signal was compared to controls with DMSO vehicle only. Error bars represent mean ±SD of two independent experiments performed with triplicate wells, n = 2. Dose-response curves were determined using GraphPad Prism software version 6.

Table 3.2 IC_{50} values of vinyl sulfone cysteine protease inhibitors against HEK293T

Entry	IC_{50} value (μM)	SE log IC_{50}
24	54.81	1.056
25	ND	-
26	ND	-
28	ND	-
29	ND	-
30	ND	-
31	ND	-
32	ND	-
33	126.8	0.377
34	ND	-

ND = not determined.

3.2.3 Visualisation of the intracellular location of vinyl sulfone cysteine protease inhibitor

Previous work done by Troeberg *et al.* showed that the major intracellular target of vinyl sulfone compound (Methylpiperazine urea-Phe-homoPhe-VS) in *T. brucei* was trypanopain-Tb, the more abundant, cathepsin L-like, lysosomal cysteine protease (Troeberg et al. 1999). Targeting of trypanopain-Tb was demonstrated by incubation and binding of biotinylated (labelled) vinyl sulfone derivatives with live and/or lysed *T. b. brucei*. Additionally, a novel computational study showed vinyl sulfone compound 29 exhibited the same key hydrogen-bonding interactions with both TbCatB and rhodesain as observed with K777, correlating binding preference of both trypanosome cysteine proteases with whole-cell trypanocidal activity (Dunny et al. 2013). Interestingly, it has been shown through immunoelectron microscopy detection that localisation of the major cysteine protease of *T. brucei* (rhodesain) is in the lysosome (Caffrey et al. 2001). Consequently, it was investigated in this study whether the target for the vinyl sulfone series, represented by derivate 19 (IC_{50} = 3.5 μM, Doherty et al. 2014), localized in a similar manner in the lysosome and thus directly correlates to parasite death. Since derivative 19 contained a dansyl functional group and fluorescence of the dansyl

functional group has been previously reported (Kim et al. 2013), it served in this assay to image and identify the location of the VS target in *T. b. brucei* cells undergoing cell death. Lysotracker red which directly binds to acidic organelles (lysosomes), was also utilized to image and identify the location of *T. b. brucei* lysosomes. As predicted, the subcellular localization of the target for derivative **19** was in the lysosome of *T. b. brucei,* same place as the lysotracker, clearly illustrated in Figure 3.7 B. However, localisation of derivative **19** also occurred in the nucleus and kinetoplast, which may suggest additional, yet unidentified target(s). Furthermore, morphological effects following 24 h treatment with derivative 19 included flagellar pocket swelling.

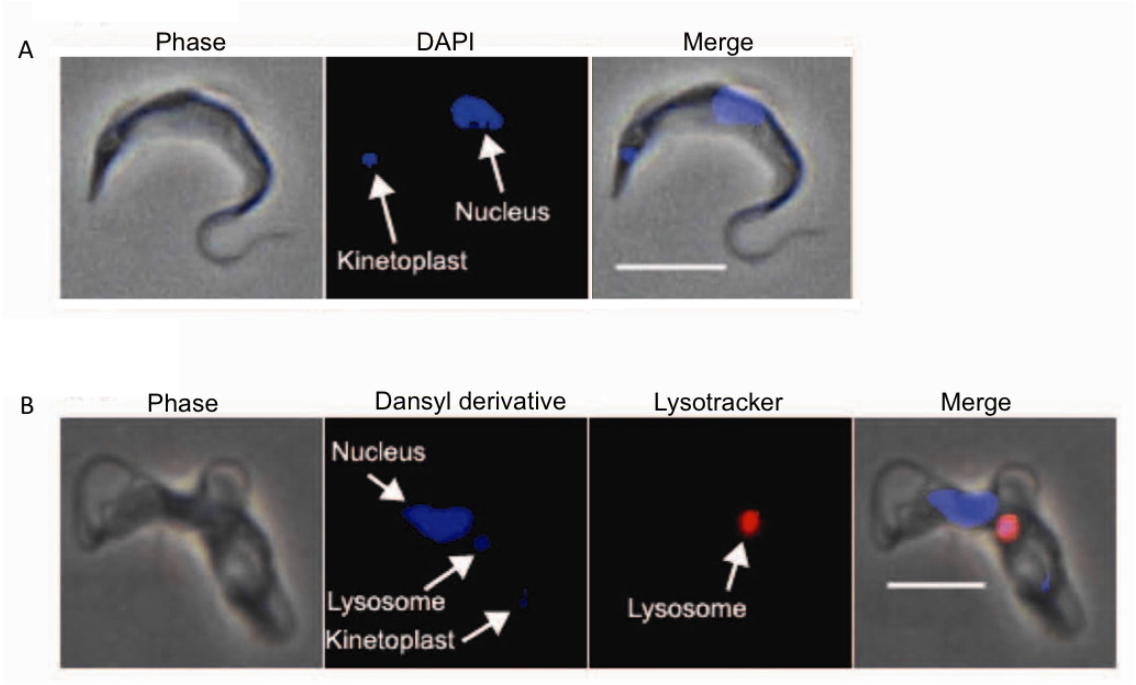

Figure 3.7 Location of cysteine protease inhibitor intracellular target. Representative images of *T. b. brucei* fixed after 24 h: **(A)** untreated cells stained with DAPI, **(B)** following treatment with derivative **19 (with dansyl functional group)** and LysoTracker, but no DAPI. Images were captured with Ziess Axiovert 100 fluorescence microscope equipped with an AxioCam HRc camera. LysoTracker Red DND-99 – red, derivative **19** – blue. Scale bar = 5 μm.

3.3 Discussion

3.3.1 Vinyl sulfone findings

The aim of the current chapter was to investigate the efficacy of a series of cysteine protease inhibitors, designed to be structurally similar to the benchmark K777 and compound 29, as trypanocidal agents. Interestingly, the most potent vinyl sulfone derivatives (21, 24-30, 32-34, 36, 37, see Table 3.1) were all analogues to compound 29 (derivate 20 here), with the presence of different inhibitor residues at P3 (position 3) in contact with the subsite binding pocket S3 of the cysteine protease enzyme (Figure 3.8). The different substrate binding domains of parasite cysteine protease can be seen in Figure 3.3, as earlier described in the introduction. To properly function, proteases must preferentially cleave their target substrates in the presence of other proteins. While many factors impact protease substrate selection, one of the key aspects is the complementary nature of the enzyme-active site with the residues surrounding the cleaved bond in the substrate. As such, determination of the residues that comprise the preferred cleavage site of a protease provides critical information regarding substrate selection (Gosalia et al., 2005) and may provide structural insights to facilitate the design or modification of other small inhibitor scaffolds. Optimum activity out of the series of P3 modified phenylalanine-lysine containing vinyl sulfones with a wide range of structurally and electronically diverse analogues of the most active compound (29) was observed for compounds with a lipophilic aromatic entity linked to the main vinyl sulfone dipeptide backbone with an H-bond donor.

Importantly the most trypanocidal vinyl sulfone derivatives in this study showed none or minimal toxicity towards mammalian cell culture (Table 3.2), as previously shown with similar vinyl sulfones (Dunny et al. 2013).

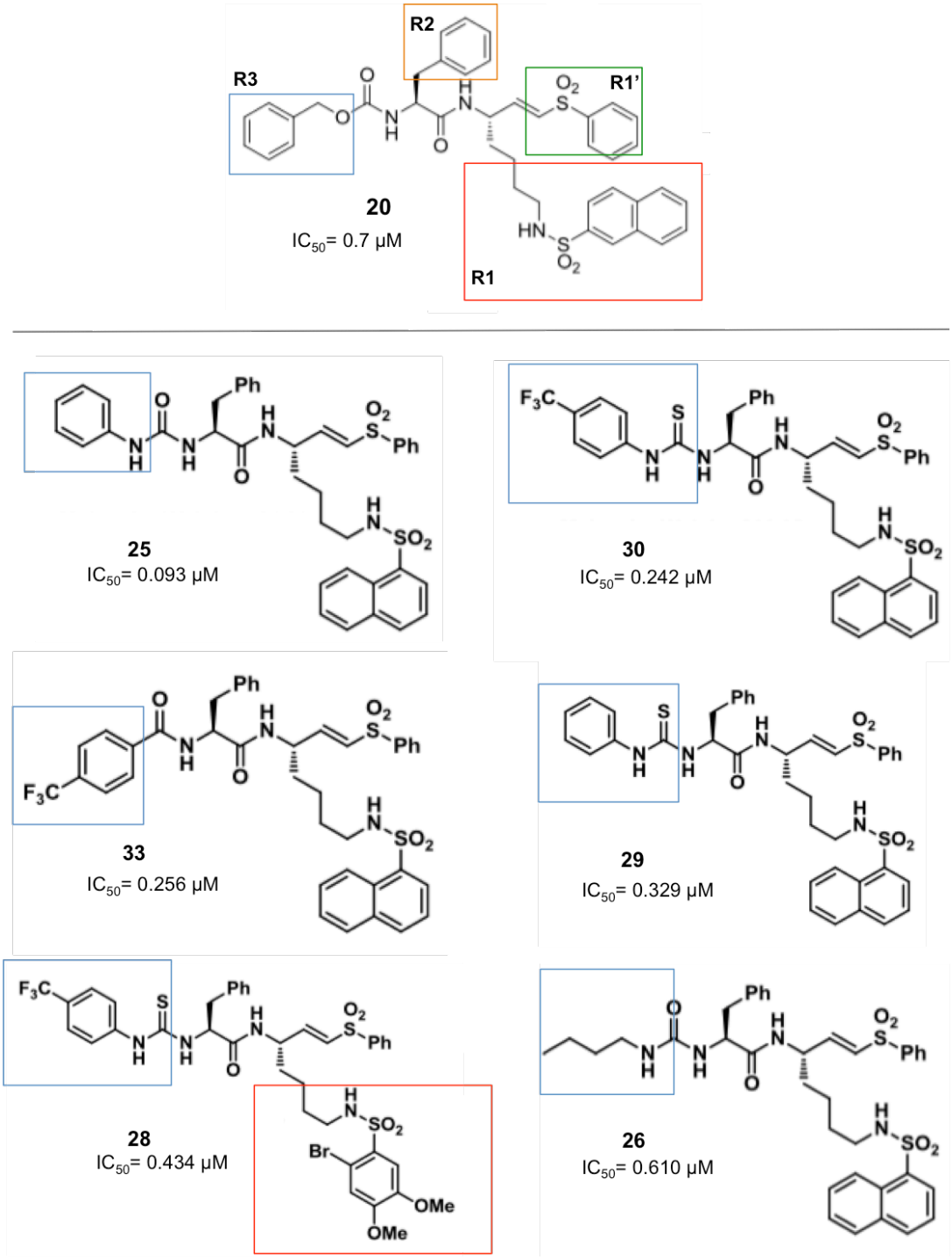

Figure 3.8 Top 6 most potent vinyl sulfone derivatives. These vinyl sulfone derivatives were structurally the most similar to compound 29 (a.k.a. derivate 20 here), with the difference of synthesis/design of inhibitor residues at P3 (position 3) in contact with the subsite binding pocket S3 (outlined in blue) of the cysteine protease enzyme. Outlined in yellow = residue at P2, green = residue at P1', and red = residue at P1).

3.3.2 Localisation of vinyl sulfone-bound targets to lysosome and other compartments

It was expected that fluorescent derivative 19 cysteine protease inhibitor would co-localise with the LysoTracker dye (Figure 3.7B) as both trypanopain-Tb and TbCatB have previously been shown to appear in lysosomal vesicles (Caffrey et al. 2001). Previously, the effects of VS on parasite morphology have been reported to appear consistent with a defect in endocytic traffic, as seen from an enlargement of the flagellar pocket ('big-eye' phenotype) (Dunny et al, 2013), which is consistent with the morphological changes (enlarged flagellar pocket) following treatment with derivative 19 (Figure 3.7B). This supports the idea that this class of VS compounds inhibit the trypanosomal cysteine proteases located in the lysosome and thus directly correlates to cell death. However, localisation of derivative 19 also occurred in the nucleus and kinetoplast, which may suggest additional, yet unidentified target(s), either as a result of binding of the dansyl moiety, or solely due to the vinyl sulfone scaffold. There are no indications to what these targets might be.

3.3.3 Conclusion

Cysteine proteases play a key role in parasitic infections (digestion of host proteins for nutrition, and inactivation of host immune defence mediators) and their inhibitors have shown little or no toxicity to the mammalian host (McKerrow et al. 1999). This lack of toxicity is in part due to the fact that the parasite targets are in a more vulnerable location within the mammalian host. For example, *T. brucei* is a bloodstream organism and is therefore more easily targeted than the homologous host proteases. Additionally, parasites may selectively take up small molecule inhibitors more readily compared to the mammalian host cells. Thus vinyl sulfones present an attractive anti-HAT potential.

Since a lot of work needs to be done to make vinyl sulfone dipeptides become drug candidates on their own, using them in combination with current treatments could be a faster route to drug/treatment development. Recent research by Steverding has shown that in fact K777 in combination with the anti-HAT drug eflornithine has a synergistic effect against BSF *T.b.b.* when tested *in vitr*o (Steverding 2015). When tested in combination with all the other current HAT treatments, however, K777 showed antagonistic effects with suramin, pentamidine and melarsoprol. The author suggests

that the underlying mechanism for synergy with only eflornithine is facilitated by a reduction in thiol levels, as opposed to for example suramin whose trypanocidal action relies on the activity of the thiol-dependent TbCATL (Alsford et al., 2012). Further investigations are required in order to establish the *in vivo* efficacy of the K777/eflornithine combination as this was only and *in vitro* study, but these findings suggest that the combination of K777 and eflornithine could be developed into an alternative treatment of HAT. It would be very interesting to investigate if other, more potent, vinyl sulfones would have a similar synergistic effect, allowing for lower eflornithine concentrations and/or treatment lengths.

CHAPTER 4. Results: Investigating anti-trypanosomal properties of repurposed drug candidates

4.1 Introduction: computational drug repurposing in drug discovery

4.1.1 New approach to drug discovery: drug repurposing

The development of a drug is an expensive and time-consuming process; going from basic research, disease assessment, lead discovery to clinical trials and production can take on average up to 14 years (Figure 4.1). An alternative and more commercially viable approach to speed up the traditional drug discovery process is to look for new uses for drugs already approved for other indications, termed drug repositioning (also called drug repurposing, drug re-profiling, drug re-tasking, therapeutic switching). Drug repurposing falls under the Food & Drug Administrations (FDAs) 505(b)(2) approval pathway (Aronson 2007; Bisson 2012; Oprea & Mestres 2012). Adopting a drug repositioning methodology has numerous benefits: 1) low development costs (160 million times less than current new chemical entity/ new molecular entity (NCE/NME) development), 2) safety issues are known (usually responsible for 30% of all drug candidate clinical failures, 3) return on investment potential is excellent (it takes an average $8.4 million to launch a successful repositioned drug vs approximately $1.3 billion per NCE/NME), 4) high out-licensing potential. Overall, drug repositioning has been shown to reduce traditional drug development timelines by 3-5 years (Ashburn & Thor 2004). Repositioned drugs generally are those marketed drugs 1) still under patent, 2) where patents have expired or 3) that have failed to reach clinical or regulatory endpoints.

Several examples of repositioning in the field of neglected diseases are highlighted in Table 4.1, many of which were discovered serendipitously. To remove the serendipitous aspect, this rapidly developing field is well suited to being driven by computational methods which can harness a plethora of data mining algorithms effectively generating and prioritising hypotheses for new indications for a drug candidate (Hurle et al. 2013).

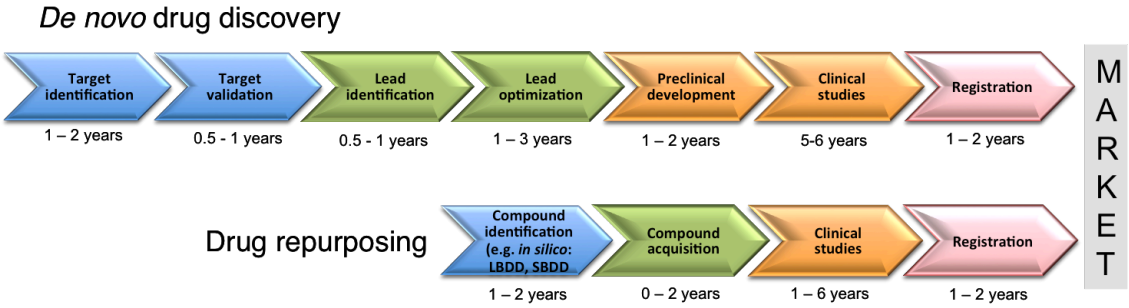

Figure 4.1 Comparison of de novo drug discovery timeline with drug repurposing timeline. The repurposing of old drugs or unsuccessful lead compounds by *in silico* approaches like ligand-based or structure-based virtual screening facilitates faster drug discovery for new indications (3-12 years) as opposed to *de novo* drug design (10-17 years) and presents a higher probability of success where safety profiles and pharmacokinetic parameters are already known. In particular, it is the process of lead discovery involving target identification and validation, hit identification, hit-to-lead process, and lead optimization, which is sped up often through computational screening means. Image adapted from Ashburn & Thor (2004).

Table 4.1 Examples of repositioned drugs for neglected diseases.

Molecule	Original indication	New indication	Refs
Paromomycin	Antibiotic	Visceral & Cutaneous Leishmaniasis	(Scott et al. 1992)
Miltefosine	Antineoplastic	Visceral & Cutaneous Leishmaniasis	(Kuhlencord et al. 1992)
Amphotericin B	Antifungal	Leishmaniasis	(Prata 1963)
Thalidomine	Morning sickness	Leprosy	(SHESKIN 1965)
Itraconazole	Antifungal	Chagas	(Apt et al. 2013)
Artemisinin	Antimalarial	Schistosomiasis	(Zhang et al. 2014)
Eflornithine	Unwanted facial hair	Human African Trypanosomiasis	(Sjoerdsma et al. 1984)
Astemizole	Antihistamine	Malaria	(Chong et al. 2006)
Cycloserine	Urinary tract infection	Tuberculosis	(Mitchell & Lester 1970)

4.1.2 Drug repurposing hit identification through computational screening: FTY720

In the previous chapter, a semi-rational approach was described whereby a library of vinyl sulfone protease inhibitors were screened against *in vitro* cultures of trypanosomes to carry out to the lead discovery part of its drug discovery pipeline. Even though the lead vinyl suflone was very potent, this drug discovery route may have associated risks and costs involved, mostly because safety profiles are not known. As an alternative approach, drug repurposing was investigated in this chapter to identify new chemical starting points as potential anti-trypanosomal compounds, especially for treating the second stage of trypanosomiasis.

Standard *in silico* drug design cycle consists of docking, scoring and ranking initial hits based on their steric and electrostatic interactions with the target site, which is commonly referred to as virtual screening (Prada-Gracia & Huerta-Yépez 2016). In the absence of structural information of a receptor and when one or more bioactive compounds are available, as was the case here, ligand-based virtual prescreening was applied (Figure 4.2). This prescreening method was carried out by similarity search. The basic principle behind similarity searching is to screen databases for similar compounds to the backbone of the lead molecule (Prada-Gracia & Huerta-Yépez 2016), in this case, lead molecules were established anti-trypanosomal inhibitors. In other words, ligand-based virtual similarity screening is based on the common assumption that two compounds that display similar chemical properties or "backbones" are likely to exhibit similar biological effects than compounds that have dissimilar structures. The choice of molecular description to calculate this similarity is not trivial and can vary depending on the compound selection (Sheridan & Kearsley 2002; Roth 2005; Bender 2010). A variety of descriptors exist which can be divided into two large groups depending if they consider only the 2D structure (topology) of a molecule or if they include 3D information (Riniker & Landrum 2013). A standard and computationally efficient abstract representation of 2D features is called molecular fingerprints (Todeschini & Consonni 2008), where bits in a bit string can represent structural features. Fingerprints are compact and allow fast comparison of chemical structures (Riniker & Landrum 2013).

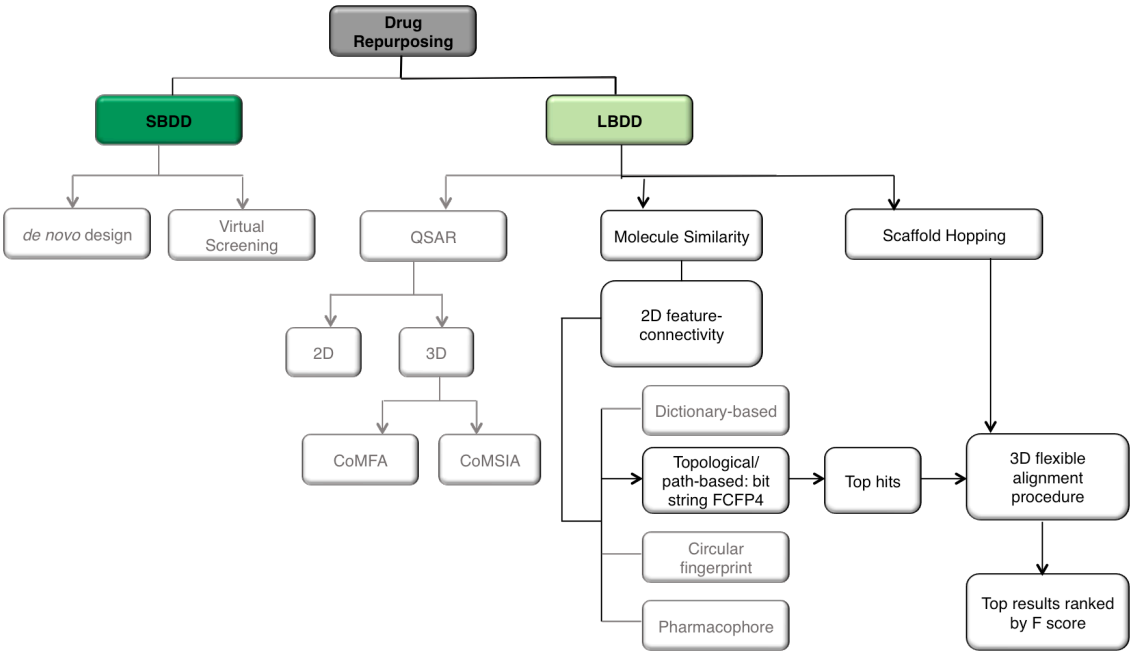

Figure 4.2 Drug discovery path showing hierarchical pathway. In the absence of structural information of a receptor and when one or more bioactive compounds are available, ligand-based virtual (LBDD) prescreening is applied. Similarity search is one such prescreening method. Adapted from Aparoy et al. (2012).

All ligand-based computational methods have their own advantages but also limitations and present significant challenges in terms of understanding their utility in the right context (Ritchie & McLay 2012; Liao et al. 2011). One way to overcome the limitations of individual methods is by exploring the different combination of approaches in a hierarchical manner (Knox et al. 2009; Zhang et al. 2013; Li et al. 2013). For the validity of any computational screening method, it must also satisfy the ability to identify known molecules from a series of unknowns. The approach taken in this study involved hierarchical computational drug repositioning where all known anti-trypanosomal inhibitors described to date in the literature were taken and initially used as templates for a series of 2D feature-connectivity bit string (FCFP4) fingerprint searches (Riniker & Landrum 2013) against an 'in-house' B^4 database previously created in the lab. The B^4 database was a manually curated database housing all drug products approved on the basis of safety and effectiveness by the Food and Drug Administration that have been described in the literature as having the ability to penetrate into the CNS.

Comparing the FCFP4 molecular fingerprints from the two compound databases resulted in finding compounds that displayed similar chemical backbones likely to exhibit similar biological effects: having the ability to pass the blood-brain barrier (important for treating the second stage of the disease) while also having anti-trypanosomal properties. To narrow down the hits and to prioritise drugs that had the most potential to act as anti-trypanocidal agents based on an overlap of molecular features, each top-ranked solution was re-evaluated for similarity to its template by an all-atom 3D flexible alignment procedure developed by Labute et al (Chan & Labute 2010; Labute et al. 2001). A prioritised list was generated based on this overlap of 3D molecular features.

Drug repurposing computational methods involve a combination of algorithms, which produce rankings (F-score) that do not correlate with one another and are hence orthogonal and considered to be ideal (Muchmore et al. 2008). Interestingly, the top four 3D flexible alignments found and ranked by F-scores by the combination of algorithms resulting in scaffold-hopping, seen in Figure 4.3, highlight common pharmacophore features correlating with drugs recently discovered as treatments for various parasitic diseases. Ranked in the top position, (A) bromocryptine has recently been shown to possess dose-dependent inhibitory activity against *Trypanosoma cruzi* and, interestingly, was also identified by computer-aided drug repurposing (Bellera et al. 2013). (B) rifabutin has been shown to be active against a related parasitic protozoan, *Cryptosporidium parvum*, and (C) etoposide, a topoisomerase inhibitor currently indicated as an anticancer agent, ranked in third position and has also been shown to possess anti-trypanosomal activity (Kulikowicz & Shapiro 2006; Shapiro & Showalter 1994; Shapiro 1994). The CNS penetrating drug (D) fingolimod/FTY720 (commercial name Gilenya) has not been reported in the literature as having been tested for its trypanocidal action at the beginning of this study and was thus chosen, along with its structural mimic sphingosine and sphingosine-1-phosphate, to be tested for its ability to firstly kill *T. brucei in vitro*. If active, it was hypothesised to have the potential to treat both stages of Human African Trypanosomiasis or Nagana.

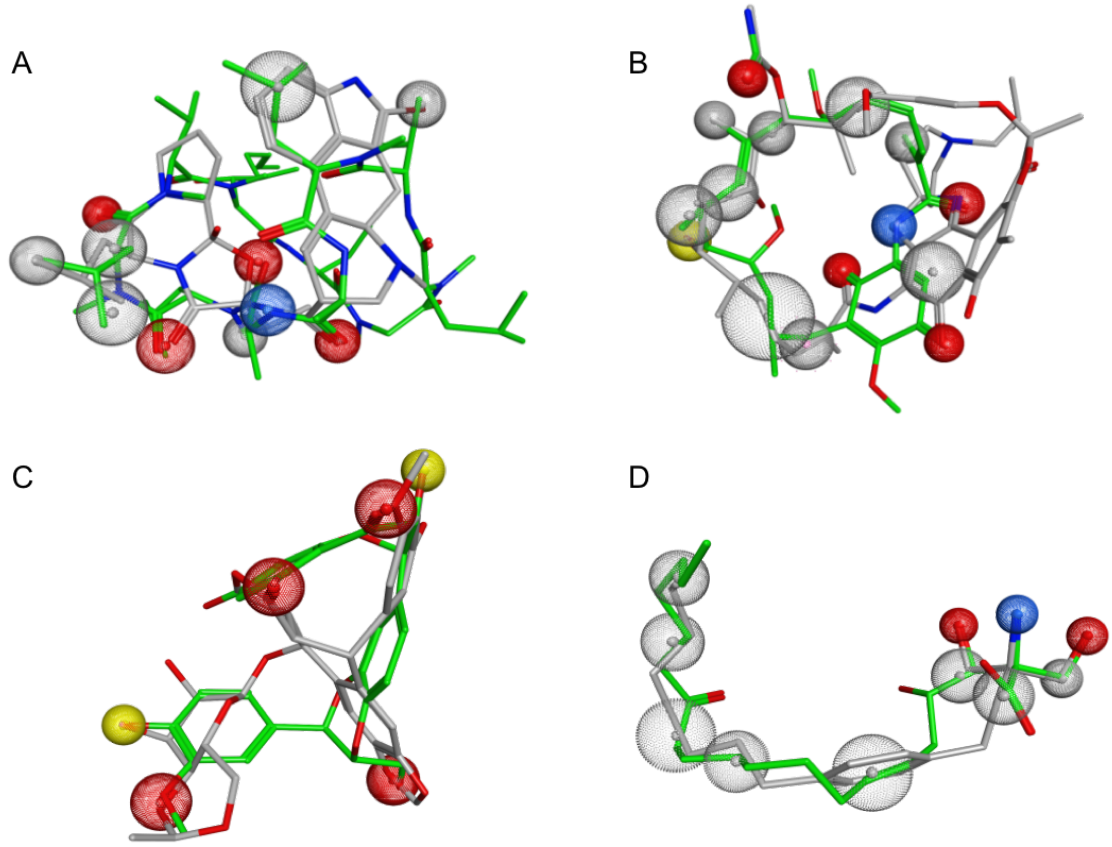

Figure 4.3 Top scoring anti-trypanosomal drugs revealed by a hierarchical computational drug repositioning approach. All known anti-trypanosomal inhibitors described to date in the literature were initially used as templates for 2D feature-connectivity bit string (FCFP4) fingerprint searches against an 'in-house' *B*[4] database of blood-brain barrier penetrating drugs. The most similar drug to each inhibitor was subsequently evaluated by an all-atom 3D flexible alignment procedure and a prioritised list was generated based on overlap of molecular features. Top four alignments highlighting common pharmacophore features – **(A)** cyclosporine and bromocriptine, **(B)** geldanamycin and rifabutin, **(C)** silybin and etoposide, **(D)** myriocin and **fingolimod**. Feature key: red=acceptor; blue=cation/donor; grey=hydrophobic; yellow=donor&acceptor.

4.1.3 Function of FTY720 & its structural mimic, sphingosine

It is important to note that fingolimod, currently approved as a treatment for relapsing forms of Multiple Sclerosis, is a synthetic structural analogue of myriocin (a fungal metabolite isolated from *Isaria sinclairii)* (Brinkmann et al. 2010; Chiba & Adachi 2012). Fingolimod is not only highly homologous in structure and function to myriocin, but also to sphingosine-1-phosphate (S1P) and its precursor D-sphingosine, see Figure 4.4 for structures (Chiba & Adachi 2012). Sphingosine and S1P are lipids part of the sphingolipid pathway naturally occurring in most living organisms.

FTY720 is phosphorylated *in vivo* by sphingosine kinase 2 (SPK2) to FTY720P, which acts as a functional agonist for a family of G protein-coupled receptors that recognize S1P (Bandhuvula et al. 2005). Evidence suggests that FTY720-phosphate-induced activation of S1P receptor type 1 (S1P1) is responsible for its mechanism of action for many of its effects, including inhibiting lymphocyte egress from secondary lymphoid organs, preventing them from contributing to an autoimmune reaction and helping to reduce the rate of relapses in relapsing-remitting multiple sclerosis, and preventing allograft rejection (Chiba & Adachi 2012). However, recently it has become evident that the action of FTY720 is more complex. Interestingly, it has been shown that FTY720 interferes with sphingolipid *de novo* biosynthesis in human cells, specifically, inhibiting ceramide synthases (by competitive inhibition of dihydrosphingosine) and modulating the intracellular balance of signaling sphingolipids, thus showing a secondary mechanism of action (Berdyshev et al. 2009), see Figure 4.5.

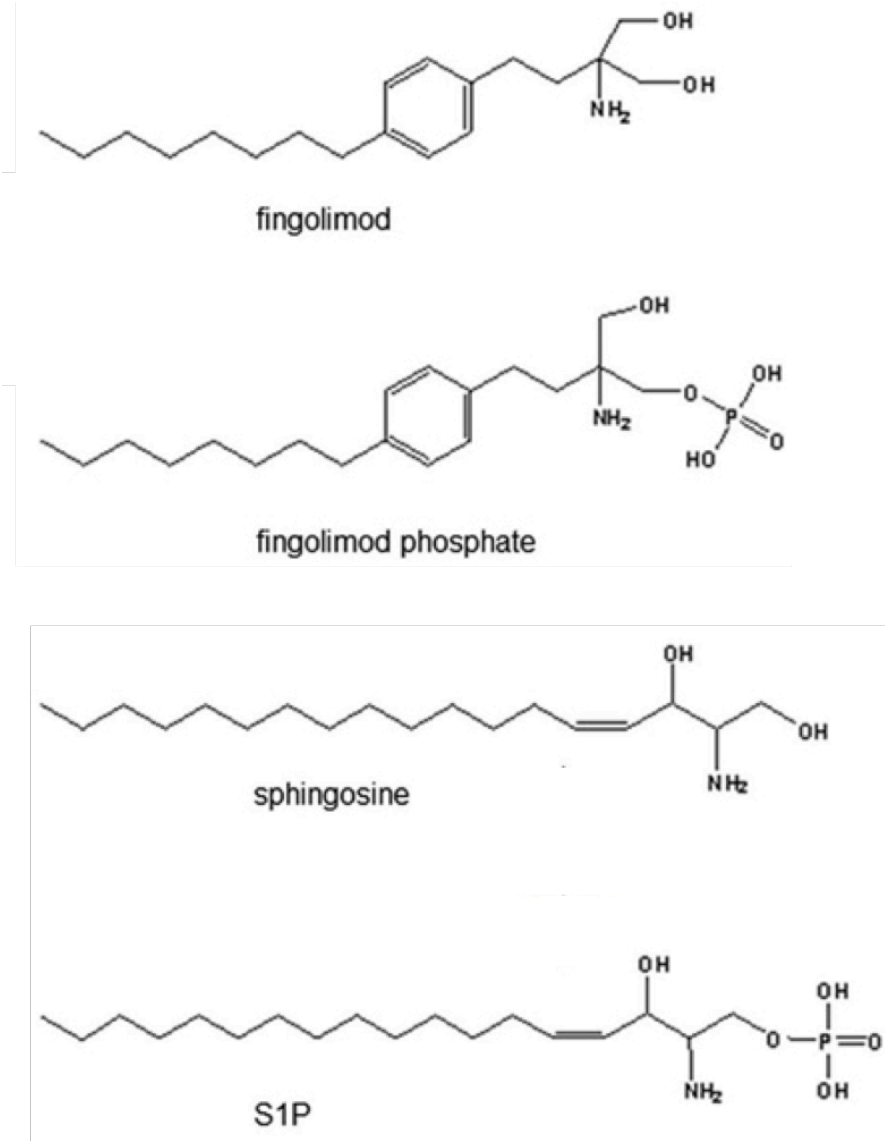

Figure 4.4 Structures of fingolimod, fingolimod phosphate, and their structural mimics sphingosine and sphingosine phosphate, respectively.

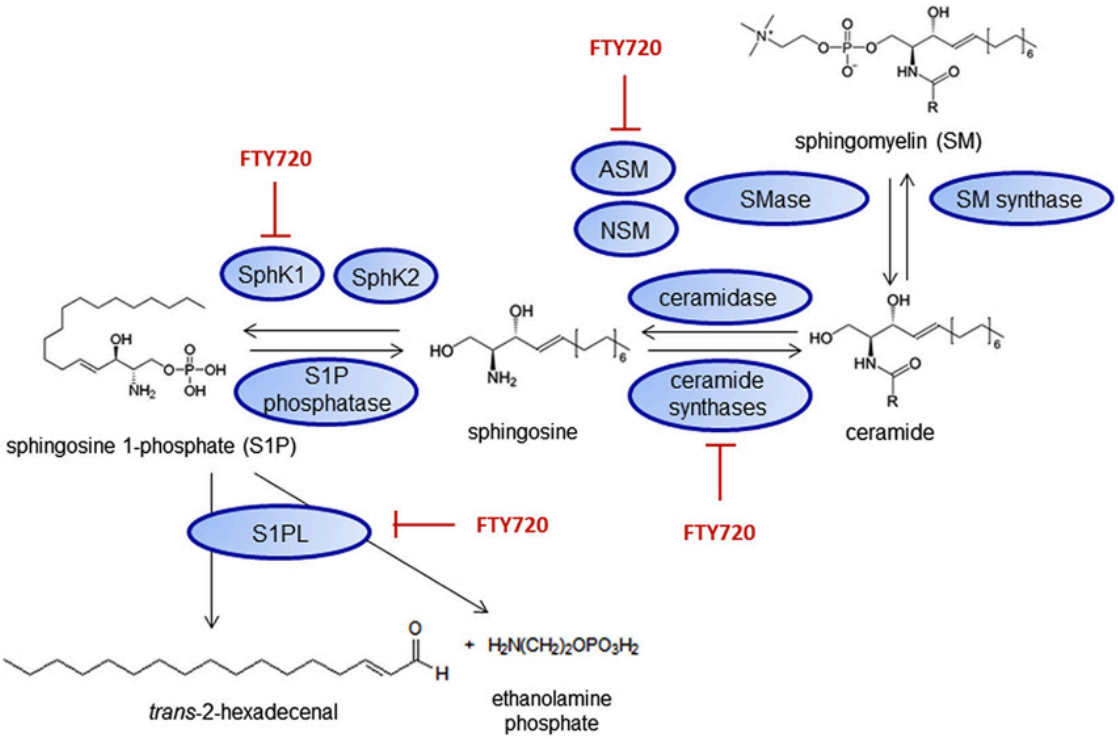

Figure 4.5 Fingolimod interacts with sphingolipid metabolizing enzymes. FTY720 has inhibitory effects on sphingosine kinase 1 (SphK1; Lim et al. 2011), sphingosine-1-phosphate lyase (SIPL; Bandhuvula et al. 2005), ceramide synthases (Berdyshev et al. 2009; Lahiri et al. 2009) and the acid sphingomyelinase (ASM; Dawson and Qin, 2011) have been shown. NSM—neutral sphingomyelinases. Schematic diagram taken from Brunkhorst et al. (2014).

As in eukaryotic cells, sphingolipids form an essential component of *T. brucei* membranes, and the *de novo* synthesis of sphingolipids is essential for parasite viability (Sutterwala et al. 2007). Sphingolipid biosynthesis is also unique in *T. brucei*, in contrast to the kinetoplastid parasites *Leishmania* (Kaneshiro et al. 1986) and *Trypanosoma cruzi* (Salto et al. 2003), which synthesize the higher-order sphingolipid, inositol phosphorylceramide (IPC). IPC is not detected in bloodstream *T. brucei* parasites (Sutterwala et al. 2007; Patnaik et al. 1993). In bloodstream *T. brucei*, the predominant higher-order sphingolipids are sphingomyelin (SM), which is normally found in mammals, and ethanolamine phosphorylceramide (EPC) (Sutterwala et al. 2008). The unique sphingolipid biosynthesis pathway in *T. brucei* has led to the pathway being proposed as a potential drug target in the parasite. Since sphingosine and sphingosine-1-phosphate are part of the sphingolipid biosynthesis pathway, it was hypothesized that both structurally similar FTY720 and FTY720P may have an effect on this pathway and thus, trypanosome viability.

4.1.4 Further drug repurposing hit identification: liposomal amphotericin B & SPK-843

A different semi-rational approach was taken yet again to further explore other potential HAT treatments. It has been described that *T. brucei, T. cruzi*, and *Leishmania major* parasites have similar biology and genomic sequence, suggesting that all three diseases could be cured with drug(s) modulating the activity of a conserved parasite target (El-Sayed et al. 2005). Evidence of promising drug leads capable of killing multiple protozoan parasites include: targeting the kinetoplastid proteasome with a selective inhibitor (GNF6702) effectively killing the causative agents of sleeping sickness, along with Chagas disease, leishmaniasis *in vivo* (Khare et al. 2016). As well as, targeting parasite cysteine proteases with a selective inhibitor (K777 vinyl sulfone) effectively killing *T. cruzi in vivo* (Engel et al. 1998), and *T. brucei in vitro* (Dunny et al. 2013), described in the previous chapter. With this idea in mind, a rational literature search was performed utilizing DNDi website to see what compound leads were under clinical investigation for similar parasitic diseases. This search resulted in amphotericin B (AmpB) and its lipid formulation (LAMB, AmBisome®) as a potential candidate to test against *T. b. brucei*.

Members of the *Trypanosomatidae* family, like other eukaryotic microorganisms such as fungi, require the sterols ergosterol and 24-methyl sterols for parasitic growth and viability (de Souza & Rodrigues 2009). In contrast, mammalian cells utilise cholesterol rather than ergosterol or 24-methyl sterols in their membranes. It therefore follows that a molecule with the ability to interfere with ergosterol synthesis or use would have the potential to cause parasite growth retardation or death. Importantly, AmpB has been shown to be ~500 times more selective for ergosterol than cholesterol (Golan et al. 2011) leading to its use as a first-line therapy in the US in its lipid formulation (AmBisome®) for the treatment of visceral leishmaniasis caused by *Leishmania donovani*. In fact, single-dose treatment with AmBisome® has shown a 91% cure rate in India but is still considered too expensive for general treatment with the cost per treatment course being $200 (Meheus et al. 2010; Sundar & Chakravarty 2012). Visceral leishmaniasis is an ideal indication for the use of antifungal therapies and due to the high efficacy and safety in treating visceral leishmaniasis patients it was hypothesized that AmpB would be a good potential candidate for the treatment of Trypanosomiasis.

Next, to locate compounds similar to amphotericin B, a semi-rational approach was taken. SureChEMBL, a publicly available large-scale resource containing compounds extracted from the full text, images and attachments of patent documents (Papadatos et al. 2016), was employed. The structure of amphotericin B (see Figure 4.5) was drawn and evaluated against the patent literature through the image-mining pipeline. The one patent extracted that was similar in structure resulted in SPK-843 (Figure 4.5), an antifungal agent.

SPK-843 is a new polyene antifungal, which is a water-soluble diascorbate salt from SPA-S-752, an amide derivative of partricin A, produced by a mutant strain of *Streptomyces aureofaciens*. Polyenes are generally macrocyclic structures, which bear a series of conjugated double bonds (Figure 4.6) that are essential for their intrinsic activity. However, they are also as a result generally water insoluble and difficult to administration via systemic routes unless they are housed within complexes such as colloidal dispersions or liposomal complexes (Hartsel & Bolard 1996). SPK-843 is currently in Phase III clinical trials for the treatment of pulmonary mycosis (Pitman et al. 2011). Since both fungi and kinetoplastids exhibit a high concentration of ergosterol in their plasma membranes compared with mammals (de Souza & Rodrigues 2009) it was hypothesised that SPK-843 may act as a selective anti-kinetoplastid agent.

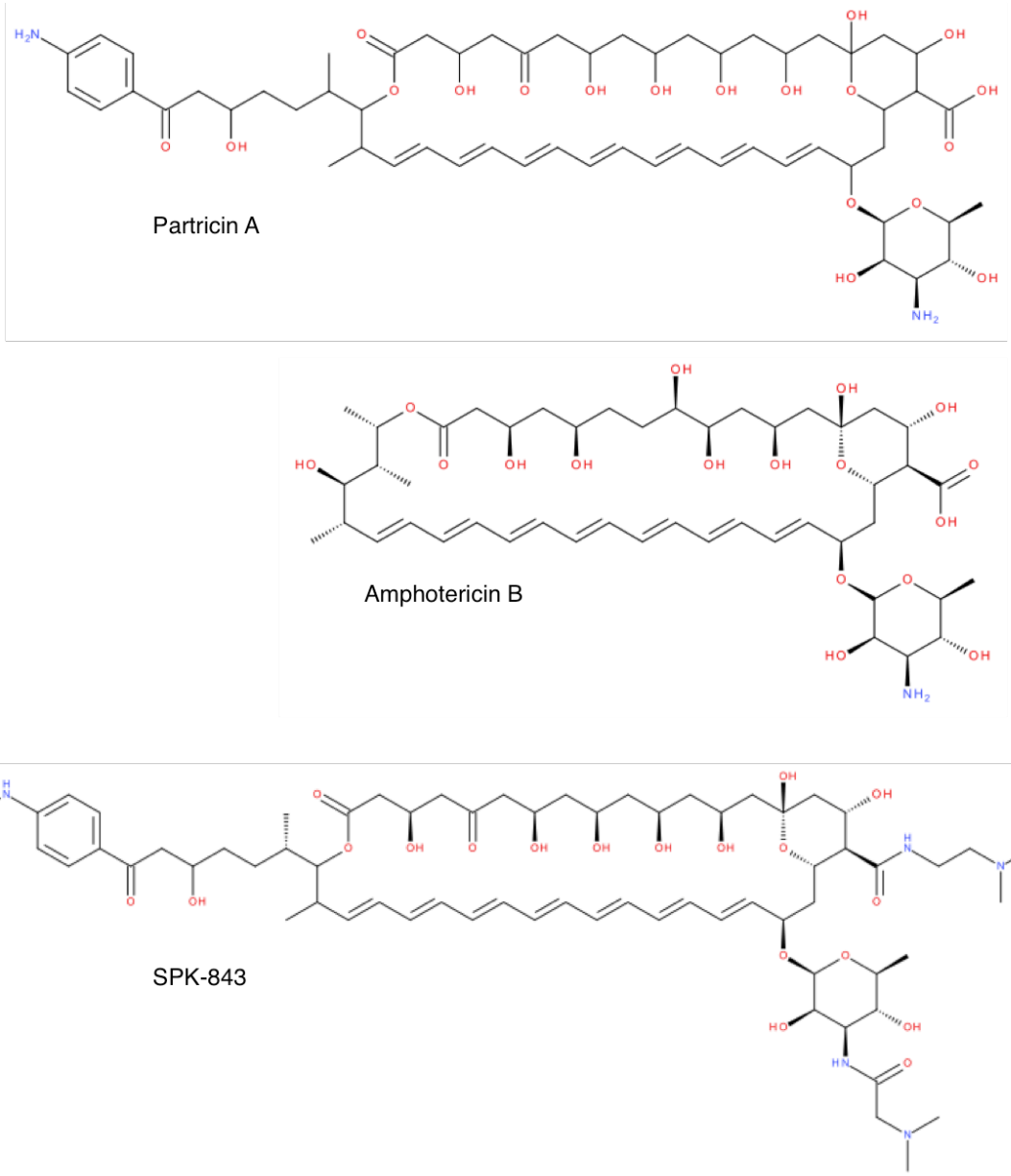

Figure 4.6 Structures of polyene macrolide antifungals partricin A, amphotericin B and SPK-843.

4.2 Results: Investigating effect of SPK843 & AmpB for the treatment of Trypanosomiasis

4.2.1 Determination of the trypanosomal action of SPK-843 & ampothericin B *in vitro*

Kinetoplastids exhibit a high concentration of ergosterol in their plasma membranes compared with mammals (de Souza & Rodrigues 2009) and we hypothesised that AmpB and SPK-843, may act as a selective anti-kinetoplastid agents due to their ergosterol binding nature. Firstly the activity of amphotericin B and SPK-843 was examined as an anti-trypanosomal monotherapy. Initially, the trypanosomal action of the antifungals amphotericin B and SPK-843 was investigated in *in vitro Trypanosoma brucei brucei* bloodstream form (BSF) cultures using the Alamar Blue viability assay. For the sake of comparison, cells were also exposed to the anti-HAT drug pentamidine. A sufficiently wide concentration range (33 μM→0.1 nM) of the test compounds was used to determine the effective concentration which killed 50% of trypanosoma population (IC_{50}) following 24 h of compound exposure. Interestingly, it was found that amphotericin B and SPK-843 inhibited *T. b. brucei* BSFs at low micromolar levels (1.38 μM and 1.53 μM, respectively) see Figure 4.7. As expected, pentamidine possessed a low submicromolar IC_{50} value. This result suggests that these lead antifungal compounds are effective trypanosomal agents, however, higher doses are required to elicit the same level of parasite cell death compared with the current first stage therapy, pentamidine.

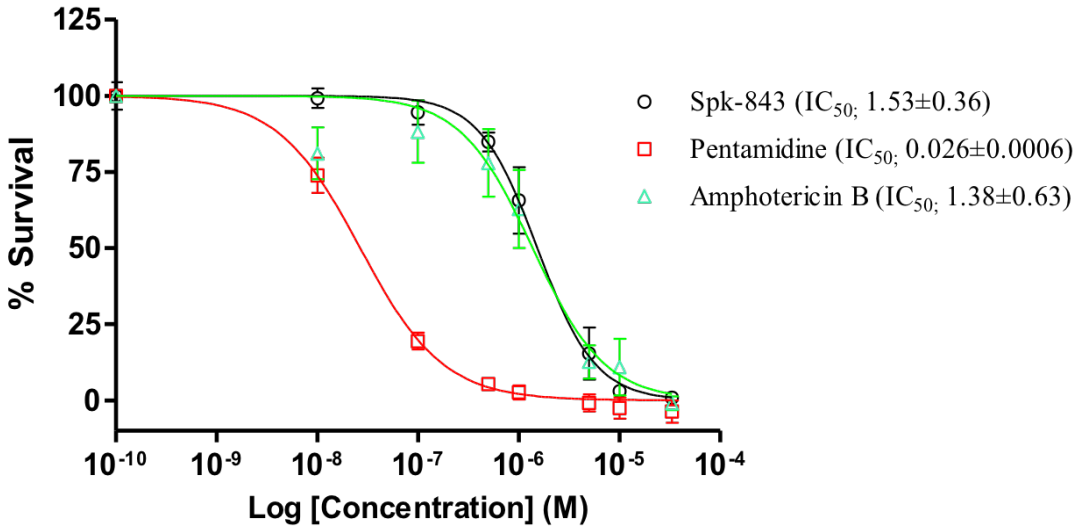

Figure 4.7 Anti-trypanosomal action of antifungals SPK-843 and amphotericin B compared with standard anti-trypanosomal treatment pentamidine. The percentage of viable *T. b. brucei* BSF (at 1 x 10^4 cells/mL) was determined with Alamar blue viability assay following a 24 h exposure to media containing serial dilutions of SPK-843, pentamidine, or amphotercin B. Error bars represent mean ±SD of two independent experiments performed in triplicate, n = 2. Dose-response curves and IC_{50} values were determined using GraphPad Prism software version 6 and are given as micromolar values. Antifungal compounds showed slightly lower activity compared to standard anti-typanosomal treatment, pentamidine.

4.2.2 Investigating time dependence of trypanosomal effects and recovery from transient exposure in *T. b. brucei*

In order to ascertain a further understanding of the pharmacodynamic parameters of the *in vitro* trypanosomal activity of SPK-843 and AmpB, time dose-dependent assays were performed. Cultured *T. b. brucei* BSF were subjected to continuous antifungal pressure over a 24 h time period and parasite ATP content was measured as a 'real-time' indicator of parasite viability (luciferase CellTiter-Glo assay) at several time-points (1, 2, 3, 5, 8, 24 h). Interestingly, a time-dependent loss of cell viability followed both SPK-843 and AmpB treatment, as reflected by the corresponding decline in IC_{50} values with prolonged incubation times (Figure 4.8c). Notably, onset of killing occurred more rapidly and at lower compound concentrations with SPK-843 than AmpB. IC_{50} values reached sub-micromolar concentrations (0.90 μM) following 5 h incubation with SPK-843, while the IC_{50} value for AmpB following 24 h exposure was still 25 fold higher (9.77 μM) compared to SPK-843 (0.393 μM). The trypanosomal activity of SPK-843 was similar to control drugs, suramin and pentamidine, after 24 h treatment as measured by the ATP assay; AmpB was not (Figure 4.8c). These results suggest that SPK-843 is a more efficacious trypanosomal agent compared to ampothericin B.

Next, to establish the time required to cause persistent or irreversible effects by SPK-843, *T. b. brucei* parasites were assessed for their ability to recover from transient exposure to test compound. Parasite cultures were exposed to SPK-843 or pentamidine for 1, 6, 12 or 24 h, after which, compounds were washed out and parasites were maintained in drug-free medium and assessed for viability at 72 h with Alamar Blue. Surprisingly, the trypanosomal effect of SPK-843 was moderately reversible when *T. b. brucei* were given time to recover following compound exposure. As observed by the IC_{50} values, the concentration of SPK-843 required to kill parasites was 5.6-fold higher following drug-washout experiments than when cells were not given time to recover without compound treatments (8.62 μM vs 1.53 μM, Figure 4.9 and Figure 4.7). In comparison, only a short period of exposure (1 h) to pentamidine was required to produce irreversible effects on *T. b. brucei* survival and the HAT treatment activity remained 33-fold lower after 24 h transient exposure than for SPK-843, 0.026 μM versus 8.62 μM, respectively (Figure 4.7 and Figure 4.9 b, c). These results may suggest that the *in vitro* potency of SPK-843 is more moderate than pentamidine and that a longer drug exposure of SPK-843 is necessary to achieve trypanosomal effects and clear infection.

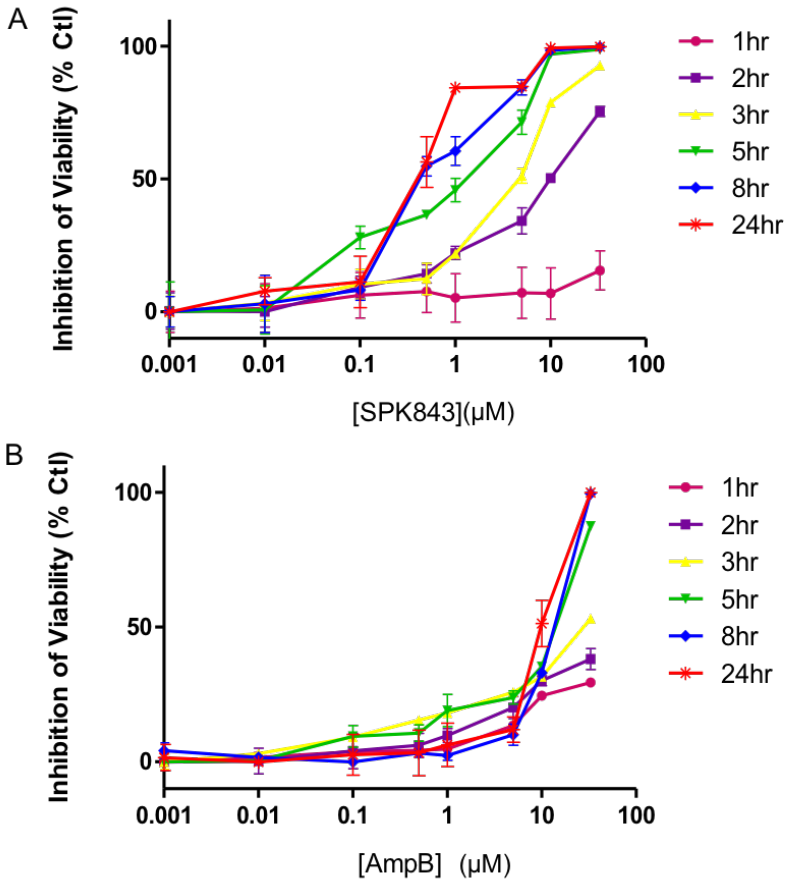

C

	1 h	2 h	3 h	5 h	8 h	24 h
(A) SPK-843	-	8.97	3.65	0.902	0.563	0.393
(B) AmpB	-	76.00	37.90	12.10	12.20	9.77
Suramin					>7*	0.200
Pentamidine					>1.6*	0.008

* Actual time point was 9 h

Figure 4.8 Time-course of *T. b. brucei* killing by SPK-843 and ampothericin B. Cultured BSF *T. b. brucei* were incubated with **(A)** SPK-843 and **(B)** ampothericin B (AmpB) for 1 - 24 h and parasite ATP content was measured as a 'real-time' indicator of cell viability. **(C)** Table of compound activities displayed as IC_{50} values (μM) at time-points. Error bars represent mean ±SD of two independent experiments performed in triplicate, n = 2. IC_{50} values were determined using GraphPad Prism software version 6.

A

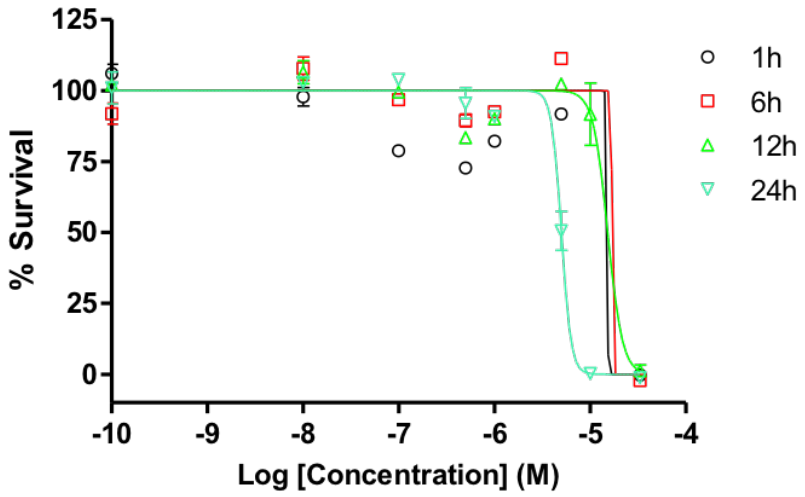

B

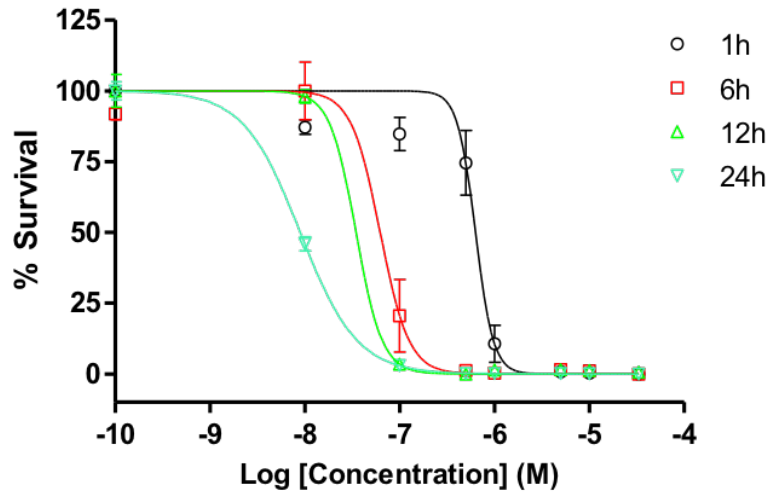

C

Compound	Activity (μM IC_{50} value)			
	1 h	6 h	12 h	24 h
(A) SPK-843	15.07	16.95	15.29	8.62
(B) Pentamidine	0.630	0.062	0.034	0.008

Figure 4.9 Reversibility of anti-trypanosomal effects of SPK-843 and pentamidine in *T. b. brucei*. *T. b. brucei* BSF (2 x 10^4/ well) were measured for their ability to recover from transient exposure to **(A)** SPK-843 and **(B)** petamidine for 1, 6, 12, or 24 h. Compounds were washed out after specified incubation times and inhibition of parasite viability measured at 72 h with Alamar Blue. **(C)** Table of compound activities displayed as IC_{50} values (μM) at time-points. Error bars represent mean ±SD of two independent experiments performed in triplicate, n = 2. Dose-response curves and IC_{50} values were determined using GraphPad Prism software version 6.

4.2.3 Investigating mechanism of action of SPK-843 & ampothericin B (cell permeabilisation) *in vitro*

It has been shown that Amphotericin B kills fungi and *Leishmania* by binding preferentially to ergosterol, the major sterol of these organisms, forming channel-like structures (pores) spanning the lipid bilayer (Neumann et al. 2009). These pores increase the permeability of cell membranes to ions and small solute molecules leading to cell death. It was hypothesized, that since SPK-843 is structurally similar to AmpB, SPK-843 would have the same mechanism of action. Thus, it was investigated if trypanosome cell death by SPK-843 involved cell membrane permeabilisation. A fluorescence assay was set up using propidium iodide (PI) to assess for disrupted plasma membrane in *T. b. brucei* following 3 h compound exposure time period. PI results in fluorescent staining of both nuclei and kinetoplasts, which is detectable with a plate reader. Parasite cultures were incubated at concentrations within the lethal range of SPK-843 and AmpB at 3 h exposure (IC_{50} values 3.65 μM and 37.9 μM, respectively shown previously with the ATP viability assay, see Figure 4.8). Pentamidine was utilized as a negative control because it's trypanocidal mechanism of action is speculated to be by interference of parasite nucleic acid metabolism and not by membrane disruption (Bacchi 2009). Interestingly, incubation of cells with SPK-843 over the 3 h did not result in any significant PI fluorescence at concentrations observed to cause 50% inhibition of trypanosomal survival (Figures 4.10). There was, however, significant PI fluorescence (60% of parasite population) for cells exposed to the highest concentration of amphotericin B (the IC_{50} value at 3 h), while concentrations below the lethal IC_{50} did not cause permeabilisation. This suggests that SPK-843 does not kill trypanosomes via cell membrane disruption, while AmpB, as expected, does.

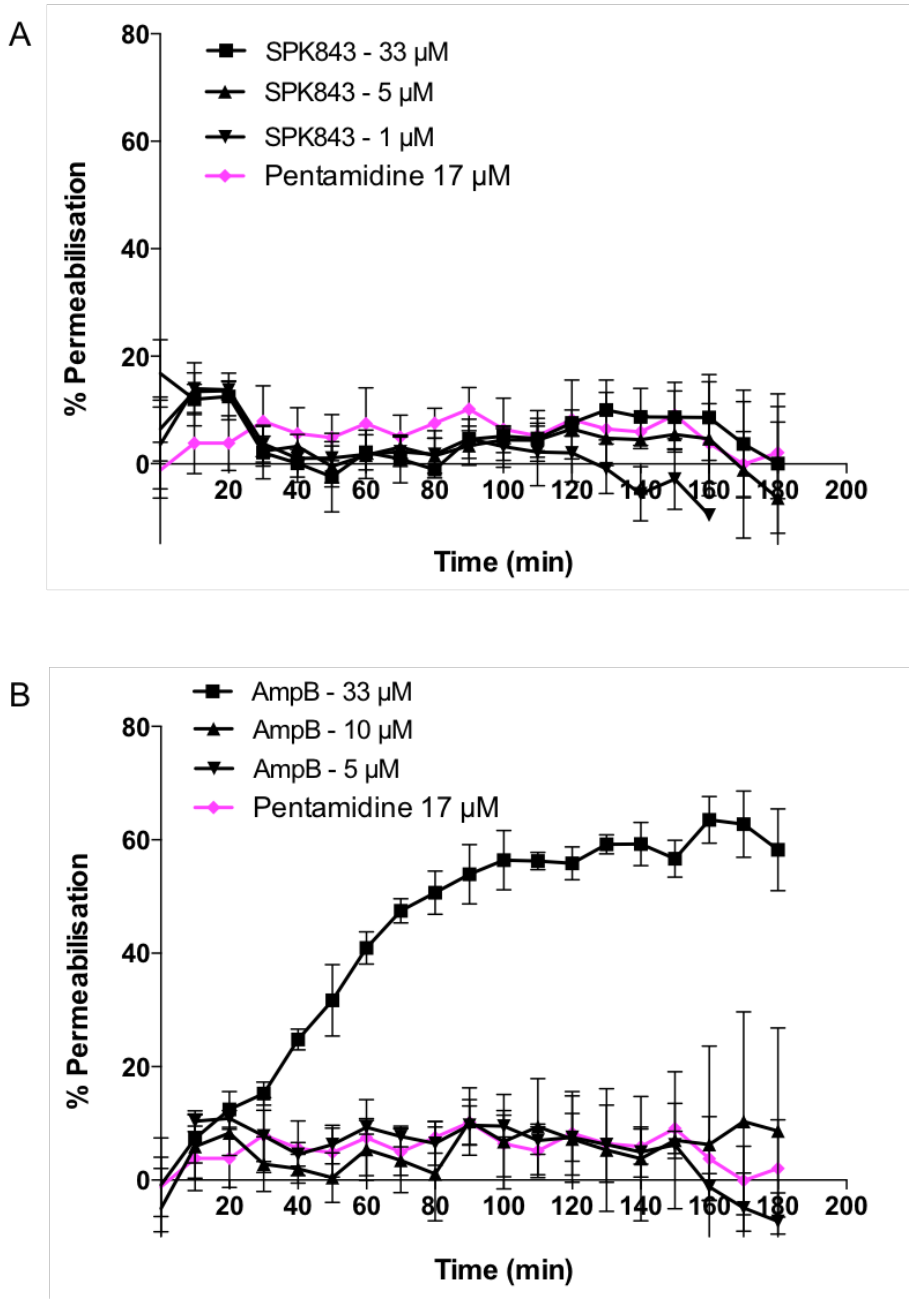

Figure 4.10 Time-course of permeabilisation of *T. b. brucei* treated with SPK-843 and AmpB. Percentage cell lysis of *T. b. brucei* BSF (2 x 10^7/well) was measured after exposure to varying concentrations of SPK-843 or AmpB for 3 h in the presence of propidium iodide, a plasma membrane-permeating nucleic acid dye. Fluorescence was monitored over time using a SpectraMax M3 plate reader. Error bars represent mean ±SD of two independent experiments performed in triplicate, n = 2. No significant PI fluorescence was detected following exposure to SPK-843 for 180 min, whereas there was with AmpB.

4.2.4 Investigating the effect of SPK-843 & ampothericin B on parasite clearance *in vivo*

To determine if the *in vitro* potency of SPK-843 and ampothericin B towards *T. b. brucei* presented a similar potential *in vivo,* a mouse model of acute trypanosomiasis was employed. An acute model was used to start off with to examine the exposure-response relationship, with the sole objective to demonstrate the acute efficacy of the biological candidates. Female NMRI mice were inoculated with *T. b. brucei* monomorphic strain Lister 427 and at 72 h post-infection, when parasites had established in their hosts, the animals were treated with a daily dose of either SPK-843 or AmBisome® at 5 mg/kg, or vehicle controls for 5 consecutive days. Notably, SPK-843 (5 mg/kg i.v in 10% intralipid) dosed over 5 days reduced parasite load and significantly increase survival time of the animals post-inoculation by a mean of five days compared to vehicle control group ($P < 0.058$, see Figure 4.11). Surprisingly, AmBisome® dosed for the same number of days was insufficient at reducing or clearing parasitemia when compared with controls. It is important to note the strain used in this study is a highly virulent monomorphic strain, which consists of only the 'slender' form *T. b. brucei,* responsible for the rapid killing triggered by uncontrollable growth *in vivo*. These results suggest that with further *in vivo* investigations SPK-843 could have the potential to completely clear parasitemia.

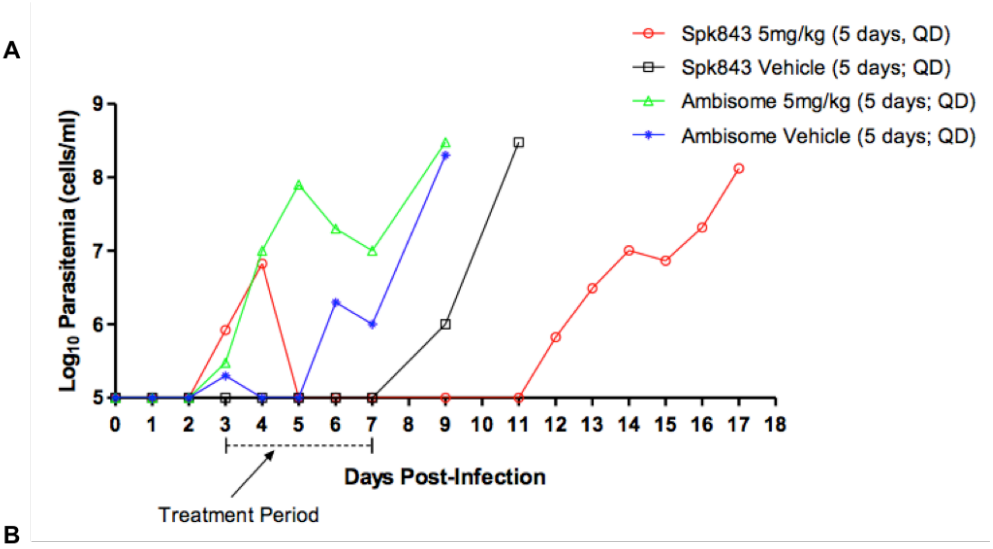

Figure 4.11 Effect of SPK-843 and AmBisome® on parasite clearance *in vivo*. Female NMRI mice were infected with 1 x 10^4 *T. b. brucei* monomorphic strain Lister 427 for 72 h prior to initiating treatment with SPK-843 (5 mg/kg), AmBisome® (liposomal amphotericin B, 5 mg/kg), or vehicle only - 10% intralipid emulsion as SPK-843 vehicle, 5 % glucose solution as AmBisome® vehicle - for 5 days. (n = 4 per treatment group, n = 3 per vehicle group). **(A)** Parasitemia was measured from peripheral blood obtained by cheek bleed as parasites were enumerated on a haemocytometer. **(B)** Survival was monitored daily throughout the course of infection, moribund mice or those with parasitemias > 10^8 cells/mL were euthanized. Unpaired t-test with Welch correction comparing treatments with vehicle control only, ** $P < 0.0058$, determined using GraphPad Prism software version 6. Only SPK-843 (5 mg/kg i.v. in 10 % intralipid) dosed over 5 days was sufficient to significantly reduce parasite load and extend survival time compared to vehicle control.

4.3 Investigation fo fingolimod for treatment of Trypanosomiasis

4.3.2 Determination of the trypanosomal action of fingolimod & structural mimics *in vitro*

Following on from the computational drug repurposing *in silico* prediction, trypanosomal action of fingolimod was investigated *in vitro* for similarity. First, the effect of fingolimod (FTY720) concentration on the viability of *Trypanosoma brucei brucei* was investigated. Drug sensitivity of both FTY720 and its metabolite FTY720P (phosphorylated *in vivo*), were analysed in cultures of *T. b. brucei* using Alamar Blue viability assay. Testing was done at a sufficiently wide concentration range (300 μM→0.3 nM) to determine the effective concentration which killed 50% of trypanosome population within 48 h of drug exposure (IC_{50}). Remarkably, FTY720 and its phosphorylated derivative FTY720P, exhibited dose-dependent growth inhibition of both *T. b. brucei* bloodstream forms (BSF) and procyclic forms (PCF) in this *in vitro* whole-cell assay, determined by reduction of the cell viability marker resazurin (Figure 4.12). As mentioned in the introduction, trypanosomes live in both a mammalian and an insect host, hence the effect of fingolimod on the growth of proliferative long slender bloodstream forms and established cultured procyclic (insect) forms was investigated. Drug activities in both life forms, as a measured by IC_{50} values, were very efficacious and ranged between 0.15 μM and 5.28 μM (Figure 4.12 C). Interestingly, two things happened. For one, both compounds showed approximately an order of magnitude more potent trypanocidal activity against BSF versus PCF. Secondly, the phosphorylated metabolite of fingolimod, FTY720P, showed a higher potency than its pre-metabolised counterpart, FTY720, with a 2-fold lower IC_{50} of 0.15 μM compared to 0.32 μM in BSF, and 1.13 μM vs 5.28 μM in PCF, respectively (Figure 4.12 C). Overall, these results correlate with that of computational methods, which had identified fingolimod as an effective trypanocidal agent (ranked number four with FCFP4 method, Figure 4.3).

As mentioned previously, fingolimod is not only highly homologous in structure and function to myriocin, but also to sphingosine-1-phosphate and its precursor D-sphingosine (Chiba & Adachi 2012); lipids that are part of the sphingolipid pathway naturally occurring in most living organisms. Thus, the effect of these structural mimics,

sphingosine and sphingosine-1-phosphate, on parasite killing was also investigated *in vitro*. Drug sensitivity was again examined by Alamar Blue viability assay in cultures of *T. b. brucei*. Sphingosine and its phosphorylated bioactive derivative, sphingosine-1-phosphate, exhibited strong dose-dependent growth inhibition of both BSF and PCF *T. b. brucei* (Figure 4.13), like that of their fingolimod counterparts (Figure 4.12). Compounds showed to be potent trypanocidal agents, with IC_{50} values of 0.10 μM and 0.13 μM in BSF for sphingosine and S1P, respectively, and approximately an order of magnitude lower in procyclic form.

Since FTY720 (fingolimod) is an FDA approved treatment (safety profiles are known), further investigation went into fingolimod. Subsequent experiments followed to work out the specifics of fingolimod, such as the time of killing, how it compares to current Human African Trypanosomiasis (HAT) treatments, and the mechanism of action.

A

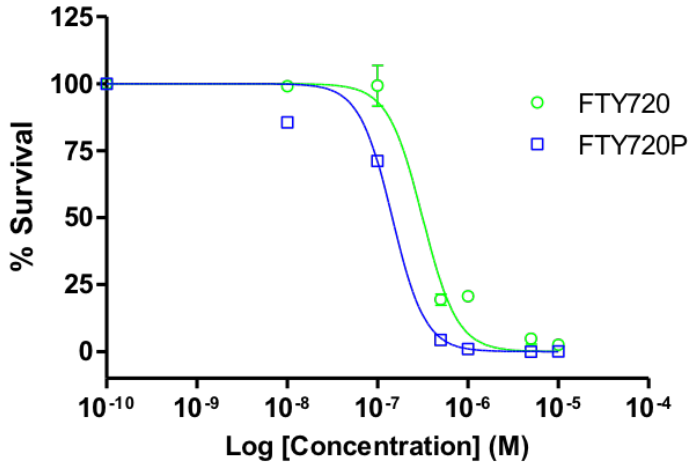

B

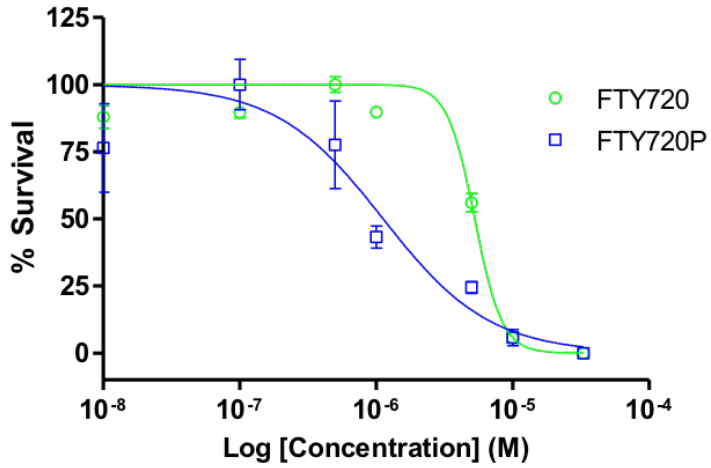

C

T. b. brucei life-cycle stage	FTY720 IC_{50} (µM)	FTY720P IC_{50} (µM)
(A) BSF	0.316±0.099	0.145±0.034
(B) PCF	5.280±0.615	1.130±0.710

Figure 4.12 *In vitro* trypanocidal activity of FTY720 and FTY720P. The percentage of viable *T. b. brucei,* **(A)** bloodstream form (BSF, seeded at 2 x 10^4 cells/mL) and **(B)** procyclic form (PCF, seeded at 2 x 10^5 cells/mL) was determined with Alamar blue viability assay following a 48 h exposure to media containing serial dilutions of FTY720 or FTY720P. **(C)** Table of compound activities from dose-response curves displayed as IC_{50} values (µM). Error bars represent mean ±SD of two independent experiments performed in triplicate, n = 2. IC_{50} values were determined using GraphPad Prism software version 6. FTY720 and FTY720P caused dose-dependent inhibition of growth in both BSF and PCF *T. b. brucei in vitro*.

A

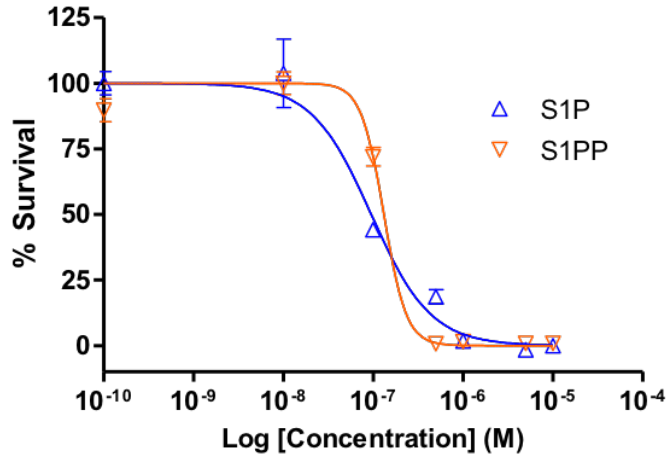

B

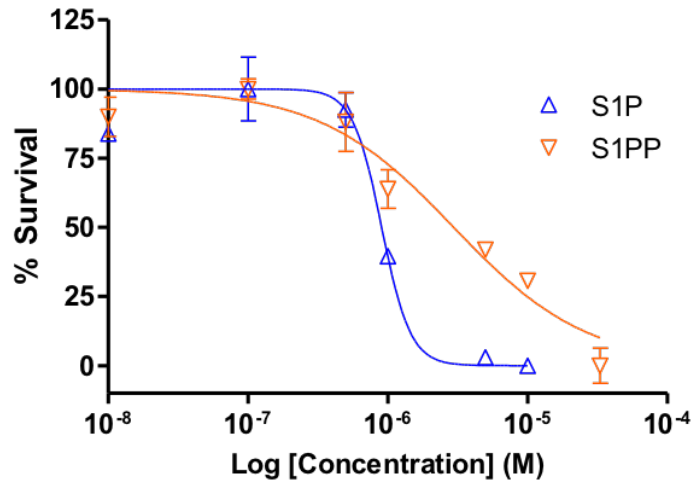

C

T.b.brucei life-cycle stage	Sphingosine IC_{50} (μM)	S1PP IC_{50} (μM)
(A) BSF	0.095±0.034	0.132±0.056
(B) PCF	0.905±0.133	2.970±1.333

Figure 4.13 *In vitro* trypanocidal activity of D-Sphingosine and Sphingosine 1-Phosphate. The percentage of viable *T. b. brucei,* **(A)** bloodstream form (BSF, at 2 x 10^4 cells/mL) and **(B)** procyclic form (PCF, at 2 x 10^5 cells/mL) was determined with Alamar blue viability assay following a 48 h exposure to media containing serial dilutions of D-Sphingosine (SIP) or Sphingosine 1-Phosphate (SIPP). **(C)** Table of compound activities from dose-response curves displayed as IC_{50} values (μM) at time-points. Error bars represent mean ±SD of two independent experiments performed in triplicate, n = 2. IC_{50} values were determined using GraphPad Prism software version 6. SIP and SIPP exhibited strong growth suppression of both forms of *T. b. brucei in vitro* with the same trend of increasing potency in BSF rather than PCF.

4.3.3 Investigating time dependence of trypanocidal effects of fingolimod in *T. b. brucei* to continuous and transient exposure

It was shown with the Alamar Blue viability assay that fingolimod and its naturally occurring structural mimic, sphingosine, kill trypanosomes after 48 h of continuous drug exposure *in vitro*. Thus, specifics of the time for FTY720 and FTY720P mediated inhibition of *T. b. brucei* viability *in vitro* were investigated next. Cultured trypanosomes were subjected to continuous drug pressure over a 48 h time period and parasite ATP content was measured as a 'real-time' indicator of cell viability at several time-points (1, 2, 3, 5, 8, 10, 24, 48 h) using CellTiter-Glo assay. Interestingly, a time-dependent loss of cell viability occurred following treatment with FTY720 and FTY720P, as illustrated by Figure 4.14. Notably, onset of killing occurred far more rapidly with FTY720 than for FTY720P, whereby parasite viability was observed as dropping below 50% following exposure to FTY720 for 8-10 h at sub-micromolar concentrations. Although this suggests that their killing mechanisms differ, both compounds appear to reach optimal killing between 24 and 48 h (Figure 4.14 C), 0.199 - 0.177 μM and 0.437 - 0.143 μM for FTY720 and FTY720P, respectively. Importantly, *in vitro* testing of both FTY720 and FTY720P compare favourably with current early stage treatments for HAT, suramin and pentamidine (4.14 C), at 24 h after exposure, 0.200 μM and 0.008 μM, respectively.

Next, to determine if the time-dependent trypanocidal effect of fingolimod was reversible, cultures were exposed to either FTY720 or pentamidine, a drug used for first stage of HAT, as a reference, for specified time periods of 1, 6, 12, and 24 h. Drugs were then washed out and all cultures were subsequently maintained in drug-free medium and assessed for viability at 72 h with Alamar Blue. Interestingly, FTY720 was shown to kill less rapidly than pentamidine, however, the killing effect was irreversible even after drug was removed following the various incubation periods (Figure 4.15). Together these results suggest that fingolimod is an effective trypanosomal agent that is on par with current HAT treatments. Pentamidine is only used as treatment during the first stage HAT as it is predominantly ineffective once the parasites have invaded the central nervous system (CNS) (Sanderson et al. 2009). Fingolimod on the other hand is known to readily penetrate the CNS and thus may provide promise for future treatment of both haemolymphatic and meningoencephalitic stages of trypanosomiasis. More *in vitro* assessments of fingolimod were necessary before testing its killing potential *in vivo*.

A

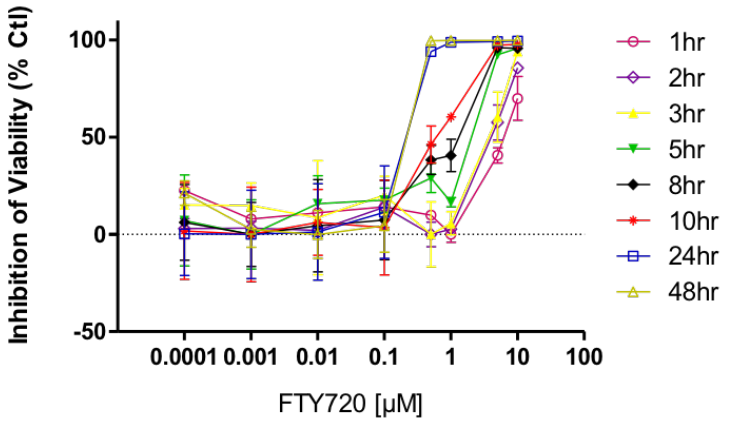

B

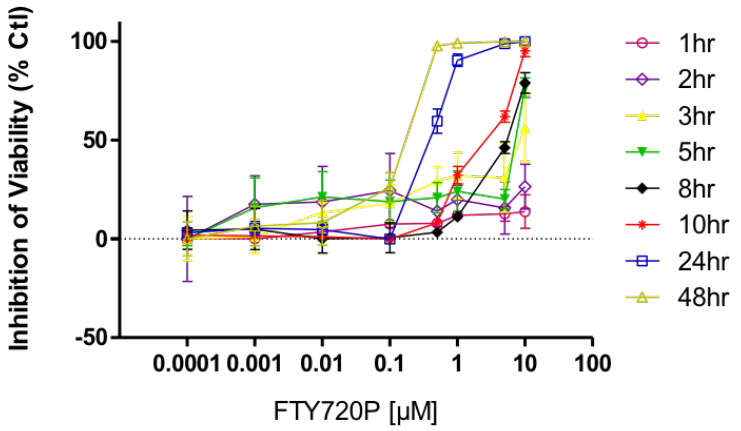

C

Compound	Activity (µM IC_{50} value)							
	1 h	2 h	3 h	5 h	8 h	10 h	24 h	48 h
FTY720	-	4.44	4.26	1.67	0.967	0.637	0.199	0.177
FTY720P	-	-	14	11.7	4.97	2.37	0.437	0.143
Suramin					>7*		0.200	
Pentamidine					>1.6*		0.008	

* Actual time point was 9 h

Figure 4.14 Time-dependent loss of *T. b. brucei* viability following treatment with FTY720 and FTY720P. Cultured BSF *T. b. brucei* were subjected to continuous drug pressure with **(A)** FTY720 or **(B)** FTY720P, over a 48 h time period and parasite ATP content was measured as a 'real-time' indicator of cell viability at several time-points using CellTiter-Glo assay. **(C)** Table of compound activities displayed as IC_{50} values (µM) at time-points. Error bars represent mean ±SD of two independent experiments performed in triplicate, n = 2. Time-response curves and IC_{50} were determined using GraphPad Prism software version 6. Parasite viability observed as dropping below 50% occurred more rapidly following exposure to FTY720 than FTY720P, however, both compounds appear to reach optimal killing between 24 and 48 h.

A

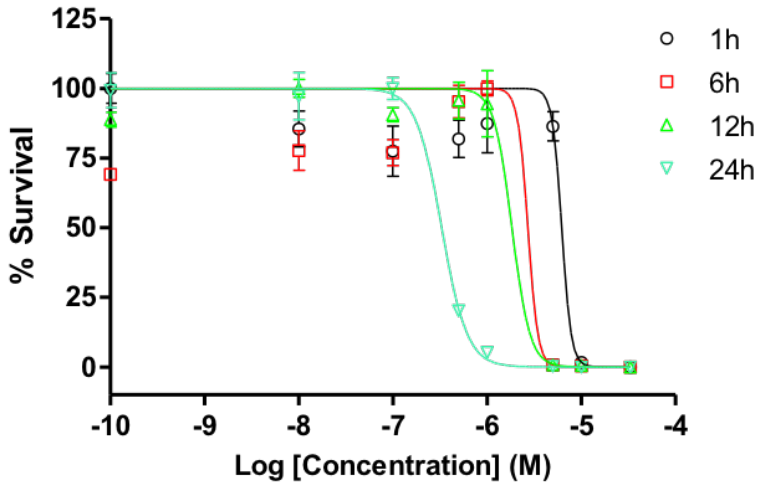

B

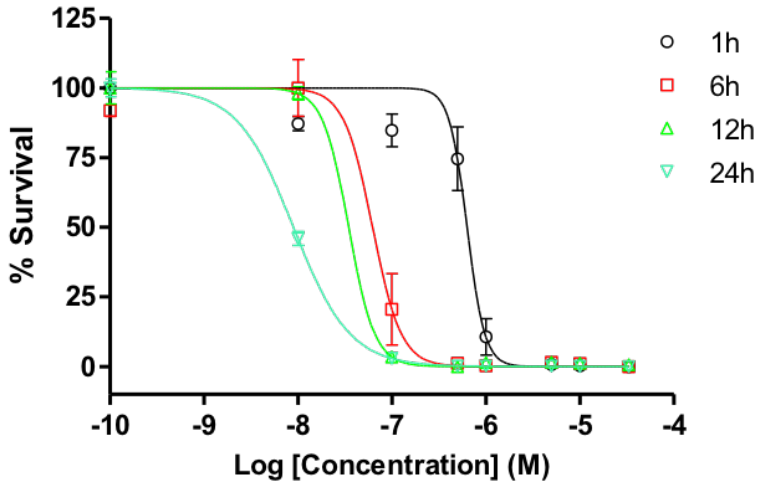

C

Compound	Activity (μM IC_{50} value)			
	1 h	6 h	12 h	24 h
(A) FTY720	6.200	2.710	1.840	0.320
(B) Pentamidine	0.630	0.062	0.034	0.008

Figure 4.15 Reversibility of trypanocidal effects of FTY720. *T. b. brucei* BSF (2 x 10^4/ well) were measured for their ability to recover from transient exposure to 1, 6, 12, or 24 h of **(A)** FTY720 and **(B)** petamidine. Compounds were washed out after specified times and viability assessed at 72 h with Alamar Blue. **(C)** Table of compound activities displayed as IC_{50} values (μM) at time-points. Error bars represent mean ±SD of two independent experiments performed in triplicate, n = 2. IC_{50} values were determined using GraphPad Prism software version 6. FTY720 kills less rapidly than pentamidine (used for first stage of HAT), however, the killing effect is irreversible even after drug washout following incubation of drug for 1, 6, 12 and 24 h.

4.3.4 Investigating the mechanism of action of fingolimod *in vitro*

Next, the possible mode of trypanocidal action of FTY720P was investigated using a fluorescence assay to assess for cell death caused by cell permeabilisation (cell lysis). Propidium iodide (PI) was used as a marker for disrupted plasma membrane in trypanosomes, as it fluorescently stains both nuclei and kinetoplasts in cells whose membrane has been compromised, making these cells then detectable with a plate reader. Pentamidine (17 μM) was used as a negative control to show time-independent baseline fluorescence values since pentamidine does not disrupt the plasma membrane. Surprisingly, incubation of cells with near-lethal concentrations of FTY720P (5 and 10 μM) resulted in PI fluorescence (> 140 min) compared with the negative pentamidine control and lowest concentration of FTY720P (1 μM) (Figure 4.16). This suggested that FTY720P may kill trypanosomes via cell lysis as a secondary mechanism.

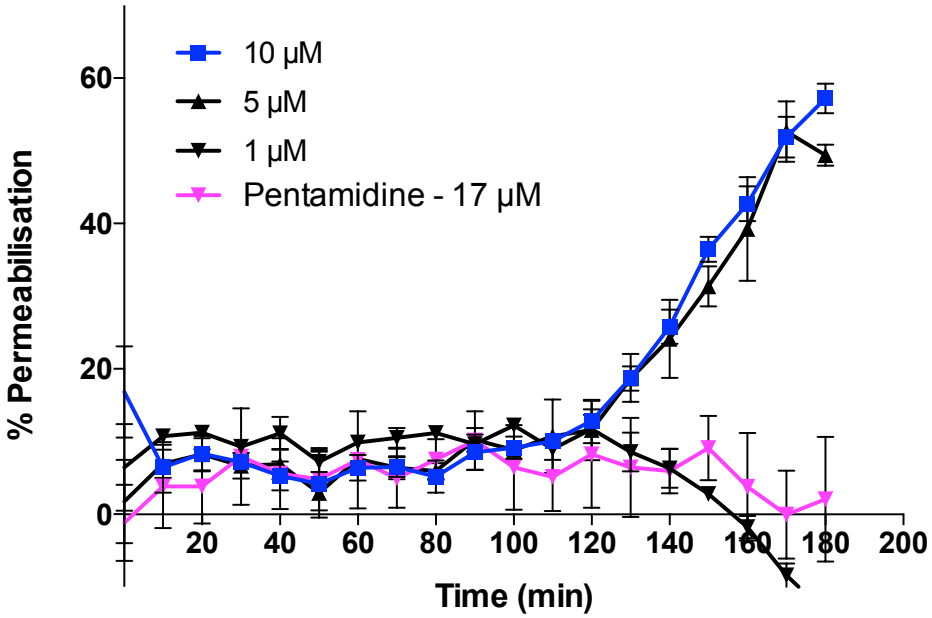

Figure 4.16 Time-course of permeabilisation of *T. b. brucei* treated with FTY720P. Percentage cell lysis of *T. b. brucei* BSF (2 x 10^7/well) was measured after exposure to FTY720P (at 1, 5, and 10 µM) for 3 h in the presence of propidium iodide, a plasma membrane-permeating nucleic acid dye. Fluorescence was monitored over time using a SpectraMax M3 plate reader. Error bars represent mean ±SD of two independent experiments performed in triplicate, n = 2. Fluorescence and thus membrane permeabilisation was detected from parasites exposed to lethal concentrations of FTY720P (IC_{50} = ~ 14 µM following 3 h exposure).

4.3.5 Investigating cell cycle and morphological changes in *T. b. brucei*

It was noted that there was a large proportion of *T. b. brucei* parasites with uncharacteristic phenotypes, mainly large swollen cells, during the various *in vitro* viability assays with fingolimod treatment compared to untreated cells, as seen under phase-contrast with a normal inverted bench microscope (data not shown). Subsequently, this trend/occurrence as cause of effect for cell death was investigated. Fluorescence microscopy analysis was carried out to monitor cell cycle and morphological effects in both untreated trypanosomes and those incubated with FTY720 or FTY720P. Initially, cell population based on morphology and kinetoplast to nucleus ratio (K/N) was assessed in untreated bloodstream form *T. b. brucei* cultures. Cells in different cell cycle stages were categorized based on the number of fluorescently stained kinetoplasts and nuclei they contained following incubation with DAPI. Overall, untreated parasite cultures were made up of an asynchronous population: cells undergoing normal cell cycles-dependent/related morphological changes (Figure 4.16 A-C), as well as some abnormal cells (Figure 4.17 D-F). Moreover, the untreated population correlated well with anticipated cell cycle progression in trypanosomes as illustrated in Figure 1.4 (Ploubidou et al. 1999; Vedrenne et al. 2002). Control cultures displayed a constant distribution of cell population over time, with a high percentage of non-diving cells (1N1K) and small percentage of cells in different phases of the cell cycle (2N1K, 2N2K).

In comparison, incubation with either 1 µM FTY720 or FTY720P generated a significant increase in cells blocked in late mitosis (2N1K, 2N2K), as well as, multinucleated cells (Figures 4.18 & 4.19). Transitioning from 0 h to 8 h in culture, trypanosomes treated with FTY720 fail to undergo cytokinesis and become blocked in late mitosis (Figure 4.18). This effect was seen as early as 3 h following exposure to FTY720, where 50% of the cell population became blocked (2N1K + 2N2K) as compared to the low level of 12% in untreated cultures. As shown earlier, even untreated cultures contain some aberrant/atypical cells. Interestingly, morphological differences were observed as cells swollen and prevented cytokinesis (Figure 4.19 B & D), in tandem with a shift in the population of predominantly 1N1K cells to 2N1K or 2N2K† cells (Figure 4.18). Endocytosis appears to be perturbed very early on after exposure to FTY720 with the appearance of a significant proportion of 'big-eye' phenotypic cells, characterised by enlargement of the flagellar pocket (Figure 4.19 B). After 24 h incubation with FTY720, the cells were no longer viable, as depicted in Figure 4.19 F.

Similar to FTY720, incubation with 1 μM of the phosphorylated metabolite FTY720P also caused cell cycle and morphological defects, albeit within a slightly extended timeframe (Figure 4.20 & 4.21 F). After 24 h FTY720P exposure, the population of 1N1K cells dropped to approximately 28%, in contrast to 82% of the control cell population of 1N1K cells. Strikingly, 22% are blocked at 2N1K and 41% at 2N2K†, whereas for the control population its altogether less than 10% (Figure 4.20). These drug treated cultures also exhibited cells with the 'big-eye' phenotype and were multinucleate (Figure 4.21 F). Again progression through the cell cycle was disrupted by failure to undergo cytokinesis as shown by the K/N ratio, indicating that FTY720s mode of killing is partly due to disruption of the cell cycle.

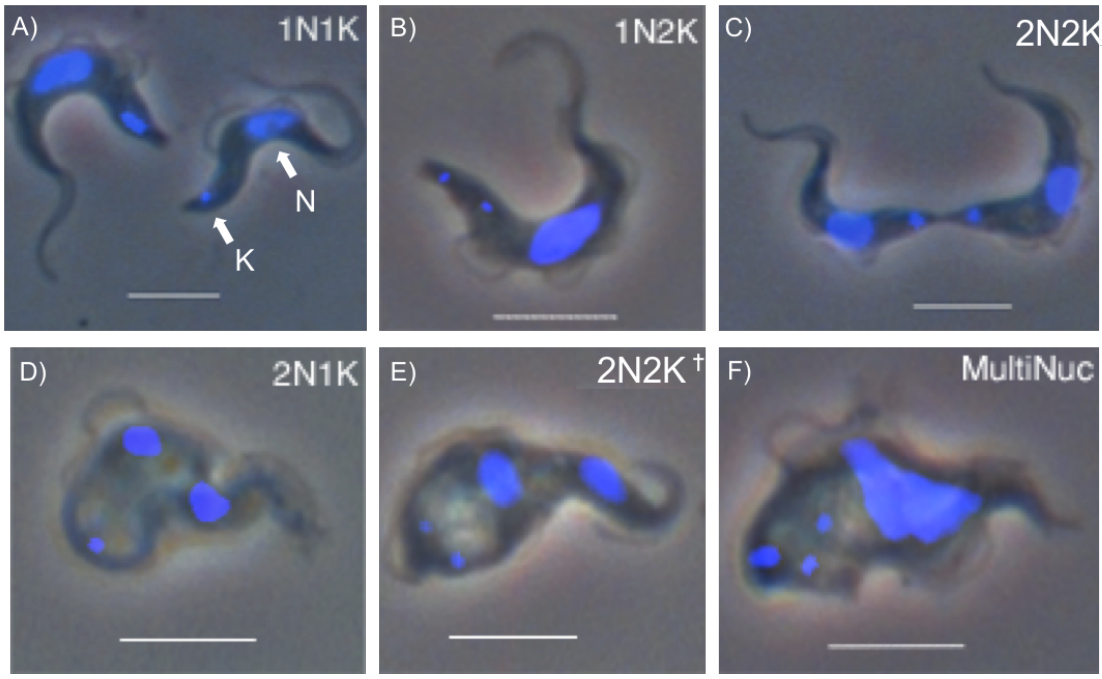

Figure 4.17 Fluorescence microscopy analysis of Trypanosome cell cycle. Untreated *T. b. brucei* BSF cultured/maintained in log phase growth, were fixed in 3% PFA and incubated with DAPI to stain nuclei and kinetoplasts. Cells were categorized according to kinetoplast-nucleus ratio, as follows: A-C; normal cells - **(A)** Cell with 1 nucleus and 1 kinetoplast (1N1K) in G1-phase. **(B)** Cell with 1 nucleus and 2 kinetoplasts (1N2K) in early S-phase. **(C)** Cell with 2 nuclei and 2 kinetoplasts (2N2K) and cell division almost complete. D-F; abnormal cells - **(D)** 2 nuclei and 1 kinetoplast (2N1K) with cell blocked in late mitosis. **(E)** Cell with 2 nuclei and 2 kinetoplasts ($2N2K^{\dagger}$) without cytokinesis occurring. **(F)** Multi-nucleated cells whereby several rounds of DNA replication progressed without cytokinesis. Images are representative of a large data set. Images captured using a Zeiss Axiovert 100 fluorescence microscope, scale bar = 5 µM. Untreated cultures were composed of an asynchronous population of parasites, cells undergoing normal cell cycle stages, along with some abnormal cells.

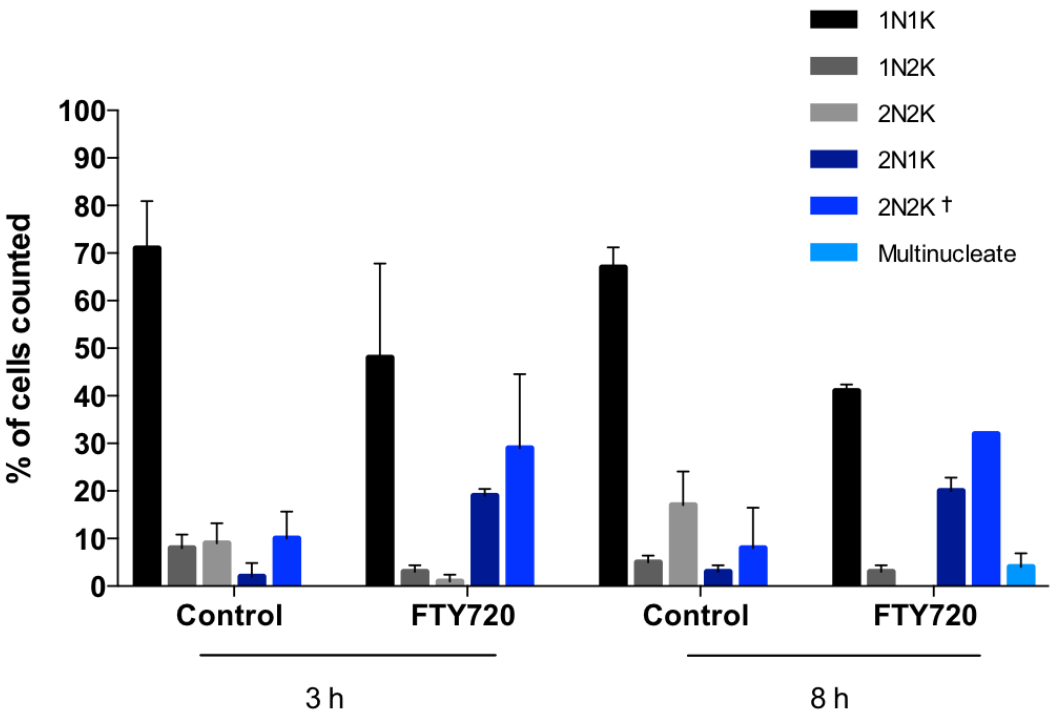

Figure 4.18 Effect of FTY720 on cell cycle. *T. b. brucei* BSF (5 x 10^5 cells/mL) were exposed to either 1 µM FTY720 or vehicle control (ethanol) for 3 h or 8 h before being fixed with 3% PFA, then stained with DAPI and quantified/counted based on their different nuclei to kinetoplast ratio and morphology. Normal cells: 1N1K, 1N2K, 2N2K; abnormal cells: 2N1K, $2N2K^{\dagger}$, multinucleated. Data are presented as the mean percentage ±SD of total cells counted (n > 100) from two independent experiments, n = 2. Images captured using a Zeiss Axiovert 100 fluorescence microscope. Short exposure to FTY720 increased the number of abnormal/aberrant *T. b. brucei* as compared to vehicle control *in vitro*.

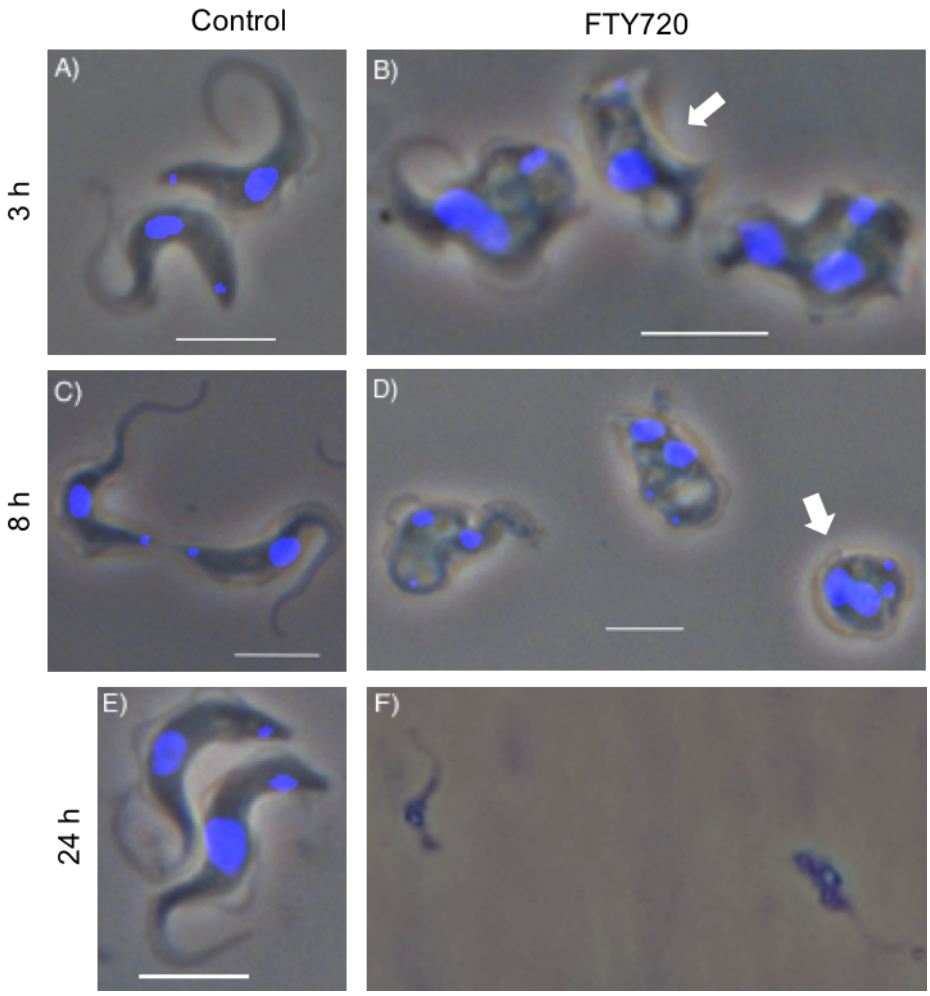

Figure 4.19 Effect of FTY720 on cell morphology. *T. b. brucei* BSF (5 x 10^5 cells/mL) were exposed to either **(A)**, **(C)**, **(E)** vehicle control (ethanol) or **(B)**, **(D)**, **(F)** 1 µM FTY720 for 3, 8, or 24 h, respectively, before being fixed with 3% PFA. Cells were incubated with DAPI and assessed for morphological and cell cycle effects. Images A-E were captured with Zeiss Axiovert 100 fluorescence microscope equipped with an AxioCam HRc camera. Image F (live) was taken with a camera mounted on an Olympus CK2 inverted microscope, scale bar = 5 µM. Images are representative images from a large data set. Short exposure to FTY720 disrupted cell cycle and caused multinucleated cell formation, while a longer exposure (24 h) caused cell death.

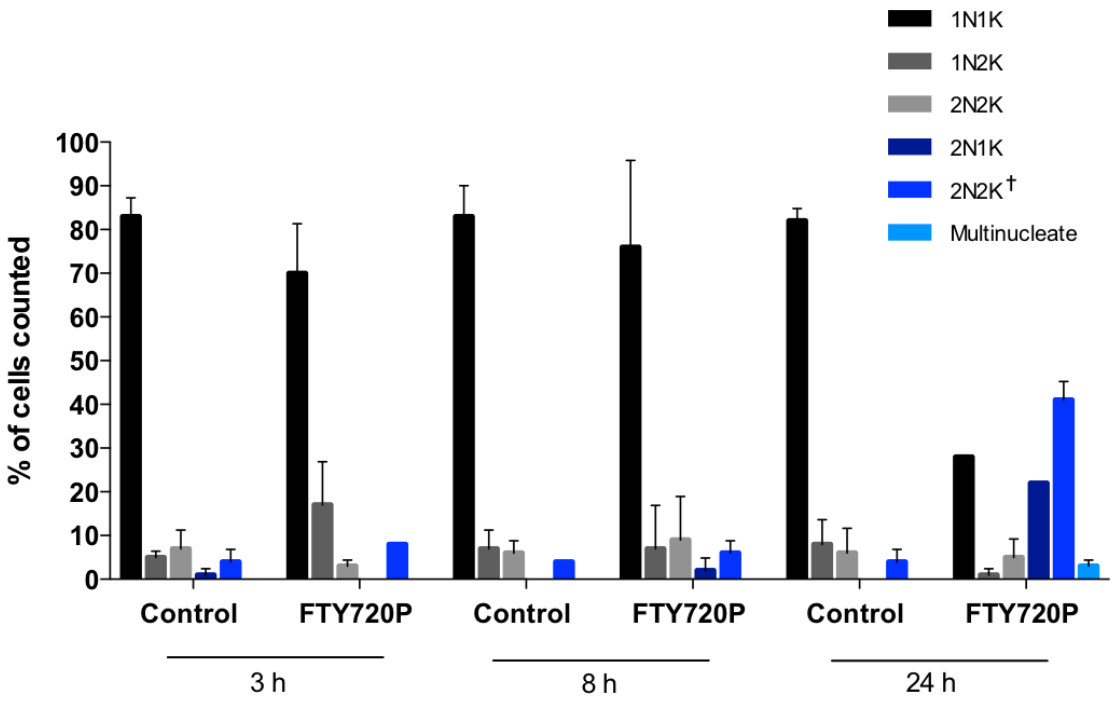

Figure 4.20 Effect of FTY720P on cell cycle. *T. b. brucei* BSF (5 x 10^5 cells/mL) were exposed to either 1 µM FTY720P or vehicle control (DMSO, HCl, ethanol mixture) for 3, 8, or 24 h before being fixed with 3% PFA, then stained with DAPI and counted based on their different nuclei to kinetoplast ratio and morphology. Normal cells: 1N1K, 1N2K, 2N2K; abnormal cells: 2N1K, $2N2K^{+}$, multinucleated. Data are presented as the mean percentage ±SD of total cells counted (n>100) from two independent experiments, n = 2. Images captured using a Zeiss Axiovert 100 fluorescence microscope. Variety of cell defects in *T. b. brucei* only observed close to the full incubation period of 24 h to FTY720P.

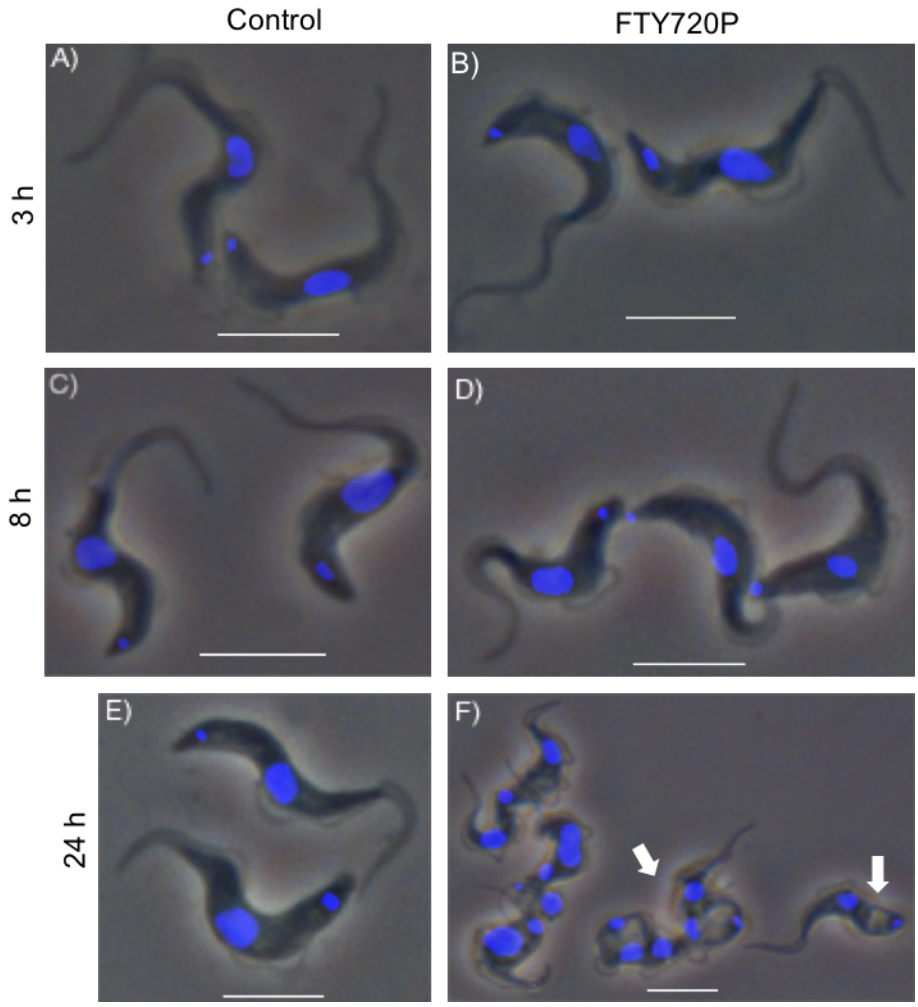

Figure 4.21 Effect of FTY720P on trypanosome cell morphology. *T. b. brucei* BSF (5 x 10^5 cells/mL) were exposed to either **(A), (C), (E)** vehicle control or **(B), (D), (F)** 1 µM FTY720P for 3, 8, or 24 h, respectively, before being fixed with 3% PFA. Cells were incubated with DAPI and assessed for morphological and cell cycle effects. Images A-E were captured with Zeiss Axiovert 100 fluorescence microscope equipped with an AxioCam HRc camera. Image F (live) was taken with a camera mounted on an Olympus CK2 inverted microscope, scale bar = 5 µM. Images are representative images from a large data set. Variety of cell defects in *T. b. brucei*, such as the 'Big Eye' phenotype was only observed following 24 h exposure to FTY720P.

4.3.6 Investigating the effect of FTY720 on parasite clearance *in vivo*

Since, fingolimod is a currently FDA approved treatment for relapsing forms of Multiple Sclerosis, coupled with the potent *in vitro* anti-trypanosomal activity demonstrated in this study, the drug candidate was next tested in an animal model of trypanosomiasis. Mice were inoculated with 1 x 10^4 trypanosomes through intraperitoneal injection (day 0). Three days later when the parasites had established in their hosts, the treatment group received FTY720 (1 mg/kg) daily for five consecutive days, control animals received vehicle only (Phosphate-buffered-Saline-Glucose: PSG). Figure 4.22 illustrates that FTY720 administration for 5 days was sufficient to reduce and control parasite load (below level of detection) onwards from the second day of treatment for a subsequent 4 day period. The parasite population stayed below the level of detection one day post-treatment with FTY720 in three out of the four mice and three days in the fourth animal. In comparison, parasites in the control group continued to proliferate exponentially, except in one animal, however, that survived as long as the fingolimod treated group. Discontinuation of treatment led to development of parasitemia similar to those of controls and all animals were culled when parasitemia had reached the critical level (> 10^8 cells/mL). This suggests that if fingolimod can supress parasitemia in a model infected with a highly virulent monomorphic strain responsible for rapid killing of the host, then it may have to potential to supress and clear *T. brucei* behind a more chronic disease model.

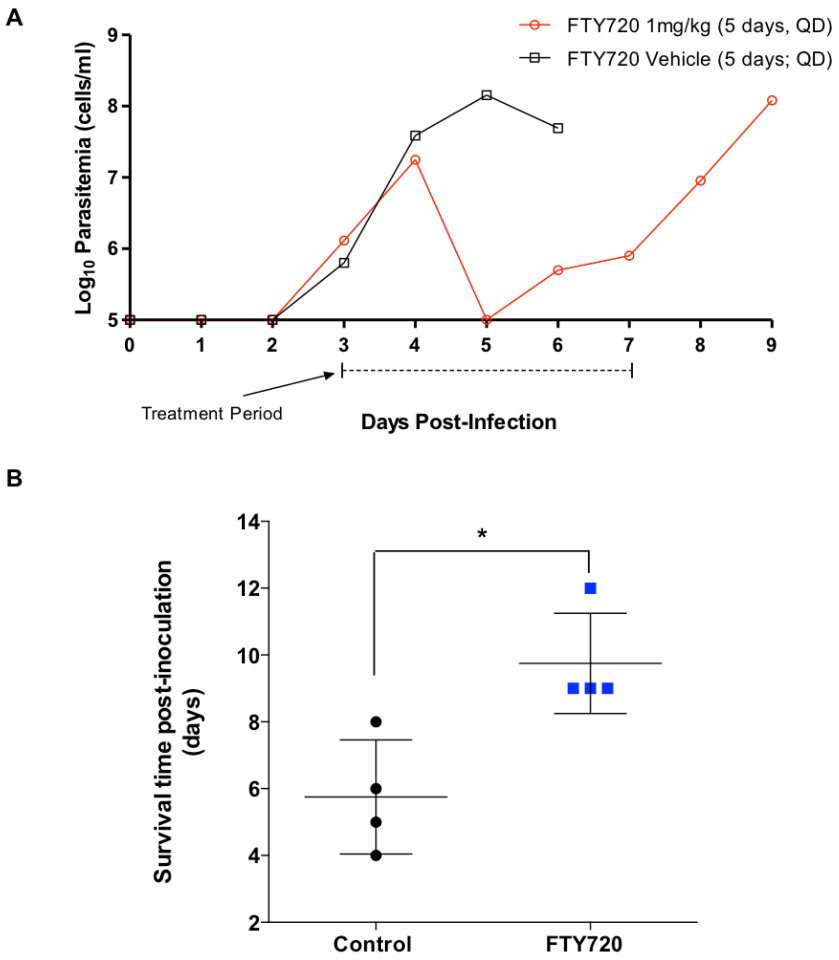

Figure 4.22 The effect of FTY720 on parasite clearance *in vivo*. Female NMRI mice were intraperitoneally infected with 1 x 10^4 parasites (*T. b. brucei* monomorphic strain Lister 427) on Day 0. Infection was allowed to progress for 72 h prior to initiating dosing control group with vehicle only (Phosphate-buffered-Saline-Glucose: PSG) vs treatment group with FTY720 (1 mg/kg; i.v.) for 5 days. **(A)** Parasitemia was quantified from peripheral blood obtained by cheek bleed, 2 µL diluted 1:200 in PSG buffer and parasites enumerated on a haemocytometer. The limit of detection using this method was > 10^6 cells/mL. Survival was monitored daily throughout the course of infection, moribund mice or those with parasitemias >10^8 cells/mL were euthanized. **(B)** Overall survival time post-inoculation data presented using GraphPad Prism software version 6. Unpaired t-test with Welch correction comparing treatments with vehicle control only. * $P < 0.05$. FTY720 (1 mg/kg) administration for 5 days was sufficient to control parasite load (below the level of detection) during treatment period and a day post-treatment, whereas the parasite population in the control group continued to proliferate exponentially.

4.4 Discussion

The aim of the current study was to investigate the efficacy of various new leads, including some already FDA-approved compounds, as anti-trypanosomal agents. It was hypothesised that drug repurposing methods can identify new chemical starting points as anti-trypanosomal compounds. These drug repurposing methods included: a) similarity searches between two databases of compounds with different properties (trypanocidal agents vs drugs with blood-brain barrier passing capabilities) that displayed similar chemical backbones, and b) compounds that modulate the activity of a conserved parasite target (ergosterol) between parasites of similar biology and genomic sequences (*T. brucei*, *T. cruzi*, *Leishmania*). The semi-rational and rational CADD re-designed leads: amphotericin B, SPK-843, fingolimod, fingolimod-phosphate, sphingosine, and sphingosine-1-phosphate were thus hypothesised to kill *T. b. brucei* in a similar manner to current anti-trypanosomal drugs (suramin and pentamidine).

We show here for the first time, using a combination of *in vivo* and *in vitro* techniques, that some of the new repurposed leads support the hypothesis as potential candidates for the treatment of trypanosomiasis, a new clinical use to their original diseases (see Table 4.2 for comparison of compound potency against current HAT treatments). For the first time, the data here show that the polyene antifungals SPK-843 and amphotericin B (AmpB) are able to kill *T. b. brucei in vitro*. Moreover, SPK-843 induces parasite death more rapidly and with a greater efficacy than AmpB. However, when *T. b. brucei* were given time to recover following 24 h transient exposure, SPK-843 showed to be a moderately reversible anti-trypanosomal agent. While the mechanism of cell death following AmpB treatment was shown to involve membrane permeabilisation, for the structurally similar SPK-843 membrane disruption was not detected. Furthermore, unlike AmpB in its lipid formulation (AmBisome®), SPK-843 (intralipid 10% emulsion) dosed at 5 mg/kg/day for five days was shown to potently suppress *T. b. brucei* parasitemia and extend the life of mice infected with the highly virulent monomorphic strain *Lister 427*.

Significantly, it was also shown that fingolimod (FTY720), the first FDA-approved oral agent for the management of relapsing forms of multiple sclerosis, its phosphorylated derivative FTY720P, and endogenous structural mimics sphingosine and sphingosine-1-phosphate, respectively, possessed potent trypanocidal activity in both life stages of *T. b. brucei*. The potency matched those of early stage treatments suramine and pentamidine.

Efficacy of all four compounds were, however, higher against bloodstream than procyclic form. FTY720 behaved differently to FTY720P in that FTY720 killed *T. brucei* faster, a sub-micromolar IC_{50} occurred after 8 h exposure to FTY720, while it took 24 h following FTY720P treatment. Significantly, the trypanocidal activity of FTY720 was irreversible at sub-micromolar concentrations (IC_{50} ~0.32 μM) after exposure for 24 h in *T. b. brucei* cultures (in contrast to reversible trypanocidal action of SPK-843, IC_{50} = 8.62 μM at 24 h transient exposure). Pharmacological time-course studies revealed that the mode of killing of FTY720 and FTY720P is partly due to membrane disruption and partly/secondary to disruption of cell division, including failure to undergo cytokinesis, which is apparent from the presence of cells with atypical DNA content observed with fluorescent imaging. Interestingly, when attempting to treat infected mice harbouring an acute strain of *T. b. brucei*, oral administration of fingolimod and intravenous injection of SPK-843 dosed over 5 days was sufficient to clear infection below detectable levels and the lives of the animals were extended by several days. Taken together these results suggest that the hierarchical computational drug repositioning approach (2D functional-class fingerprint (FCFP4) and 3D flexible alignment similarity searches) applied here led to the discovery of a new trypanocidal drug, fingolimod and was a more targeted approach to identifying SPK-843 with other semi-rational approaches.

Table 4.2 Trypanosomal potency of repurposed leads vs current treatments

Compound	**Activity (μM IC_{50} value)**			**Original Indication**
Exposure / Assay type	**24 h / ATP assay**	**24 h / Resazurin assay**	**24 h transient / Resazurin assay**	
AmpB	9.77	1.38	-	Fungal infections, Visceral Leishmaniasis
SPK-843	0.393	1.53	8.62	Fungal infections
FTY720	0.199	0.316*	0.320	Multiple Sclerosis
FTY720P	0.437	0.145*	-	
Sphingosine	-	0.095*	-	
S1P	-	0.132*	-	
Current Treatmenst	**Activity (μM IC_{50} value)**			
Pentamidine	0.008	0.026	0.008	
Suramin	0.200	-	-	
SCYX-6759**	-	0.280	-	

*Actual time-point was 48 h
**SCYX-6759 is currently being developed by Scynexis and DnDi (http://www.dfid.gov.uk/R4D/PDF/Outputs/DNDI/steve_wring_scynexis_astmh2009.pdf)

4.4.1 Cell viability assays give different compound activities

When investigating initial *in vitro* activity and pharmacological time-course for the test compounds, there was a slight discrepancy between the compound activities seen in the resazurin reduction viability assay and luminescent ATP viability assay (see IC_{50} values for SPK-843, amphotericin B, FTY720 and pentamidine in Table 4.3). For example, the positive control pentamidine used in the Alamar Blue assay, had an IC_{50} value of 26 nM, while it was 8 nM with the CellTiter-glo assay. Why could this difference have occurred? When data was compared to those in the literature, similar IC_{50} values were attained following 24 h exposure to pentamidine when assessed with the Alamar Blue assay. Examples of pentamadine activity from studies include, 14.7 nM (Sykes et al. 2012), 15 nM (Thao et al. 2014) and as low as 4 nM and 5.97 nM (Sun et al. 2016, Faria et al. 2015). The IC_{50} value for pentamidine from the ATP assay fell within the range found in the literature, more than the IC_{50} from the Alamar Blue assay.

However, the differences between values are more likely due to the two viability assays operating on different principles. Resazurin is a cell permeable redox indicator, and cells with active metabolism can reduce resazurin into the fluorescent resorufin product (Sittampalam et al. 2004). Resazurin is required to be present in the cell media for a sufficient period of time to be metabolised into resorufin by the cells. It has been shown that the fluorescent Alamar Blue signal (quantity of resorufin produced) correlates directly with the number of *T. b. brucei* cells in a well, therefore providing a good indication of viable cell numbers (Sykes & Avery 2009). In contrast, cells in the chemiluminescence assay are immediately lysed following the addition of the Celltiter-glo reagent, releasing ATP into the surrounding media. The ATP released from the lysed cells is directly proportional to the number of cells present in the culture, making this assay more sensitive than Alamar Blue. For example, the sensitivity of detection with the Alamar Blue assay is 390 mammalian cells in a 96-well plate, while the luminescent ATP viability assay can detect as low as 50 cells, according to the Promega protocol and application guide. The different compound activities from the two assays may have been due to higher sensitivity and endpoint measurement protocol produced by the luminescent ATP viability assay.

Table 4.3 Comparison of compound activities from 2 cell viability assays at 24 or 48 h time-points

Compound	Activity (μM IC_{50} value)	
	Resazurin Reduction Assay (Alamar Blue)	**Luminescent Assay (ATP)**
SPK-843	1.53	0.393
AmpB	1.38	9.77
FTY720	0.316*	0.177*
FTY720P	0.145*	0.143*
Pentamidine	0.026	0.008

*48 h time-point, all others taken at 24 h

4.4.2 SPK & Amphotericin B do not show the same effectiveness as anti-trypanosomal agents

Liposomal amphotericin B is already being used to treat visceral leishmaniasis (causative agent is *Leishmania donovani*), while the structurally similar SPK-843 is an antifungal that is currently in Phase III clinical trials for the treatment of pulmonary mycosis (ClinicalTrials.gov) and has exhibited efficacy in other bacterial infections. Currently there are no published studies on the use of these antifungals as treatment for *Trypanosomal brucei* infections. Since SPK-843 and AmpB are able to target the ergosterol in fungi, yeast, and other protozoa it was hypothesised that they might possess anti-trypanosomal properties and possibly through a similar mechanisms of action (by binding to sterols and create pore-forming complexes). Significantly, both antifungals were potent towards *T. b. brucei.* The efficacy of these compounds against *T. b. brucei* is important at it supports the idea that compounds that modulate the activity of a conserved parasite target (ergosterol) between parasites of similar biology and genomic sequences (*T. brucei*, *T. cruzi*, *Leishmania*) can be effective and may be repurposed as anti-trypanosomal therapeutics.

Interestingly, even though these two lead candidates are structurally similar, SPK-843 induced parasite death *in vitro* much more rapidly and with a greater efficacy than AmpB (Figure 4.8) and most significantly was better able to supress parasitemia in an *in vivo* model of trypanosomiasis (Figure 4.11). Due to the lack of studies on the use of these antifungals against *T. brucei,* their actions against other indications are compared

to the data in this study. In agreement with our results, studies that assessed the antifungal activity of SPK-843 and AmpB against clinical isolates of yeasts and fungi *in vitro* have shown SPK-843 to be similar or more potent than AmpB. For example, SPK-843 has better inhibitory activity than amphotericin B against filamentous fungi of *Aspergillus spp*, and similarly potent against *R. oryzae*, *P. variotii*, *Penicillium spp*., and *S. schenkii* (Rimaroli & Bruzzese 2000). Better activity against *fungi: Candida albicans* (Strippoli et al. 2000), *Candida glabrata, Candida krusei* and *Candida tropicali,* and higher activity towards *yeasts: S cerevisiae, C neoformans* (Rimaroli & Bruzzese 1998). Further studies showed SPK-843 possessed *in vitro* inhibitory activity comparable to or better than that of AmpB against *Candida spp*., *Cryptococcus neoformans*, and *Aspergillus spp*. (Senda et al 2000, Kantarcioglu et al. 2003).

A similar case can be seen with studies investigating fungal/yeast clearance *in vivo*. In a murine model of systemic candidiasis, after five doses of intravenous therapy at 0.8 mg/kg, SPK-843 completely eradicated the pathogen in eight out of ten mice, whereas the same dose of D-AMPH (amphotericin B deoxycholate) had no effect (Senda et al 2000). In another different study, a lower concentration of SPK-843 (0.25 mg/kg) compared to amphotericin B (1 mg/kg), micafungin (4 mg/kg) or voriconazole (16 mg/kg) was enough to eradicate *C albicans* in a mouse model (Senda et al 2000). Furthermore, SPK-843 exhibited dose-dependent efficacy on murine pulmonary aspergillosis models and SPK-843 doses of higher than 1.0 mg/kg of body weight exhibited no renal toxicities and a tendency toward better survival prolongation than the estimated maximum tolerated doses of amphotericin B (Fungizone) (1.0 mg/kg) and liposomal amphotericin B (AmBisome) (8.0 mg/kg) (Kakeya et al. 2008). The mechanism behind the difference in potency between the two compounds is not fully understood, but one possibility is different modes of action.

4.4.3 Different mechanism of action between SPK-843 & Amphotericin B

One obvious possibility to account for the difference between SPK-843 and amphotericin B efficacy towards *T. b. brucei in vitro* and *in vivo* is a difference in their respective mechanism of action. For example, AmpB has been shown to induce cell death in *Leishmania donovani* by binding to sterols in the cell membrane causing aqueous pore formation and as a result cells become permeable to small cations, anions and the negative plasma or surface membrane potential collapses (Saha et al. 1986,

Ramos et al. 1996). In this study, it was clear that AmpB parasite killing was likely due to disruption/permeabilisation of the plasma membrane, as demonstrated by the entry of fluorescent propidium iodide into the cells in the permeability assay (Figure 4.8). Approximately, 50% of cell population was permeable to propidium iodide after 70 min following treatment with the lethal concentration of AmpB (33 μM, IC_{50} of AmpB at 3 h was 37.9 μM), which is a reasonable indication that membrane disruption was the primary mechanism of action for the anti-trypanosomal property of AmpB.

The *T. brucei* parasite encounters diverse environments during its life cycle, and in the different hosts take on very different sterol compositions. Of particular interest is the variance in the ergosterol homoeostasis, which is poorly understood (Haubarich et al 2015). Studies indicate that ergosterol is the major sterol of *T. brucei* procyclic cells (Dixon et al. 1972; Gros et al. 2006; Furlong 1989). In mammalian hosts where cholesterol may be abundant (i.e. in humans), the ergosterol pathway is significantly downregulated in BSF and sterol requirements are met via receptor-mediated endocytosis of host cholesterol (Coppens et al. 1988). As a result, it has long been held that *T. brucei's* ability to scavenge cholesterol from their animal hosts, and their inability to undergo sterol biosynthesis in this adaptive stage, makes them resistant to antiparasitic drugs that target ergosterol or ergosterol biosynthesis (Gros et al. 2006; Hinshaw et al. 2003). However, it has since been demonstrated that *T. brucei* BSF satisfy two different functions with the two sterols: exogenous cholesterol (from the host) functions as structural component in membranes, while there is endogenously formed ergosterol that functions as a signal molecule, essential to their growth and survival (Nes et al. 2012, Roberts et al. 2003). Interestingly, one study showed that in cases in which cholesterol from the diet is minimal for BSF, the ergosterol pathway is upregulated (Zhou et al. 2007). Alternatively, in cases in which cholesterol availability is significant, the endogenous pathway to ergosterol is downregulated but not eliminated.

Results from the *in vitro* assays in this study showed AmpB to be a potent trypanosomal agent (Figure 4.7 & 4.8), while in our *in vivo* experiment liposomal amphotericin B was unable to slow down or clear trypanosome infection. One possible reason for this could be that there is less cholesterol available in the media containing 10% FCS under *in vitro* conditions while there is in 100% mouse serum in an animal model and this could effect the level of ergosterol biosynthesis in the parasites and the available ergosterol in the plasma membranes. In addition, it has been shown, that AmpB is ~500 times more

selective for ergosterol than cholesterol (Golan et al. 2011), while concurrently molecular modelling studies have shown that AmpB channels were more stable in the presence of ergosterol-containing as compared to cholesterol-containing membranes (Baginski et al. 2002). Interestingly, a study using the polyene antibiotic nystatin, showed that the ability of nystatin to permeabilise ternary lipid vesicles and the rate of pore formation was dependent on the ergosterol/cholesterol molar ratio of the lipid vesicles (Silva et al. 2006). Thus, it is proposed here that due to the larger quantity of cholesterol available in the host for the parasites to scavenge, the ergosterol pathway was more down-regulated than under *in vitro* conditions and there was not enough ergosterol in the trypanosome membrane for liposomal amphotericin B to bind to and form stable pore-inducing complexes with. Overall, this suggests that the presence of ergosterol in the parasite membrane, to which AmpB can bind to and create pores, is necessary for the trypanocidal action of AmpB.

In contrast, the same propidium iodide permeability assay (Figure 4.10 A) showed no significant fluorescence in the cells treated with above lethal concentrations of SPK-843. The IC_{50} of SPK-843 at 3 h was 3.65 μM (determined with ATP assay) and the highest concentration of SPK-843 used in this permeability assay was 33 μM, thus increasing concentration or time would not lead to permeabilisation. This result indicates intact cell membranes and that the mechanism behind parasite death was something other than membrane permeabilisation. No studies have examined the use of SPK-843 as a treatment for protozoan infections, so comparisons were drawn from results of fungicidal studies. A study assessing the killing action of SPK-843 and amphotericin B on the *Candida albicans* showed that they induced leakage of K^+ ions (Strippoli et al. 2000). However, this fungal study result does not fit with the data presented here showing no permeation occurring in *T. b. brucei* following lethal doses of SPK-843. Furthermore, our *in vivo* study showed SPK-843 was able to extend the life of our acute mouse model of trypanosomiasis by dampening down parasitemia (Figure 4.11), unlike liposomal amphotericin B, which was not able to extend the life of the animals.

A recent study Gray et al challenged the widely accepted model of AmpB killing yeast primarily via channel-mediated membrane permeabilisation (Gray et al. 2012). Alternatively, they showed that AmpB primarily killed yeast by simply binding ergosterol, a lipid that is vital for many aspects of yeast cell physiology, including vacuole fusion (Kato & Wickner 2001), endocytosis (Heese-Peck et al. 2002),

pheromone signalling (Jin et al. 2008), membrane compartmentalization (Klose et al. 2010), and the proper functioning of membrane proteins (Zhang et al. 2010). They suggest that membrane permeabilisation via channel formation represents a second complementary mechanism that further increases drug potency and the rate of yeast killing (Figure 4.23 D). In addition, a study showed another antifungal polyene macrolide natural product, natamycin, was shown to bind ergosterol directly without causing membrane permeabilisation of vacuoles isolated from yeast (te Welscher & Jones 2010). It was proposed that a similar mechanism of action is occurring when treating *T. b. brucei* with SPK-843 (Figure 4.23 C). While it was predicted that the hydroxyl group on carbon35 of AmpB (Figure 4.23 B) is critical for ion channel self-assembly as seen in Figure 4.23 D, SPK-843, even though structurally similar, has a functional group in place of this hydroxyl group (Figure 4.23 A) that could potentially impede the ion channel self-assembly. The sterols ergosterol and 24-methyl sterols are critical for *T. brucei* growth and viability (de Souza & Rodrigues 2009) so it is highly possible that simply binding these sterols would impede necessary cell functions.

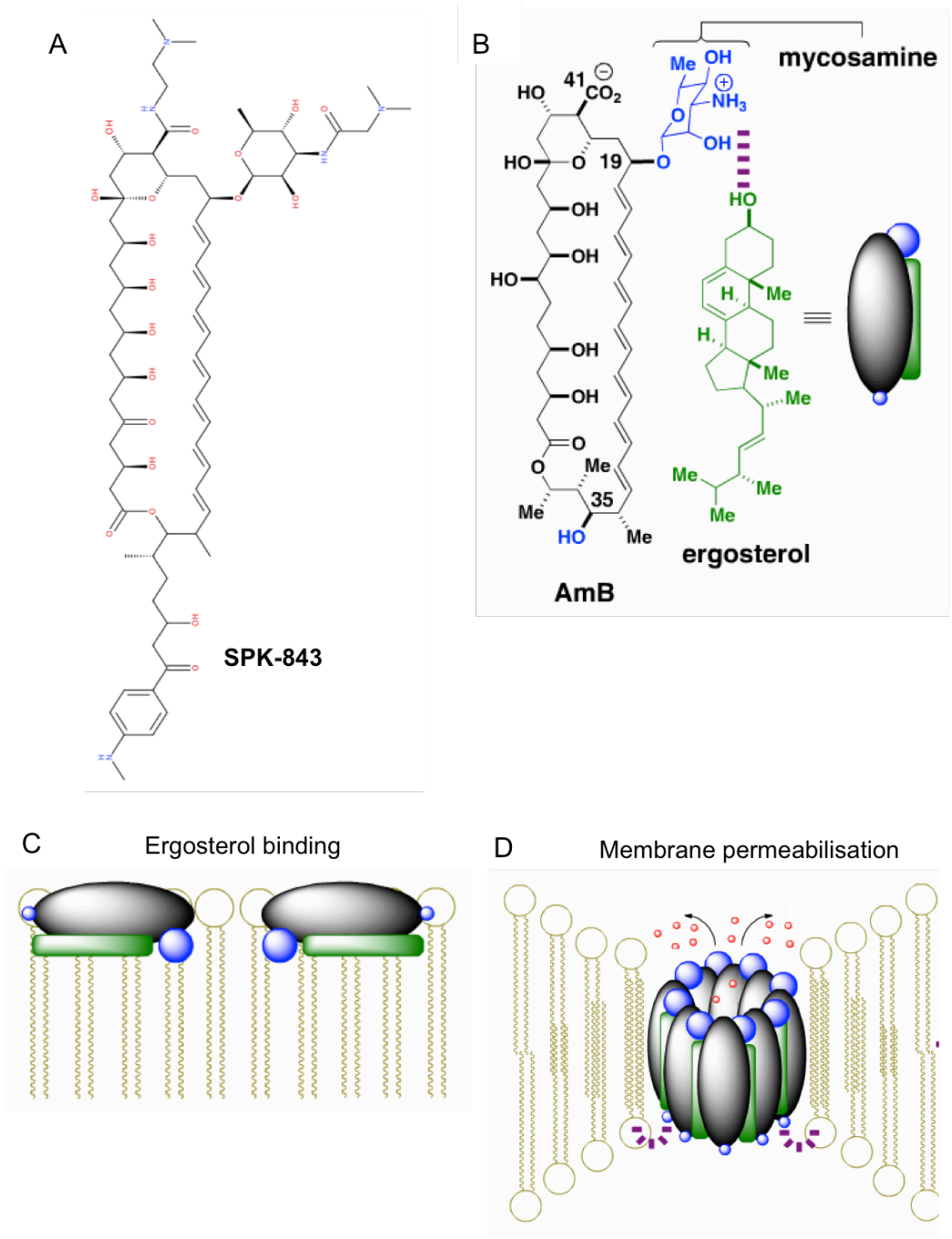

Figure 4.23 Suggested mechanistic difference behind the anti-trypanosomal activity of SPK-843 and ampothericin B. **(A)** Molecular structure of SPK-843 in comparison to **(B)** molecular structure of amphotericin B bound to an ergosterol molecule. Representations of the two mechanisms of action for antifungal activity of AmpB as suggested by Gray et al (2012): **(C) primary mechanism** of simply binding of antifungals to ergosterol within plasma membrane **(D) secondary mechanism** of membrane permeabilisation following channel formation. Importance of hydroxyl group on C35 in blue in (B) is critical for ion channel self-assembly, as indicated with the purple squares in (D). Adapted from Gray et al. (2012).

4.4.4 SPK & Amphotericin B overall efficiency compared to current HAT treatments

Prolonged period of treatment (24 h) with SPK-843, was on par with the HAT drug suramin, as seen by the similar IC_{50} values: 0.393 μM and 0.2 μM, respectively (Figure 4.8). SPK-843 however was slightly less potent and less robust at killing when compared to the current HAT treatment pentamidine in drug-washout experiments (Figure 4.9). Overall, SPK-843 was able to extend the life of mice an in acute model of trypanosomiasis. However, 95% of Human African Trpanosomiasis cases are caused by the chronic infective parasite, *T. b. gambiense*, so a chronic model of infection is more representative of typical cases. If, SPK-843 is capable of slowing down an acute disease model, it is possible that it may be capable of clearing parasitemia in a chronic disease model. These results may suggest that the *in vitro* potency of SPK-843 is more moderate than pentamidine and that a continuous drug exposure of SPK-843 for longer treatment regimen is necessary for trypanosomal killing and clearance. Indeed, in a study where AmBisome was tested in a murine model of Chagas disease (American trypanosomiasis), another protozoan indication, AmBisome was capable of extending the life of the infected animals and reducing the *T. cruzi* load in most tissues, but was not able to completely clear the infection (Cencig et al. 2011). In this it was suggested that AmBisome might be a good drug to use concomitantly with current drugs. Due to the broad-spectrum of activity and the low frequency of resistant pathogens to AmpB seen in antifungal disease/treatment (Kasanah et al 2005) it is useful to consider further investigations into SPK-843. It is proposed here that SPK-843 might be effective in combination use with current HAT drugs. These results demonstrate that SPK-843 promising drug hits/lead and they have the potential to become trypanosomal agents, to be used for further investigations, but eventually join the list of those in line to be clinically tested.

4.4.5 Fingolimod trypanocidal activity

Fingolimod is currently approved as an oral treatment for relapsing forms of Multiple Sclerosis. The mode of action appears somewhat complex, as fingolimod acts as a functional agonist to S1P receptors but also interferes with sphingolipid de novo biosynthesis. Interestingly, all four sphingoid base analogues or sphingolipid derivatives FTY720, FTY720P, sphingosine, and S1P displayed potent concentration- and time-dependent anti-trypanosomal properties when examined via time-kill experiments in this study. A summary of submicromolar IC_{50} values following Alamar blue and ATP viability assays is presented in Table 4.2 (IC_{50} = 0.095 – 0.437 µM). The efficacy of these compounds against *T. b. brucei* is important for a number of reasons: a) it validates the computer-aided drug design (CADD) similarity search, b) it agrees with the hypothesis that the phosphorylated and un-phosphorylated version would both have an effect on parasite viability, c) it demonstrates that these compounds meet part of the criteria for the selection of hit compounds for Human African Trypanosomiasis defined as possessing IC_{50}s of < 10 µM by the Drugs for Neglected Diseases *initiative* (DND*i*) (Don & Ioset 2014), and d) they may have a similar mechanism of action to each other and may target the same part of the sphingolipid synthesis pathway.

A recent study by Jones et al (published in 2016) screened a large library of compounds and identified fingolimod as a potent selective anti-trypanosomal agent (Jones et al. 2016). This is the only study to date examining the efficacy of fingolimod and other sphingoid compounds against *Trypanosome brucei*. The authors evaluated the efficacy of FTY720, both FTY720P enantiomers (S and R), and sphingosine, among other related sphingolipids, against various *T. brucei* species *in vitro* and *in vivo* and they showed all four to be very potent at killing *T. b. brucei* (see Table 4.4). Jones et al (2016) reported IC_{50} values of a slightly lower potency than in this study (Table 4.4) using the same Alamar Blue assay. The authors did not, however, investigate any specific pharmacodynamics, while it was demonstrated in this study that the trypanocidal action of FTY720 is irreversible and that parasite killing occurs faster with FTY720 than FTY720P.

Table 4.4. Comparison of *in vitro* trypanocidal activity of compounds agaisnt *T. brucei brucei* BSF.

Compound	Activity (μM IC_{50} value ± SD)*	
	This study	**Jones et al (2015)**
FTY720	0.316 ± 0.10	0.59 ± 0.01
FTY720P	0.145 ± 0.03	1.21 (S), 1.98 (R)
Sphingosine	0.095 ± 0.03	1.26 ± 0.35
Sphingosine-1-phosphate	0.132 ± 0.06	--

***** All values determined with Alamar Blue viability assay and activity (IC_{50}) values given as μM as determined by non-linear regression analysis of curve-fitting and ±SD calculated based on the average of triplicate values from two-three independent experiments.

4.4.6 Limitations of the *in vivo* experiment

The *in vivo* data presented here also contrast the data obtained by Jones et al (2015). This study demonstrated the ability of oral administration of FTY720 (1 mg/kg/day) to reduce significantly the parasite load in a highly virulent animal model of trypanosomiasis (strain *Lister 427*) for a mean of 4 days (Figure 4.22). Whereas, Jones at el (2015) stated that there was no effect in the animal model used in their study, though, these data were not shown (Jones et al. 2015). It is important to note that *Lister 427* is a highly virulent monomorphic strain, which consists solely of the 'slender' form *T. b. brucei*, responsible for the rapid killing triggered by uncontrollable growth *in vivo* (mice exposed to high parasitemia, exceeding 10^9 parasites/mL of blood die if not culled). Future *in vivo* studies may benefit from the alternative use of a pleomorphic strain instead, in which the mammalian immune system induces some trypanosomes to differentiate from the proliferating long slender form to the non-replicative 'stumpy' forms in order to maintain a chronic and sublethal level of parasitemia. This would be more representative of HAT caused by the chronic infective parasite *T. b. gambiense*. A sub-chronic or chronic animal model could be used to better explore dose-exposure-response relationships and could also be utilized to determine an effective concentration range of the fingolimod against trypanosomiasis.

4.4.7 Potential mechanism behind trypanocidal action of FTY720

The mode of action of FTY720 against *Trypanosoma brucei* is partly due to disruption of cell division, as shown by the presence of cells with atypical DNA content (abnormal K/N ratios), but the exact mechanism of action remains to be established (Figure 4.17 – 4.21). In order, to investigate whether trypanosomes have S1P receptors (S1PR) or receptor-like proteins a BLAST analysis was conducted against both human S1P receptor protein and gene sequences (tritypdb.org). This analysis resulted in no matches with trypanosome proteins, while the 50 gene sequence matches all scored 44 and below out of 100, too low to be significant. The lack of S1PRs or receptor-like proteins in *T. brucei* ruled out fingolimod mode of action to be through plasma membrane receptor binding.

As observed for FTY720 and FTY720P, sphingosine and sphingosine 1-phosphate also exhibited strong growth suppression of both BSF and PCF forms of *T. b. brucei* (Figure 4.13 & Table 4.4). Therefore, it is possible that fingolimod may act through the same pathway as the endogenous structural analogues, sphingosine. On moving from the insect vector to the mammalian host, *T. b. brucei* is required to be highly adaptive and it adapts to these new environments via morphological and metabolic changes, including lipid content and localisation (Smith & Bütikofer 2010). Both BSF and PCF trypanosomes do not utilise phospholipids scavenged from their hosts, but use their repertoire of metabolic and anabolic enzymes to de novo synthesise their own phospholipids and glycolipids for their specific requirements (Dixon et al. 1971; van Hellemond & Tielens 2006). Typical phospholipids found in these parasites include: phosphotidylcholine (PC), phosphatidyl-ethanolamine (PE), phosphatidylinositol (PI), phosphatidylserine (PS), whilst the typical sphingophospholipids are sphingomyelin (SM), inositol phosphorylceramide (IPC) and ethanolamine phosphorylceramide (EPC)(Dixon & Williamson 1970; Patnaik et al. 1993; Sutterwala et al. 2007; Sutterwala et al. 2008).

Significantly, a number of findings have shown that inhibition of various enzymes in the sphingolipid de novo pathway result in parasite death with aberrant cytokinesis and abnormal DNA content (Figure 4.24). First, serine palmitoyltransferase (SPT) catalyses the first reaction step in sphingolipid biosynthesis, condensation of palmitoyl CoA and serine to generate keto-dihydrosphingosine (3-KDS) (Hanada 2003). SPT is suggested to be a key enzyme for the regulation of sphingolipid levels in cells, preventing harmful accumulation of metabolic sphingolipid-intermediates including sphingoid bases and

ceramide (Hanada 2003). Depletion of SPT subunit 2 by both RNA interference and inhibition with myriocin in PCF parasites has been shown to result in substantially reduced levels of inositolphosphorylceramide, and incomplete cleavage furrow formation, promoting aberrant cytokinesis, delayed kinetoplast segregation and polyploidy (Fridberg et al. 2008).

Secondly, RNAi silencing of sphingolipid synthases (TbSLS1-4) has been shown to lead to growth arrest and trypanosomal cell death (Sutterwala et al. 2008). Sutterwala et al (2008) showed that after 24 h of dsRNA induction cellular morphology was significantly disrupted, cell division stopped while DNA and organelles replication continued, giving rise to cells containing multiple nuclei, kinetoplasts and flagella. RNAi silencing of the TbSLS locus also lead to elevated ceramide levels. Thirdly, Pasternack et al (2015) demonstrated attenuated cell division, microtubule elongation at the posterior tip, and altered organelle positioning through RNA interference-mediated depletion of sphingosine kinase (TbSPHK) in PCF *T. brucei*, as well as, BSF cell death following low micromolar treatments of specific SPHK inhibitors (IC_{50} of 1.5 μM and 12. 8 μM for dimethylsphingosine and L-threodihydrosphingosine (safingol, respectively) (Pasternack 2015). Parasite cell death was further demonstrated following the use of the sphingosine kinase inhibitors CAY10621, PF543, SKI2 in all three *T. brucei* subspecies (Jones et al. 2016).

Due to the critical importance of sphingolipid de novo synthesis for trypanosome viability, it is tempting to speculate that the mode of FTY720 killing trypanosomes may in part be by inhibiting de novo sphingolipid synthesis. Specifically, by inhibiting the trypanosomal enzymes involved in controlling the S1P, sphingosine, and ceramide (all bioactive intermediates) signal molecule formation and accumulation, as is the case in mammalian cells (Patmanathan et al. 2015), see Figure 4.24. Fingolimod has been reported to inhibit sphingosine kinase 1 (SPHK1), an enzyme that catalyzes the phosphorylation of sphingosine to produce the bioactive S1P in mammalian cell lines and induced apoptosis (Tonelli et al. 2010; Pchejetski et al. 2010). While also demonstrating cell death following the use of sphingosine kinase inhibitors CAY10621, PF543, SKI2 in all three *T. brucei* subspecies, Jones et al (2016) were unable to find a direction correlation between SPHK inhibition and the trypanocidal activity of FTY720 (Jones et al. 2016).

Additionally, FTY720 but not FTY720-P was shown to inhibit S1P lyase, which degrades S1P to ethanolamine phosphate and (*E*)-2-hexadecenal and regulates the removal of sphingoid bases from the pool of sphingolipids (Bandhuvula et al. 2005). Furthermore, FTY720 has also been demonstrated to inhibit mammalian ceramide synthases through a competitive inhibition of dihydrosphingosine and thus affecting the intracellular balance of signalling sphingolipids (Berdyshev 2009). In the presence of FTY720, cellular levels of dihydroceramides, ceramides, sphingosine and S1P decreased, while dihydrosphingosine and dihydrosphingosine 1-phosphate (DHS1P) levels increased (Berdyshev 2009). Furthermore, Lahiri et al (2009) demonstrated FTY720 also inhibited ceramide synthase activity, which resulted in elevated levels of ceramide, sphingomyelin, and hexosylceramides (Lahiri et al. 2009). Overall, these results suggest that FTY720 and analogues may have utility in regulating sphingolipid bioactive intermediate production and their signalling cascades involved in trypanosome cell death, but no direct correlation has been shown in the literature or in this current study.

Interestingly, the onset of killing occurred more rapidly with FTY720 than for FTY720P in the 'time-to-kill' assay, whereby a sub-micromolar IC_{50} occurred after 8 h exposure to FTY720, which in contrast took 24 h following FTY720P treatment. A possible reason why FTY720 has a more rapid effect is due to the preferred uptake/affinity for FTY720 over FTY720P at endocytotic vesicles at the flagellar pocket. Alternatively, the two sphingoid compounds may inhibit different enzymes in the de novo sphingosine synthesis pathway, or perhaps FTY720P has to be converted to FTY720 before it is capable of killing the cells.

Interestingly, all four sphingoid compounds tested (FTY720, FTY720P, sphingosine, S1P) showed approximately an order of magnitude more potent trypanocidal activity against BSF compared to PCF cells (EC_{50} values seen in Figure 4.12 & 4.13). This difference in potency may be due to the difference in the rates of endocytosis of the two life stages. Both BSF and PCF scavenge phospholipids from their hosts and since both FTY720 and FTY720P are highly protein bound, (99.7%, mainly to albumin; Portaccio 2011; Guarnera et al. 2017) they would be taken up by the parasites. In *T. brucei*, endocytosis and exocytosis occur exclusively at the flagellar pocket and both bloodstream and procyclic trypanosomes are capable of internalizing macromolecules (Liu 2000). However, the flagellar pocket volume for the bloodstream form is approx. 3-fold larger than that in the procyclic form (Webster & Shapiro 1990) and it has been shown that procyclic form

trypanosomes take up fluid-phase markers at a rate much slower than in BSF (LANGRETH & LBER 1975). Thus the PCF rely less on the uptake of proteins from the host, and would have internalized the test compounds at a slower rate.

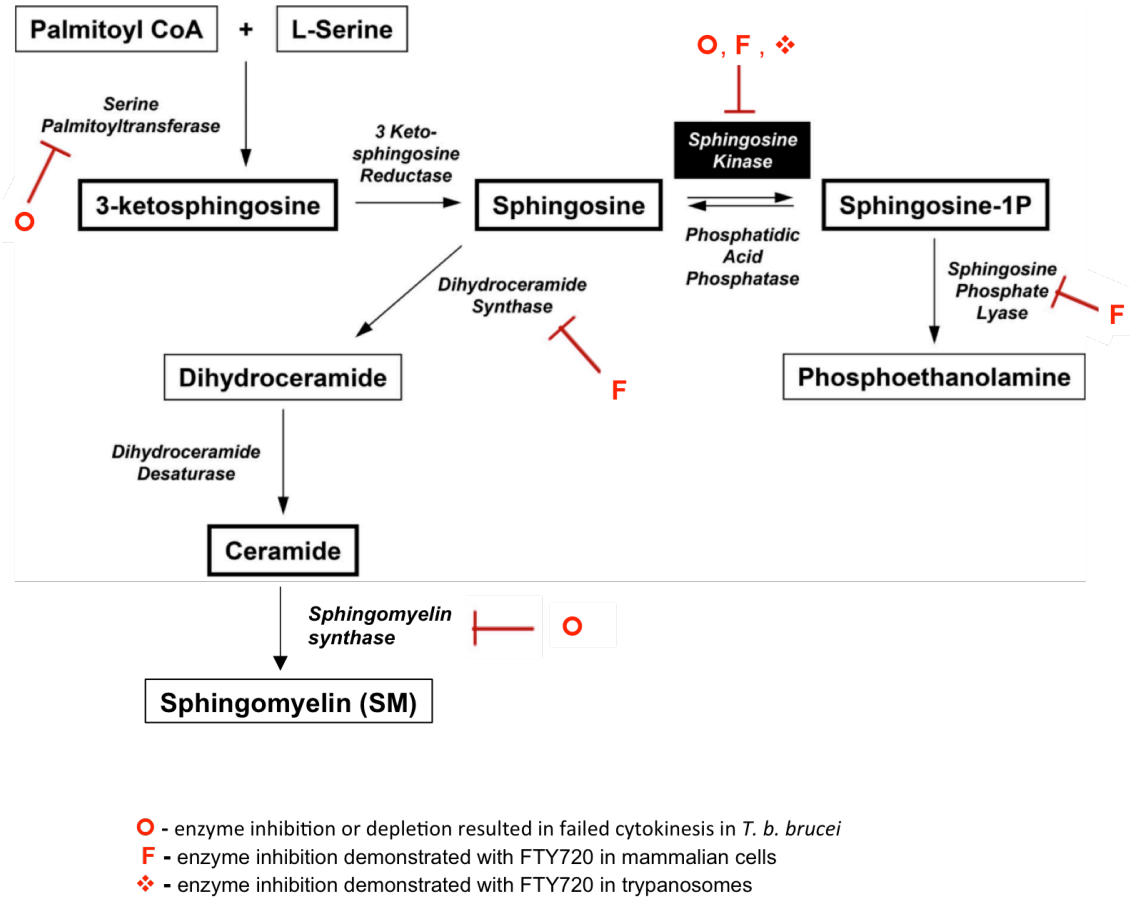

O - enzyme inhibition or depletion resulted in failed cytokinesis in *T. b. brucei*
F - enzyme inhibition demonstrated with FTY720 in mammalian cells
❖ - enzyme inhibition demonstrated with FTY720 in trypanosomes

Figure 4.24 Sphingosine metabolic pathway in Trypanosomes. The de novo biogenesis of sphingolipids begins with the condensation of serine and palmitoyl CoA by serine palmityoltransferase. Bioactive sphingolipids (bold outlined), generated by de novo or via breakdown of sphingomyelin, function as potent regulators of cellular proliferation and survival. Sphingosine phosphate lyase catalyzes the irreversible cleavage of S1P to phosphoethanolamine, facilitating movement of bioactive sphingolipids into the ethanolamine biosynthesis pathway. Sphingosine may also be converted to dihydroceramide and then to ceramide, through the actions of dihydroceramide synthase and desaturase, respectively, then sphingomyelin by sphingomyelin synthase. Inhibition or knockdown of enzymes in the de novo pathway in *T. b. brucei* has been shown to result in cell cycle arrest and cell death (Hanada 2003;

Fridberg et al. 2008; Sutterwala et al. 2007; Pasternack et al. 2015). FTY720 has been reported to inhibit some of these enzymes (Bandhuvula et al. 2005; Berdyshev et al. 2009; Lahiri et al. 2009; Tonelli et al. 2010; Pchejetski et al. 2010; Jones et al. 2015). Image adapted from Pasternack et al (2015).

CHAPTER 5. Final Discussion

5.1 Clinical relevance

The need for new drugs drives antiparasitic drug discovery research globally and requires a range of innovative strategies to ensure a sustainable pipeline of lead compounds. The DNDi highlighted in their Target Product Profile (TPP) that an ideal candidate for drug research and development for the treatment of HAT requires safe, effective, and practical stage 2 drug to replace current first-line treatments, and to improve and simplify the current case management. Ideally, TPP includes: a new treatment for adults and children effective against both stages of the disease and both parasite sub-species, non-toxic, have at least 95% efficacy at 18 months post end of dosing follow-up examination, effective in melarsoprol refractory patients, cidal, multitarget, be safe for pregnant and breastfeeding women, easy to use (short-course or once a day), oral, require no monitoring, affordable, and adapted to tropical climates.

How do the tested compounds vinyl sulfone dipeptides, SPK-843, amphotericin B, fingolimod measure up against these TPP criteria seen in Table 5.1? In the case of vinyl sulfones, K777 has been shown to kill *T. b. brucei in vitro* (Dunny et al. 2013), as well as in combination with eflornithine *in vitro* (Steverding 2015), which could indicate its effectiveness potentially in Stage 1 HAT. Not much is known in terms of vinyl sulfone broad-spectrum effect on *T. b. gambiense* or *rhodesiense*. Additionally, oral administration of K777 for 14 days at 50 mg/kg twice daily in a study of *T. cruzi* infection in the dog was sufficient to protect against cardiac damage (Barr et al. 2005). Vinyl sulfones have the potential for an oral formula and that would make treatment administration easier. Consequently, it may be possible to create an oral formula for the more active 1-naphthyl vinyl sulfone, compound 29.

AmBisome (liposomal ampothericin B) may have the potential to treat Stage 1 HAT as this study showed how ampothericin B is effective against *T. b. brucei in vitro*. Large clinical experience exists in the successful use of different AmpB preparations for other CNS infections in humans, despite the lack of measurable CSF AmpB concentrations (Kethireddy & Andes 2007). Which may suggest the possible use of AmBisome against second stage HAT. The mechanism of action is suggested to be through pore formation in trypanosome plasma membrane as it has been shown in treating Leishmaniasis, liposomal AmpB binds to parasite ergosterol precursors causing membrane disruption, resulting in cell death, and amphotericin B formulations may thus be effective in

melarsoprol refractory patients. In terms of adult & paediatric formulations: AmpB of adult dosing, and pediatric patients (302) have been given to treat fungal infections.

SPK-843 has the potential to cure Stage 1 HAT as this study showed it kills *T. b. brucei in vitro* and also slowed down parasitemia in an animal model, however further. There is no clinical data to support the potential use for Stage 2 HAT. Mechanism of action and route into the cell are unknown, there is little clinical evidence thus far in the literature that would help support SPK-843 and so it is not known if it would be effective in melarsoprol refractory cases.

Significantly, fingolimod is known to readily penetrate the CNS and may provide promise for future treatment of both haemolymphatic and meningoencephalitic stages of trypanosomiasis. Fingolimod has been shown to not only decrease the permeability of the blood-brain barrier but also to cross it, where it is phosphorylated by endogenous SPHKs in the CNS. It has been well established that brain levels of both forms are >10 times higher than in the blood in both rats and humans, which could be harnessed to also treat stage 2 of the disease. Follow-up studies will be needed to determine the efficacy of fingolimod in this regard as well. A clinical study showed no difference in incidence of mortality between treatment groups when used for treating MS patients (up to 5 mg/kg), supporting the safe use of fingolimod (Francis et al. 2010). Breast-feeding during fingolimod treatment is not advised (Novartis Pharmaceuticals, Product Information) and there is known risks of teratogenicity in animals and humans (Karlsson et al. 2014). Overall, fingolimod presents the most attractive potential as a new HAT candidate out of the compounds tested here to due having the capability of passing into the CNS, the oral formulation, as well as the extensive safety data from clinical studies for other diseases (MS and immonumodulation).

Table 5.1 DNDi* target product profile (TPP) criteria for treating sleeping sickness with current treatment NECT. According to the DNDi website, first priority of TPP is "the development of a safe, effective, and practical stage 2 HAT drug to replace current first-line treatments, and to improve and simplify the current case management".

TPP1 criteria	**Current treatment – NECT***
Effective against stage 1 & 2	Stage 1 + 2 (used stage 2 only)
Broad Spectrum (*gambiense* & *rhodesiense*)	gambiense
Clinical efficacy >95% at 18 months follow up	Clinical efficacy: 96.5% (ITT NECT Study)
Effective in melarsoprol refractory patients	Effective
<0.1% drug related mortality	1.2% possibly related mortality (NECT field)
Safe during pregnancy and for lactating women	No specific adverse event found in babies born or being breastfed after treatment (NECT field)
Adult & paediatric formulations	DFMO paediatric dosing available + Nifurtimox 5 mg tablets to be cut
No monitoring of AEs	Hospitalization required
<7 days p.o. once daily (DOT)	7 days IV infusion (bid) + 10 days po (tid)
<7 days i.m. once daily	
Stability in Zone 4 for >3 years	Stability in Zone 4 for > 24 months
Cidal	DFMO static + Nifurtimox cidal
Multitarget	
< 30 € / course (only drug cost)	222.5 € / course (in 4 treatments kits; WHO)

*DNDi website: http://www.dndi.org/diseases-projects/hat/hat-target-product-profile/

5.3 Conclusion & suggestions for further research

The protozoan parasite *Tryapnosoma brucei* is responsible for causing sleeping sickness, which if left untreated eventually leads to coma and death. It is highly adapted for immune evasion, especially when it has reached the meningo-encephalic stage, while also showing resistance to current Human African Trypanosomiasis (HAT) treatments (eflornithine, melarsoprol, nifurtimox) (Lutje et al. 2010). New treatments are desperately needed as current therapeutics are highly toxic (e.g. Melarsoprol) and generally difficult to administer (Nifurtimox combined with Eflornithine; NECT). Unlike traditional drug discovery, drug repositioning offers the chance to reduce some of the inherent risk associated with drug development and the potential to fill NTD pipelines and bring a New Chemical Entity (NCE) to market. Drug repurposing through computational methods is an attractive option for pharmaceutical companies' drug development and delivery while simultaneously reducing the associated costs and they can also provide the tools and understanding needed to develop second-generation drugs. In an effort to repurpose oral FDA-approved drugs for the treatment of trypanosomiasis 2D functional-class fingerprint, FCFP4 and 3D flexible alignment computational approaches were undertaken and similarity searches led to the identification of FTY720. This study showed fingolimod to be potent *in vitro* against *T. b. brucei* and slow down infection *in vivo* against. SPK-843 and the 1-naphthyl vinyl sulfone (compound 29) analogues also demonstrated efficacy against *in vitro* BSF *T. b. brucei* and further investigations would allow these compounds to stay in the drug development pipeline.

It is well established that drug combination regimes often achieve greater therapeutic efficacy than monotherapies (e.g. in the treatment of cancer, AIDS and tuberculosis). Drug combinations may be less toxic than monotherapy regimes and have the additional advantage of reducing the risk for development of drug resistance. This is because drug combinations may interact synergistically, i.e. their combined effect may be greater than the sum of their separate effects (Chou, 2006). Thus for future experiments, it would be worth investigating combination use of fingolimod with current HAT treatments as well as further testing in a chronic disease model with longer treatment times.

Appendix

A1. Schematic structures of dipeptide vinyl sulfone compounds 13-53 designed and synthesized by Paul Evans and his group, University College Dublin.

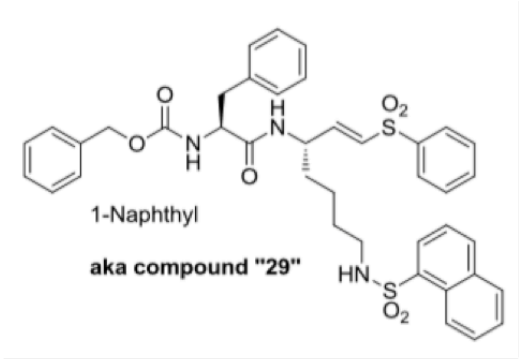

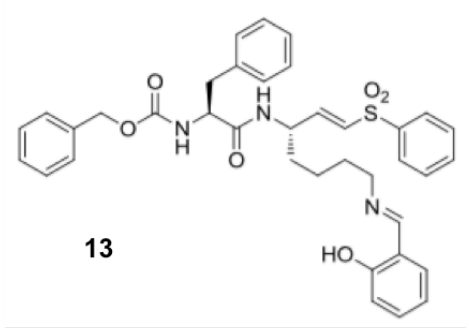

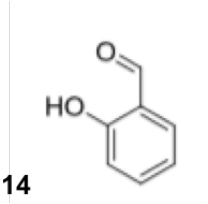

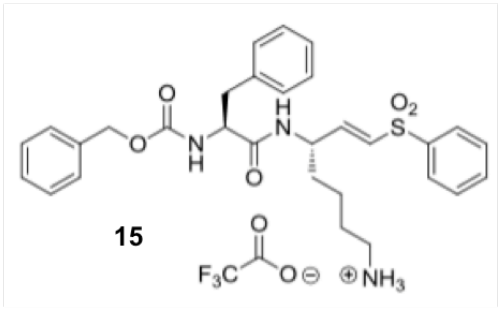

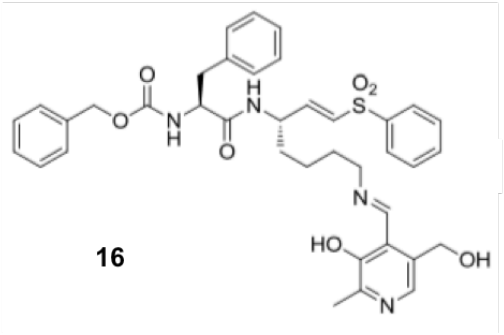

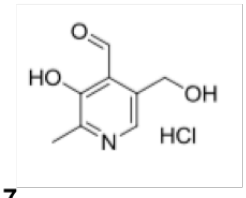

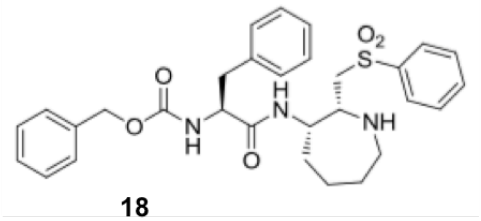

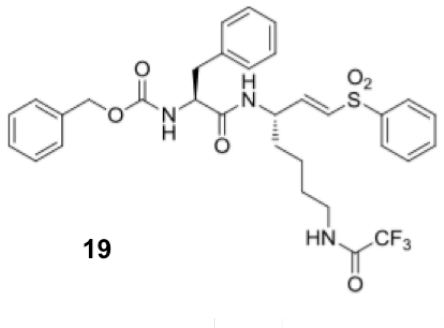

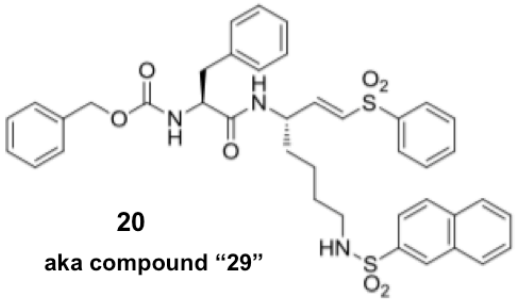

20

aka compound "29"

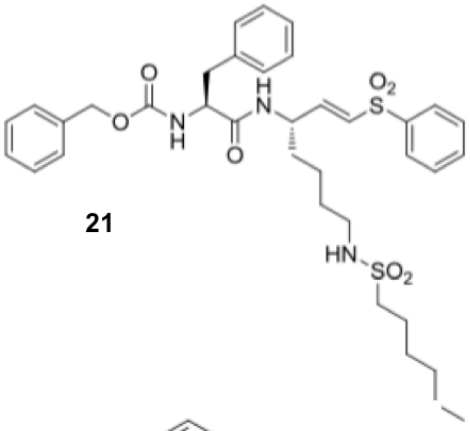

21

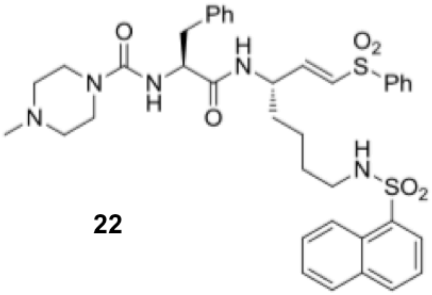

22

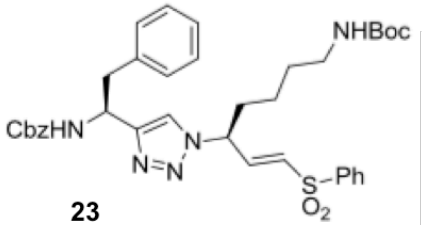

23

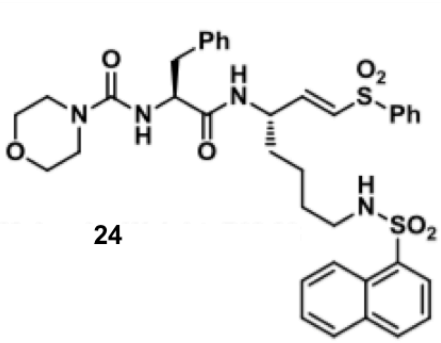

24

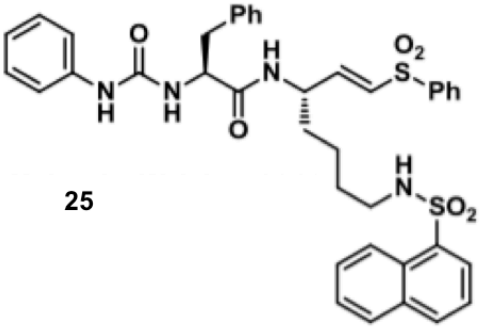

25

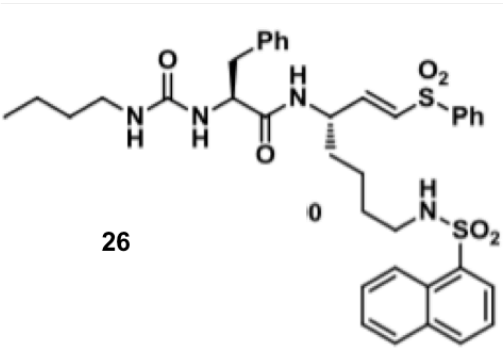

26

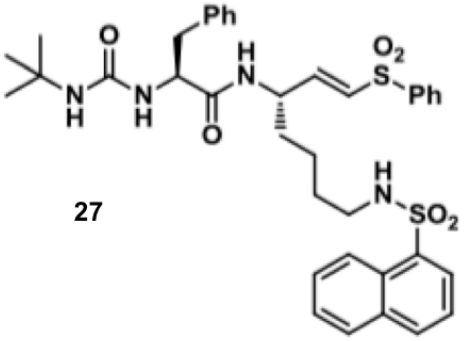

27

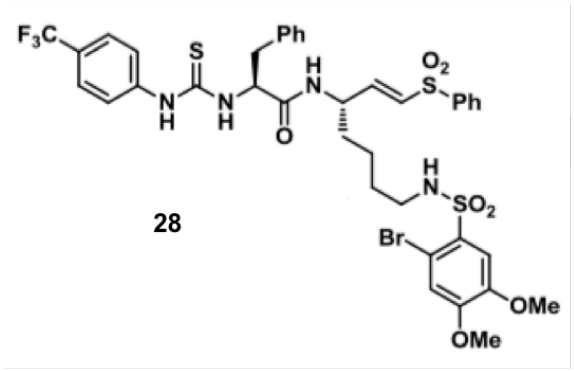

28

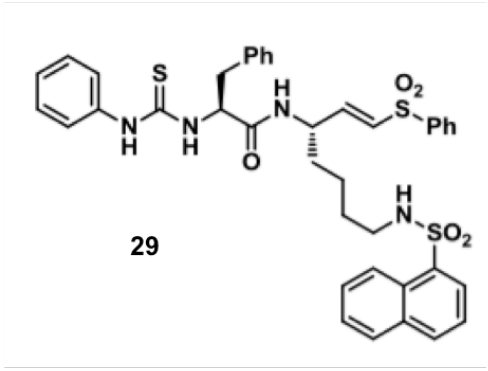

29

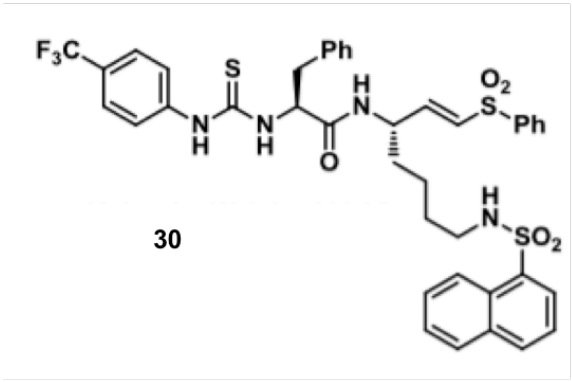

30

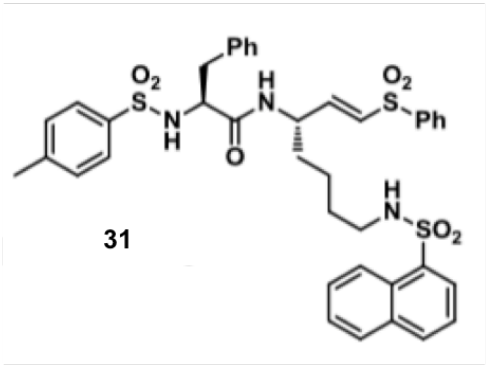

31

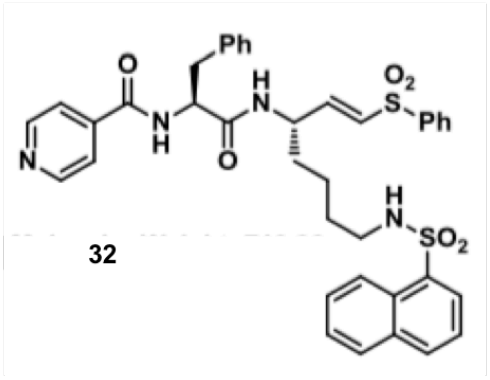

32

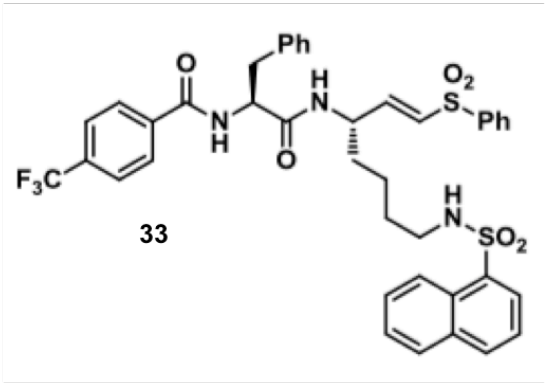

33

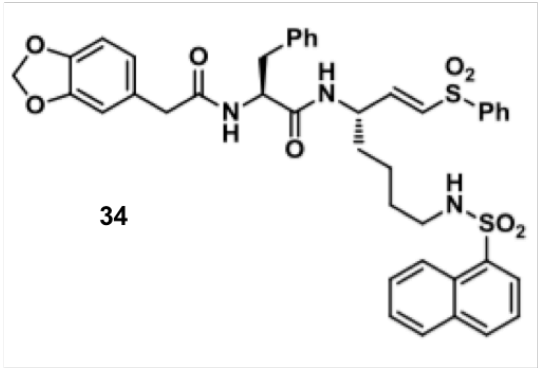

34

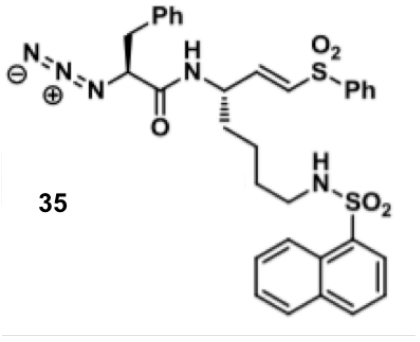

35

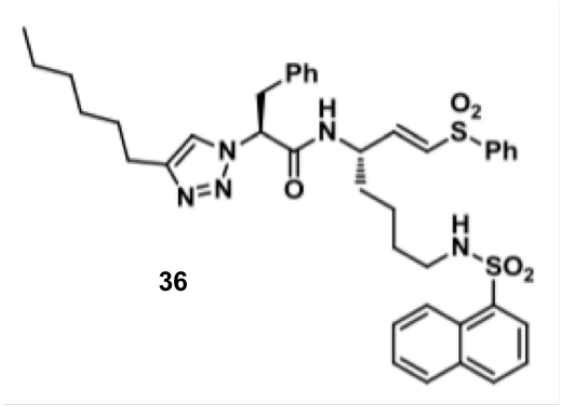

36

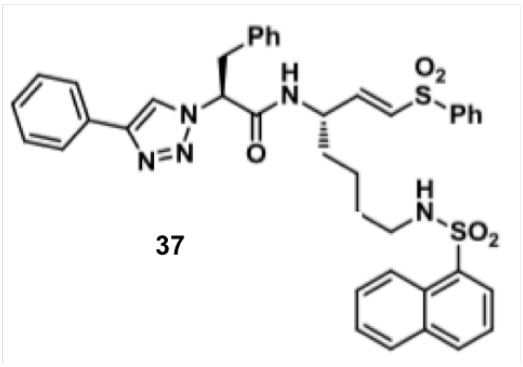

37

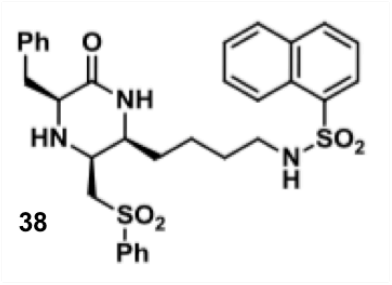

38

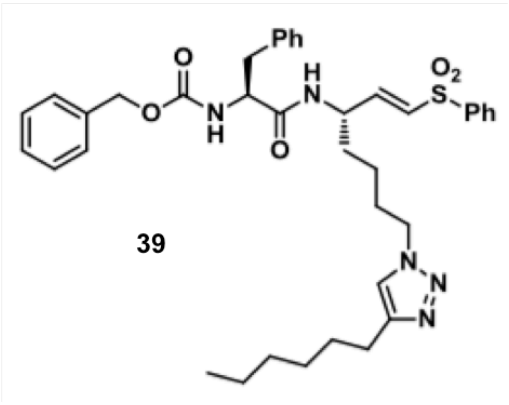

39

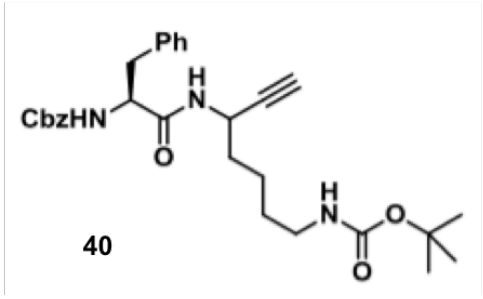

40

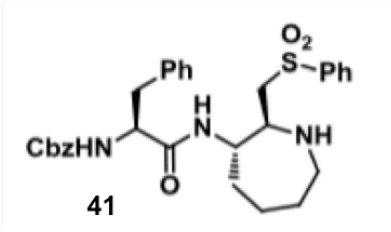

41

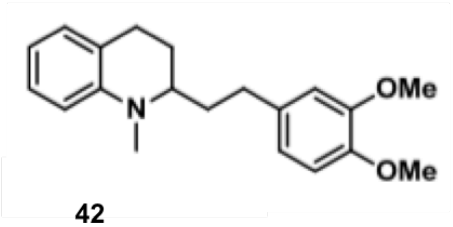

42

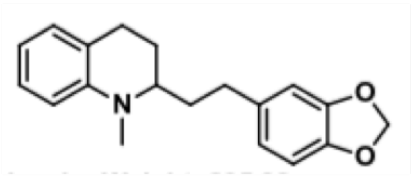

43

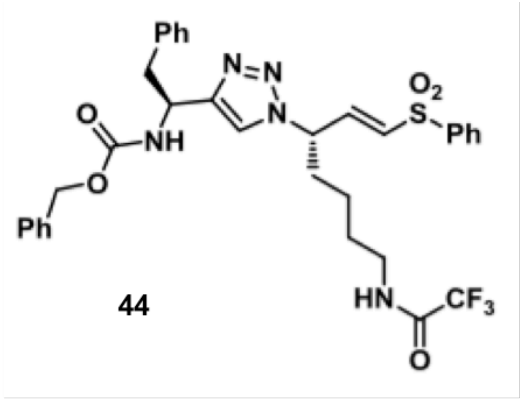

44

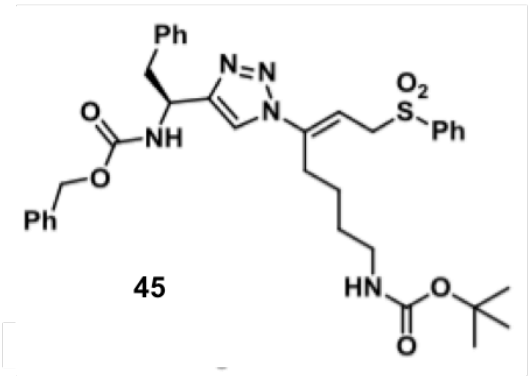

45

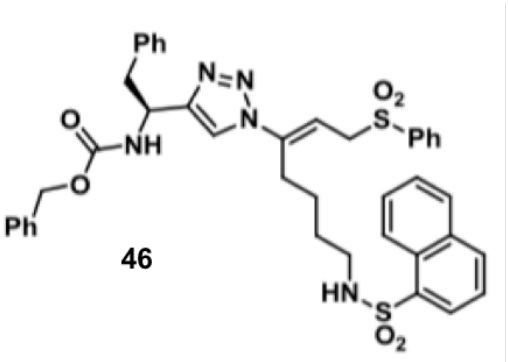

46

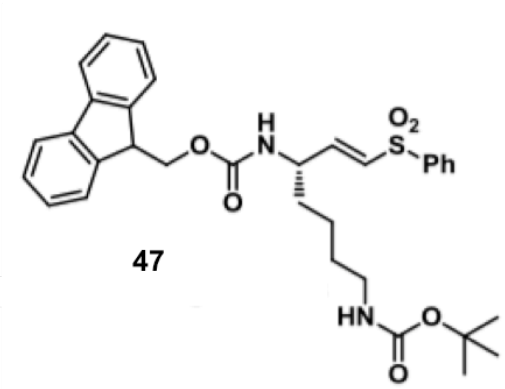

47

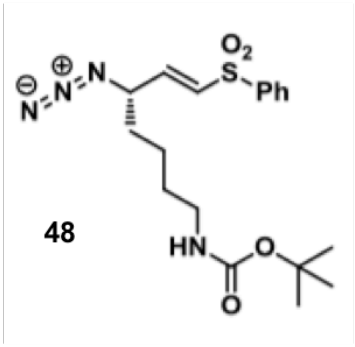

48

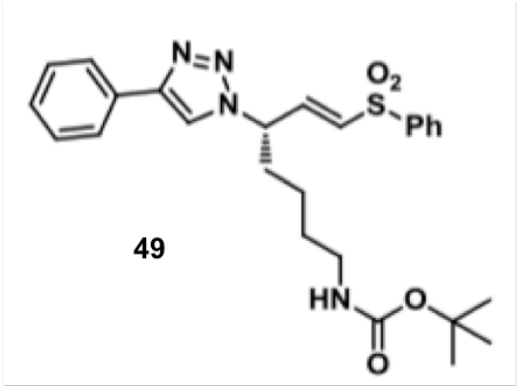

49

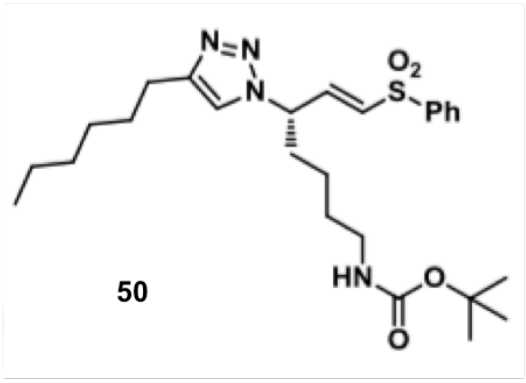

50

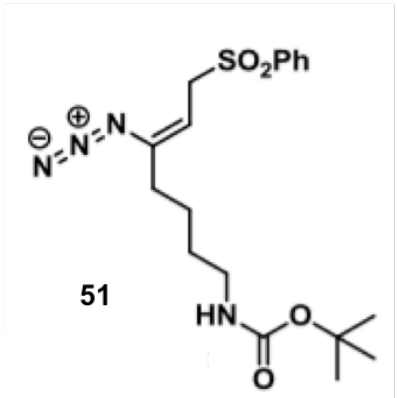

51

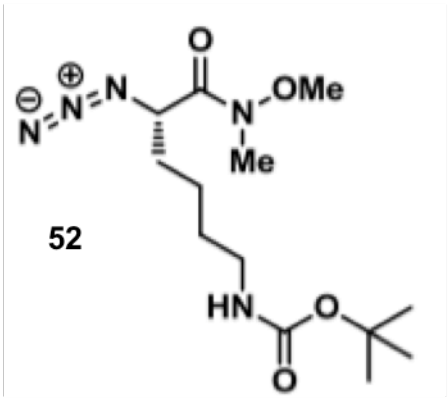

52

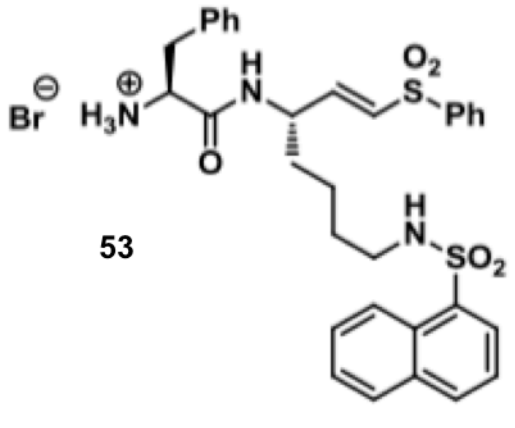

53

References

Abdulla MH, O'Brien TC, Mackey ZB, Sajid M, Grab DJ & McKerrow JH (2008). RNA interference of Trypanosoma brucei cathepsin B and L affects disease progression in a mouse model. *PLoS Negl Trop* 9, e298.

Alsford S, Eckert S, Baker N, Glover L, Sanchez-Flores A, Leung KF, Turner DJ, Field MC, Berriman M & Horn D (2012). High-throughput decoding of antitrypanosomal drug efficacy and resistance. *Nature* 482, 232-236.

Aparoy P, Reddy KK & Reddanna P (2012). Structure and ligand based drug design strategies in the development of novel 5- LOX inhibitors. *Curr. Med. Chem.* 19, 3763–3778.

Apt W, Arribada A, Zulantay I, Rodriguez J, Saavedra M & Munoz A (2013). Treatment of Chagas' disease with itraconazole: electrocardiographic and parasitological conditions after 20 years of follow-up. *J of Antimicrob Chemother* 68, 2164-2169.

Aronson JK (2007). Old drugs – new uses. *Br J of Clin Pharmacol* 64, 563–565.

Arias JLL, Unciti-Broceta JD, Maceira J, Del Castillo T, Hernández-Quero J, Magez S, Soriano M & García-Salcedo JAA (2015). Nanobody conjugated PLGA nanoparticles for active targeting of African Trypanosomiasis. *J Control Release* 197, 190–198.

Ashall F, Angliker H & Shaw E (1990). Lysis of trypanosomes by peptidyl fluoromethyl ketones. *Biochem. Biophys. Res. Commun.* 170, 923–929.

Ashburn T & Thor K (2004). Drug repositioning: identifying and developing new uses for existing drugs. *Nat Rev Drug Discov* 3, 673–683.

Auty H, Torr SJ, Michoel T & Jayaraman S (2015). Cattle trypanosomosis: the diversity of trypanosomes and implications for disease epidemiology and control. *Rev sci Tech Off Int Epiz* 34, 587-598.

Babokhov P, Sanyaolu AO & Oyibo WA (2013). A current analysis of chemotherapy strategies for the treatment of human African trypanosomiasis. *Pathogens and Global Health* 107, 242-252.

Bacchi CJ (2009). Chemotherapy of human african trypanosomiasis. *Interdiscip Perspect Infect Dis* 2009, 195040.

Baker N, Alsford S & Horn D (2011). Genome-wide RNAi screens in African trypanosomes identify the nifurtimox activator NTR and the eflornithine transporter AAT6. *Mol Biochem Parasitol* 172, 55-57.

Baker N, Glover L & Munday JC, Andres DA, Barrett MP, Koning HP & Horn D (2012). Aquaglyceroporin 2 controls susceptibility to melarsoprol and pentamidine in African trypanosomes. *PNAS* 109, 10996-11001.

Bandhuvula P, Tam YY, Oskouian B & Saba JD (2005). The immune modulator FTY720 inhibits sphingosine-1-phosphate lyase activity. *J Biol Chem* 280, 33697-33700.

Barr SC, Warner KL, Kornreic BG, Piscitelli J, Wolfe A, Benet L & McKerrow JH (2005). A cysteine protease inhibitor protects dogs from cardiac damage during infection by Trypanosoma cruzi. *Antimicrob Agents Chemother* 49, 5160–5161.

Barrett M, Burchmore R, Stich A, Lazzari J, Frasch A, Cazzulo J & Krishna S (2003). The trypanosomiases. *The Lancet* 362, 14691480.

Barrett AJ & Kirschke H (1981). Cathepsin B, Cathepsin H, and cathepsin L. *Meth Enzymol* 80, 535–61.

Bellera CL, Balcazar DE & Alberca L (2013). Application of computer-aided drug repurposing in the search of new cruzipain inhibitors: discovery of amiodarone and bromocriptine inhibitory effects. *J Chem Inf Model* 53, 2402-2408.

Bender A (2010). How similar are those molecules after all? Use two descriptors and you will have three different answers. *Expert Opin Drug Discov* 12, 1141-1151.

Berdyshev EV, Gorshkova I, Skobeleva A, Bittman R, Lu X, Dudek SM, Mirzapoiazova T, Garcia JG & Natarajan V (2009). FTY720 inhibits ceramide synthases and upregulates dihydrosphingosine 1-phosphate formation in human lung endothelial cells. *J Biol Chem* 284, 5467–5477.

Bisson W (2012). Drug repurposing in chemical genomics: can we learn from the past to improve the future? *Curr Top Med Chem* 12, 1883–1888.

Brinen LS, Hansell E, Cheng J, Roush WR, McKerrow JH & Fletterick RJ (2000). A target within the target: probing cruzain's P1' site to define structural determinants for the Chagas' disease protease. *Structure* 8, 831–840.

Brinkmann V, Billich A, Baumruker T, Heining P, Schmouder R, Francis G, Aradhye S & Burtin P (2010). Fingolimod (FTY720): discovery and development of an oral drug to treat multiple sclerosis. *Nat Rev Drug Discove* 9, 883–897.

Brömme D, Klaus JL, Okamoto K, Rasnick D & Palmer JT (1996). Peptidyl vinyl sulphones: a new class of potent and selective cysteine protease inhibitors: S2P2 specificity of human cathepsin O2 in comparison with cathepsins S and L. *Biochem J* 315, 85–89.

Brun R & Schonenberger (1979). Cultivation and in vitro cloning or procyclic culture forms of Trypanosoma brucei in a semi-defined medium. *Acta Trop* 36, 289-292.

Brunkhorst R, Vutukuri R & Pfeilschifter W (2014). Fingolimod for the treatment of neurological diseases-state of play and future perspectives. *Front Cell Neurosci* 8, 283.

Bruzzese T, Rimaroli C, Bonabello A, Ferrari E & Signorini M (1996). Amide derivatives of partricin A with potent antifungal activity. *Eur J Med Chem* 31, 965–972.

Buguet A, Bourdon L, Bouteille B, Cespuglio R, Vincendeau P, Radomski MW & Dumas M (2001). The duality of sleeping sickness: focusing on sleep. *Sleep Med Rev* 5, 139–153.

Caffrey CR, Hansell E, Lucas KD & Brinen LS (2001). Active site mapping, biochemical properties and subcellular localization of rhodesain, the major cysteine protease of Trypanosoma brucei rhodesiense. *Mol Biochem Parasitol* 118, 61-73.

Caffrey CR & Steverding D (2009). Kinetoplastid papain-like cysteine peptidases. *Mol Biochem Parasitol* 167, 12-19.

Caffrey C, Scory S & Steverding D (2000). Cysteine Proteinases of Trypanosome Parasites Novel Targets for Chemotherapy. *Curr Drug Targets* 1, 155–162.

Caporuscio F & Tafi A (2011). Pharmacophore modelling: a forty year old approach and its modern synergies. *Curr Med Chem* 18, 2543–53.

Cencig S, Coltel N, Truyens C & Carlier Y (2011). Parasitic loads in tissues of mice infected with Trypanosoma cruzi and treated with AmBisome. *PLoS Negl Trop Dis* 5, e1216.

Chan S & Labute P (2010). Training a Scoring Function for the Alignment of Small Molecules. *J Chem Inf Model* 50, 1724–1735.

Checchi F, Filipe J & Barrett MP (2008). The natural progression of Gambiense sleeping sickness: what is the evidence? *PLoS Negl Trop* 2(12), e303.

Checkley, Pepin, Gibson, Taylor, Jäger & Mabey (2007). Human African trypanosomiasis: diagnosis, relapse and survival after severe melarsoprol-induced encephalopathy. *Tran R Soc Trop Med Hyg* 101, 523–526.

Chiba K & Adachi K (2012). Discovery of fingolimod, the sphingosine 1-phosphate receptor modulator and its application for the therapy of multiple sclerosis. *Future Med Chem* 4, 771-781.

Chong C, Chen X, Shi L, Liu J & Sullivan D (2006). A clinical drug library screen identifies astemizole as an antimalarial agent. *Nat Chem Bio* 2, 415–416.

Choy J, Bryant C, Calvet C, Doyle P, Gunatilleke S, Leung S, Ang K, Chen S, Gut J, Oses-Prieto J, Johnston J, Arkin M, Burlingame A, Tauton J, Jacobson M, McKerrow J, Podust L & Rensto A (2013). Chemical–biological characterization of a cruzain inhibitor reveals a second target and a mammalian off-target. Beilstein J Org Chem 9, 15-25.

Clemons KV & Stevens DA (2001). Efficacy of the partricin derivative SPA-S-753 against systemic murine candidosis. *J Antimicrob Chemother* 47, 183-186.

Coppens I, Baudhuin P, Opperdoes FR & Courtoy PJ (1988). Receptors for the host low density lipoproteins on the hemoflagellate Trypanosoma brucei: purification and involvement in the growth of the parasite. *Proc Natl Acad Sci USA* 85, 6753–6757.

De Cazzulo B & Martínez J (1994). Effects of proteinase inhibitors on the growth and differentiation of Trypanosoma cruzi. *FEMS Microb Lett* 124, 81-86.

Demuth HU (1990). Recent developments in inhibiting cysteine and serine proteases. *J Enzym Inhib* 3, 249–78.

Dixon H, Ginger CD & Williamson J (1971). The lipid metabolism of blood and culture forms of Trypanosoma lewisi and Trypanosoma rhodesiense. *Comp Biochem Physiol* 39, 247–66.

Dixon H & Williamson J (1970). The lipid composition of blood and culture forms of Trypanosoma lewisi and Trypanosoma rhodesiense compared with that of their environment. *Comp Biochem Physiol* 33, 111–28.

Dixon H, Ginger CD & Williamson J (1972). Trypanosome sterols and their metabolic origins. *Comp Biochem* 41, 1-18.

Doherty W, James J, Evans P, Martin L, Adler N, Nolan D & Knox A (2014). Preparation, anti-trypanosomal activity and localisation of a series of dipeptide-based vinyl sulfones. *Org Biomol Chem* 12, 7561–71.

Doyle PS, Zhou YM, Engel JC & McKerrow JH (2007). A Cysteine Protease Inhibitor

Cures Chagas' Disease in an Immunodeficient-Mouse Model of Infection. *Antimicrob Agents Chemother* 51, 3932–3939.

Dunny E & Evans P (2011). Vinyl sulfone containing parasitic cysteinyl protease inhibitors. *Curr Bioact Compd* 7, 218-236.

Dunny E, Doherty W, Evans P, Malthouse P, Nolan D & Knox A (2013). Vinyl Sulfone-Based Peptidomimetics as Anti-Trypanosomal Agents: Design, Synthesis, Biological and Computational Evaluation. *J Med Chem* 56, 6638–6650.

Eakin AE, Mills AA, Harth G & McKerrow JH (1992). The sequence, organization, and expression of the major cysteine protease (cruzain) from Trypanosoma cruzi. *J Biol Chem* 267, 7411-7420.

Ekwanzala M, Pépin J, Khonde N, Molisho S, Bruneel H & De Wals P (1996). In the heart of darkness: sleeping sickness in Zaire. *Lancet* 348, 1427–30.

Engel J, Doyle P, Hsieh I & McKerrow J (1998). Cysteine protease inhibitors cure an experimental Trypanosoma cruzi infection. *J Exp Med* 188, 725-734

El-Sayed NM, Myler PJ, Blandin G, Berriman M, Crabtree J, Aggarwal G, Caler E, Renauld H, Worthey EA, Hertz-Fowler C, Ghedin E, Peacock C, Bartholomeu DC, Haas BJ, Tran A-NN, Wortman JR, Alsmark UC, Angiuoli S, Anupama A, Badger J, Bringaud F, Cadag E, Carlton JM, Cerqueira GC, Creasy T, Delcher AL, Djikeng A, Embley TM, Hauser C, Ivens AC, Kummerfeld SK, Pereira-Leal JB, Nilsson D, Peterson J, Salzberg SL, Shallom J, Silva JC, Sundaram J, Westenberger S, White O, Melville SE, Donelson JE, Andersson B, Stuart KD & Hall N (2005). Comparative genomics of trypanosomatid parasitic protozoa. *Science* 309, 404–409.

Ettari R, Previti S, Tamborini L, Cullia G, Grasso S & Zappalà M (2016). The Inhibition of Cysteine Proteases Rhodesain and TbCatB: A Valuable Approach to Treat Human African Trypanosomiasis. *Mini Rev Med Chem* 16, 1374–1391.

Francis G, Collins W & Burtin P. Fingolimod (NDA 22-527) Briefing Document: Prepared by Novartis Pharmaceuticals for the Peripheral and Central Nervous System Drugs Advisory Committee Meeting 10 June 2010 (online). Available at: http://docplayer.net/6962885-Prepared-by-novartis-pharmaceuticals-for-the-peripheral-and-central-nervous-system-drugs-advisory-committee-meeting-10-june-2010.html

Frearson J, Brand S, McElroy S, Cleghorn L, Smid O, Stojanovski L, Price H, Guther L, Torrie L, Robinson D, Hallyburton I, Mpamhanga C, Brannigan J, Wilkinson

A, Hodgkinson M, Hui R, Qiu W, Raimi O, van Aalten D, Brenk R, Gilbert I, Read K, Fairlamb A, Ferguson M, Smith D & Wyatt P (2010). N-myristoyltransferase inhibitors as new leads to treat sleeping sickness. *Nature* 464, 728–732.

Faria J, Moraes CB, Song R, Pascoalino BS, Lee N, Siqueira-Neto JL, Cruz DJ, Parkinson T, Ioset J-RR, Cordeiro-da-Silva A & Freitas-Junior LH (2015). Drug discovery for human African trypanosomiasis: identification of novel scaffolds by the newly developed HTS SYBR Green assay for Trypanosoma brucei. *J Biomol Screen* 20, 70–81.

Fridberg A, Olson CL, Nakayasu ES, Tyler KM, Almeida IC & Engman DM (2008). Sphingolipid synthesis is necessary for kinetoplast segregation and cytokinesis in Trypanosoma brucei. *J Cell Sci* 121, 522–35.

Furlong ST (1989). Sterols of parasitic protozoa and helminths. *Exp Parasitol* 68, 482-485.

Garcia-Salcedo JA, Unciti-Broceta JD, Valverde-Pozo J & Soriano M (2016). New Approaches to Overcome Transport Related Drug Resistance in Trypanosomatid Parasites. *Front Pharmacol* 7, 351.

Gibson W, Stevens J & Truc P (1999). Identification of trypanosomes: from morphology to molecular biology. *Progress in Human African Trypanosomiasis, Sleeping Sickness,* 7-29.

Goebel-Stengel M, Stengel A, Taché Y & Reeve JR (2011). The importance of using the optimal plasticware and glassware in studies involving peptides. *Anal Biochem* 414, 38–46.

Golan DE, Tashjian AH & Armstrong EJ (2011). Principles of pharmacology: the pathophysiologic basis of drug therapy. .

Gómez-Muñoz A (2006). Ceramide 1-phosphate/ceramide, a switch between life and death. *Biochim Biophys Acta* 1758, 2049–2056.

Gosalia DN, Salisbury CM, Ellman JA & Diamond SL (2005). High throughput substrate specificity profiling of serine and cysteine proteases using solution-phase fluorogenic peptide microarrays. *Mol Cell Proteomics: MCP* 4, 626–636.

Gould MK, Vu XL, Seebeck T & de Koning HP (2008). Propidium iodide-based methods for monitoring drug action in the kinetoplastidae: comparison with the Alamar Blue assay. *Anal Biochem* 382, 87-93.

Graf FE, Ludin P, Wenzler T, Kaiser M & Brun R (2013.) Aquaporin 2 mutations in Trypanosoma brucei gambiense field isolates correlate with decreased susceptibility to pentamidine and melarsoprol. *PLoS Negl Trop*.

Gray KC, Palacios DS & Dailey I (2012). Amphotericin primarily kills yeast by simply binding ergosterol. *PNAS* 109, 2234-2239.

Gros L, Castillo-Acosta VM & Jiménez CJ (2006). New azasterols against Trypanosoma brucei: role of 24-sterol methyltransferase in inhibitor action. *Antimicrob Agents Chemother* 50, 2595-2601.

Grzonka Z, Jankowska E, Kasprzykowski F, Kasprzykowska R, Lankiewicz L, Wiczk W, Wieczerzak E, Ciarkowski J, Drabik P, Janowski R, Kozak M, Jaskólski M & Grubb A (2001). Structural studies of cysteine proteases and their inhibitors. *Acta Biochim Pol* 48, 1–20.

Guarnera C, Bramanti P & Mazzon E (2017). Comparison of efficacy and safety of oral agents for the treatment of relapsing-remitting multiple sclerosis. *Drug Des Devel Ther* 11, 2193–2207.

Güner O, Clement O & Kurogi Y (2004). Pharmacophore modeling and three dimensional database searching for drug design using catalyst: recent advances. *Curr Med Chem* 11, 2991–3005.

Hall BS, Bot C & Wilkinson SR (2011). Nifurtimox activation by trypanosomal type I nitroreductases generates cytotoxic nitrile metabolites. *J Biolog Chem* 286, 13088-13095.

Hammarton TC (2007). Cell cycle regulation in Trypanosoma brucei. *Mol Biochem Parasitol* 153, 1-8.

Hanada K (2003). Serine palmitoyltransferase, a key enzyme of sphingolipid metabolism. *Biochim Biophys Acta* 1632, 16–30.

Hanzlik RP & Thompson SA (1984). Vinylogous amino acid esters: a new class of inactivators for thiol proteases. *J Med Chem* 27, 711–712.

Harth G, Andrews N, Mills AA, Engel JC, Smith R & McKerrow JH (1993). Peptide-fluoromethyl ketones arrest intracellular replication and intercellular transmission of Trypanosoma cruzi. *Mol Biochem Parasitol* 58, 17–24.

Hartsel S & Bolard J (1996). Amphotericin B: new life for an old drug. *Trends pharmacol Sci* 17, 445-449.

Haubrich, BA, Singha, UK, Miller, MB, and Nes, CR (2015). Discovery of an ergosterol-

signaling factor that regulates Trypanosoma brucei growth. *J Lipid Res* 56, 331-341.

Heese-Peck A, Pichler H & Zanolari B (2002). Multiple functions of sterols in yeast endocytosis. *Mol Biol Cell* 12, 2664-2680.

Van Hellemond JJ & Tielens AG (2006). Adaptations in the lipid metabolism of the protozoan parasite Trypanosoma brucei. *FEBS Lett* 580, 5552–8.

Hinshaw JC, Suh DY & Garnier P (2003). Oxidosqualene cyclase inhibitors as antimicrobial agents. *J Med Chem* 46, 4240-4203.

Hirumi H & Hirumi K (1989). Continuous cultivation of Trypanosoma brucei blood stream forms in a medium containing a low concentration of serum protein without feeder cell layers. *J Parasitol* 75, 985–989.

Huang H-J, Yu H, Chen C-Y, Hsu C-H, Chen H-Y, Lee K-J, Tsai F-J & Chen C (2010). Current developments of computer-aided drug design. *J Taiwan Inst Chem Eng* 41, 623–635.

Hurle, Yang, Xie, Rajpal, Sanseau & Agarwal (2013). Computational Drug Repositioning: From Data to Therapeutics. *Clin Pharmacol Ther* 93, 335–341.

Ioset J-R & Chang S (2011). Drugs for Neglected Diseases initiative model of drug development for neglected diseases: current status and future challenges. *Future Med Chem* 3, 1361–1371.

Irvine JW & North MJ (1997). Use of inhibitors to identify essential cysteine proteinases of Trichomonas vaginalis. *FEMS Microbiol Lett* 149, 45-50.

Jacobs RT, Nare B, Wring SA, Orr MD & Chen D (2011). SCYX-7158, an orally-active benzoxaborole for the treatment of stage 2 human African trypanosomiasis. *PLoS Negl Trop* 5(6), e1151.

Jennings FW & Urquhart GM (1983). The use of the 2 substituted 5-nitroimidazole, fexinidazole (Hoe 239) in the treatment of chronicT. brucei infections in mice. *Parasitol Res* 69, 577-581.

Jin H, McCaffery JM & Grote E (2008). Ergosterol promotes pheromone signaling and plasma membrane fusion in mating yeast. *J Cell Biol* 180, 813-826.

Jones AJ, Kaiser M & Avery VM (2015). Identification and Characterization of FTY720 for the Treatment of Human African Trypanosomiasis. *Antimicrob Agents Chemother* 60, 1859–61.

Jones N, Thomas E, Brown E, Dickens N, Hammarton T & Mottram J (2014). Regulators of Trypanosoma brucei Cell Cycle Progression and Differentiation Identified Using a Kinome-Wide RNAi Screen. *Plos Pathog* 10, e1003886.

Jordan AM (1976). Tsetse flies as vectors of trypanosomes. *Vet Parasitol* 2, 143–152.

Kaiser M, Bray MA, Cal M & Trunz BB (2011). Antitrypanosomal activity of fexinidazole, a new oral nitroimidazole drug candidate for treatment of sleeping sickness. *Antimicrob Agents Chemother* 55, 5602-5608.

Kakeya H, Miyazaki Y, Senda H, Kobayashi T, Seki M, Izumikawa K, Yanagihara K, Yamamoto Y, Tashiro T & Kohno S (2008). Efficacy of SPK-843, a novel polyene antifungal, in comparison with amphotericin B, liposomal amphotericin B, and micafungin against murine pulmonary aspergillosis. *Antimicrob Agents Chemother* 52, 1868–1870.

Kantarcioglu AS, Yucel A & Vidotto V (2003). In vitro activity of a new polyene SPK-843 against Candida spp, Cryptococcus neoformans and Aspergillus spp clinical isolates. *J Chemother* 15, 296–298.

Karlsson G, Francis G, Koren G, Heining P, Zhang X, Cohen JA, Kappos L & Collins W (2014). Pregnancy outcomes in the clinical development program of fingolimod in multiple sclerosis. *Neurology* 82, 674–80.

Kato M & Wickner W (2001). Ergosterol is required for the Sec18/ATP-dependent priming step of homotypic vacuole fusion. *EMBO J* 20, 4035-4040.

Keating J, Yukich JO, Sutherland CS & Woods G (2015). Human African trypanosomiasis prevention, treatment and control costs: a systematic review. *Acta tropica* 150, 4-13.

Kerr ID, Wu P, Marion-Tsukamaki R, Mackey ZB & Brinen LS (2010). Crystal Structures of TbCatB and rhodesain, potential chemotherapeutic targets and major cysteine proteases of Trypanosoma brucei. *PLoS Negl Trop Dis* 4, e701.

Kerr, Lee, Farady, Marion, Rickert, Sajid, Pandey, Caffrey, Legac, Hansell, McKerrow, Craik, Rosenthal & Brinen (2009). Vinyl Sulfones as Antiparasitic Agents and a Structural Basis for Drug Design. *J Biol Chem* 284, 25697–25703.

Kethireddy S & Andes D (2007). CNS pharmacokinetics of antifungal agents. *Expert Opin Drug Metab & Toxicol* 3, 573-581.

Khare S, Nagle AS, Biggart A, Lai YH, Liang F, Davis LC, Barnes SW, Mathison CJ, Myburgh E, Gao M-YY, Gillespie JR, Liu X, Tan JL, Stinson M, Rivera IC, Ballard J, Yeh V, Groessl T, Federe G, Koh HX, Venable JD, Bursulaya B, Shapiro M, Mishra PK, Spraggon G, Brock A, Mottram JC, Buckner FS, Rao

SP, Wen BG, Walker JR, Tuntland T, Molteni V, Glynne RJ & Supek F (2016). Proteasome inhibition for treatment of leishmaniasis, Chagas disease and sleeping sickness. *Nature* 537, 229–233.

Kim K-H, Kim N & Seong B-L (2010). Pharmacophore-based virtual screening: a review of recent applications. *Expert Opin Drug Dis* 5, 205–222.

Kim SJ, Rhee HW, Park HJ, Kim HY, Kim HS & Hong JI (2013). Fluorescent probes designed for detecting human serum albumin on the basis of its pseudo-esterase activity. *Bioorg Med Chem Lett* 23, 2093-2097.

Kirschke H, Schmidt I & Wiederanders B (1986). Cathepsin S The cysteine proteinase from bovine lymphoid tissue is distinct from cathepsin L (EC 3.4. 22.15). *Biochem J* 240, 455-459.

Kirschke H, Wiederanders B & Brömme D (1989). Cathepsin S from bovine spleen. Purification, distribution, intracellular localization and action on proteins. *Biochem J* 264, 467-473.

Klose C, Ejsing CS, García-Sáez AJ & Kaiser HJ (2010). Yeast lipids can phase-separate into micrometer-scale membrane domains. *J Biol Chem* 285, 30224-30232.

Kore PP, Mutha MM, Antre RV & Oswal RJ (2012). Computer-Aided drug design: an innovative tool for modeling. OJMC 2, 139-148 Available at: http://file.scirp.org/Html/5-1790023_26238.htm.

Knox AJ, Price T, Pawlak M, Golfis G, Flood CT, Fayne D, Williams DC, Meegan MJ & Lloyd DG (2009). Integration of ligand and structure-based virtual screening for the identification of the first dual targeting agent for heat shock protein 90 (Hsp90) and tubulin. *J Med Chem* 52, 2177–80.

Kristjanson, Swallow, Rowlands, Kruska & de Leeuw (1999). Measuring the costs of African animal trypanosomosis, the potential benefits of control and returns to research. *Agricultural Systems* 59, 7998.

Kuhlencord, Maniera, Eibl & Unger (1992). Hexadecylphosphocholine: oral treatment of visceral leishmaniasis in mice. *Antimicrob Agents Chemother* 36, 1630-1634.

Kulikowicz T & Shapiro TA (2006). Distinct genes encode type II topoisomerases for the nucleus and mitochondrion in the protozoan parasite Trypanosoma brucei. *J Biol Chem* 281, 3048-3056.

Labute P, Williams C, Feher M, Sourial E & Schmidt J (2001). Flexible Alignment of Small Molecules. *J Med Chem* 44, 1483-1490.

Lancien J (1991). Lutte contre la maladie du sommeil dans le sud-est Ouganda par piégeage des Glossines. *Ann Soc Belg Med Trop* 71, 35-47.

Lahiri S, Park H, Laviad EL, Lu X, Bittman R & Futerman AH (2009). Ceramide synthesis is modulated by the sphingosine analog FTY720 via a mixture of uncompetitive and noncompetitive inhibition in an Acyl-CoA chain length-dependent manner. *J Biol Chem* 284, 16090–16098.

Langousis G & Hill KL (2014). Motility and more: the flagellum of Trypanosoma brucei. *Nat Rev Microbiol* 12, 505-518.

Langreth SG & Balber AE (1975). Protein Uptake and Digestion in Bloodstream and Culture Forms of Trypanosoma brucei. *J Protozool* 22, 40–53.

Lecaille, Kaleta & Brömme (2002). Human and parasitic papain-like cysteine proteases: their role in physiology and pathology and recent developments in inhibitor design. *Chem Rev* 102, 4459-4488.

Leelananda SP & Lindert S (2016). Computational methods in drug discovery. *Beilstein J Org Chem* 12, 2694–2718.

Leung-Toung R, Li W, Tam TF & Karimian K (2002). Thiol-dependent enzymes and their inhibitors: a review. *Curr Med Chem* 9, 979–1002.

Leung-Toung R, Zhao Y, Li W, Tam TF, Karimiam K & Spino M (2006). Thiol proteases: inhibitors and potential therapeutic targets. *Curr Med Chem* 13, 547-581.

Li H, Ren X, Leblanc E, Frewin K, Rennie P & Cherkasov A (2013). Identification of Novel Androgen Receptor Antagonists Using Structure- and Ligand-Based Methods. *J Chem Inf and Model* 53, 123–130.

Liao C, Sitzmann M, Pugliese A & Nicklaus MC (2011). Software and resources for computational medicinal chemistry. *Future Med Chem* 3, 1057–1085.

Lim KG, Tonelli F, Li Z, Lu X, Bittman R, Pyne S & Pyne NJ (2011). FTY720 analogues as sphingosine kinase 1 inhibitors: enzyme inhibition kinetics, allosterism, proteasomal degradation, and actin rearrangement in MCF-7 breast cancer cells. *J Biol Chem* 286, 18633–18640.

Lutje V, Seixas J & Kennedy A (2010). Chemotherapy for second-stage Human African trypanosomiasis. *Cochrane Database Syst Rev* 8, CD006201.

Maceyka M, Payne SG, Milstien S & Spiegel S (2002). Sphingosine kinase, sphingosine-1-phosphate, and apoptosis. *Biochim Biophys Acta* 1585, 193–201.

Magnus E, Vervoort T & Meirvenne VN (1978). Communications—Mededelíngen. *Ann Soc Belge Med Trop* 58, 169-176.

Manna PT, Boehm C, Leung KF & Natesan SK (2014). Life and times: synthesis, trafficking, and evolution of VSG. *Trends Parasitol* 30, 251-8.

Martí-Renom M, Stuart A, Fiser A, Sánchez R, Melo F & Šali A (2000). Comparative protein structure modeling of genes and genomes. *Annu Rev Bioph Biom* 29, 291–325.

Mäser P, Wittlin S, Rottmann M & Wenzler T (2012). Antiparasitic agents: new drugs on the horizon. *Curr Opin Pharmacol* 12, 562-566.

Matthews KR (1999). Developments in the differentiation of Trypanosoma brucei. *Parasitology Today*. 15, 76-80.

Matthews K (2005). The developmental cell biology of Trypanosoma brucei. *J Cell Sci* 118, 283–290.

Mbawa ZR, Gumm ID & Shaw E (1992). Characterisation of a cysteine protease from bloodstream forms of Trypanosoma congolense. *FEBS* 204, 371-379.

McKerrow J, Engel J & Caffrey C (1999). Cysteine protease inhibitors as chemotherapy for parasitic infections. *Bioorganic Med Chem* 7, 639–644.

Melagraki G & Afantitis A (2011). Ligand and structure based virtual screening strategies for hit-finding and optimization of hepatitis C virus (HCV) inhibitors. *Curr Med Chem* 18, 2612–9.

Meheus F, Balasegaram M & Olliaro P (2010). Cost-effectiveness analysis of combination therapies for visceral leishmaniasis in the Indian subcontinent. *PLoS Negl Trop Dis* 4, pii: e818.

Merrill AH (2011). Sphingolipid and glycosphingolipid metabolic pathways in the era of sphingolipidomics. *Chem Rev* 111, 6387–6422.

Minovski N & Novič M (2017). Integrated in Silico Methods for the Design and Optimization of Novel Drug Candidates: A Case Study on Fluoroquinolones–Mycobacterium tuberculosis DNA Gyrase. *Oncology: Breakthroughs in Research and Practice*.

Mitchell & Lester (1970). Clinical experience with cycloserine in the treatment of tuberculosis. *Scandinavian journal of respiratory diseases. Supplementum* 71, 94–108.

Moitessier N, Englebienne P, Lee D, Lawandi J & Corbeil CR (2008). Towards the development of universal, fast and highly accurate docking/scoring methods: a long way to go. *Br J Pharmacol* 153 Suppl 1, S7–26.

Moore A & Richer M (2001). Re emergence of epidemic sleeping sickness in southern Sudan. *Trop Med Int Health* 6, 342–347.

Muchmore SW, Debe DA & Metz JT (2008). Application of belief theory to similarity data fusion for use in analog searching and lead hopping. *J Chem Inf Model* 48, 941-948.

Munday JC, Settimo L & de Koning HP (2015). Transport proteins determine drug sensitivity and resistance in a protozoan parasite, Trypanosoma brucei. *Front Pharmacol* 6, 32.

Nes CR, Singha UK, Liu J, Ganapathy K, Villalta F, Waterman MR, Lepesheva GI, Chaudhuri M & Nes WD (2012). Novel sterol metabolic network of Trypanosoma brucei procyclic and bloodstream forms. *Biochem J* 443, 267–77.

Neumann A, Czub J & Baginski M (2009). On the possibility of the amphotericin B-sterol complex formation in cholesterol- and ergosterol-containing lipid bilayers: a molecular dynamics study. *J Phys Chem B* 113, 15875–85.

Ngoyi D, Lejon V, Pyana P, Boelaert M, Ilunga M, Menten J, Mulunda J, Nieuwenhove S, Tamfum J & Büscher P (2010). How to Shorten Patient Follow-Up after Treatment for Trypanosoma brucei gambiense Sleeping Sickness. *J Infect Dis* 201, 453–463.

Odiit M, Kansiime F & Enyaru JC (1997). Duration of symptoms and case fatality of sleeping sickness caused by Trypanosoma brucei rhodesiense in Tororo, Uganda. *East Afr Med J* 74, 792-795.

Oprea & Mestres (2012). Drug Repurposing: Far Beyond New Targets for Old Drugs. *AAPS J* 14, 759–763.

Organization W (2013). Control and surveillance of human African trypanosomiasis. *World Heal Organization Technical Rep Ser*, 1–237.

Otto H-HH & Schirmeister T (1997). Cysteine Proteases and Their Inhibitors. *Chem. Rev.* 97, 133–172.

Overath P & Engstler M (2004). Endocytosis, membrane recycling and sorting of GPI-anchored proteins: Trypanosoma brucei as a model system. *Mol Microbiol* 53, 735–744.

Palmer J, Rasnick D, Klaus J & Bromme D (1995). Vinyl Sulfones as Mechanism-Based Cysteine Protease Inhibitors. *J Med Chem* 38, 3193–3196.

Papadatos G, Davies M, Dedman N, Chambers J, Gaulton A, Siddle J, Koks R, Irvine S, Pettersson J, Goncharoff N, Hersey A & Overington J (2016). SureChEMBL: a large-scale, chemically annotated patent document database. *Nucleic Acids Res* 44, D1220–D1228.

Pasternack DA, Sharma AI, Olson CL, Epting CL & Engman DM (2015). Sphingosine Kinase Regulates Microtubule Dynamics and Organelle Positioning Necessary for Proper G1/S Cell Cycle Transition in Trypanosoma brucei. *MBio* 6, e01291–15.

Patmanathan SN, Yap LF, Murray PG & Paterson IC (2015). The antineoplastic properties of FTY720: evidence for the repurposing of fingolimod. *J Cell Mol Med* 19, 2329–2340.

Patnaik PK, Field MC, Menon AK & Cross G (1993). Molecular species analysis of phospholipids from Trypanosoma brucei bloodstream and procyclic forms. *Mol Biochem Parasitol* 58, 97-105.

Pays E (1999). Antigenic variation in African trypanosomes. *Progress in human African trypanosomiasis, Sleeping Sickness*, 31-52.

Pchejetski D, Bohler T, Brizuela L, Sauer L, Doumerc N, Golzio M, Salunkhe V, Teissié J, Malavaud B, Waxman J & Cuvillier O (2010). FTY720 (fingolimod) sensitizes prostate cancer cells to radiotherapy by inhibition of sphingosine kinase-1. *Cancer Res* 70, 8651–8661.

Ploubidou A, Robinson DR, Docherty RC, Ogbadoyi EO & Gull K (2000). Evidence for novel cell cycle checkpoints in trypanosomes: kinetoplast segregation and cytokinesis in the absence of mitosis. *J Cell Sci* 112 (Pt 24), 4641–4650.

Pitman SK, Drew RH & Perfect JR (2011). Addressing current medical needs in invasive fungal infection prevention and treatment with new antifungal agents, strategies and formulations. *Expert Opin Emerg Drugs* 16, 559–586.

Portaccio E (2011). Evidence-based assessment of potential use of fingolimod in treatment of relapsing multiple sclerosis. *Core Evid* 6, 13–21.

Potashman M & Duggan M (2009). Covalent modifiers: an orthogonal approach to drug design. *J Med Chem* 52, 1231–46.

Prada-Gracia D & Huerta-Yépez S (2016). Application of computational methods for anticancer drug discovery, design, and optimization. *Boletín Médico del Hospital Infantil de Mexico* 73, 411-423.

Prata A (1963). Treatment of kala-azar with amphotericin B. *Trans R Soc Trop Med Hyg* 57, 266–268.

Raether W & Seidenath H (1983). The activity of fexinidazole (HOE 239) against experimental infections with Trypanosoma cruzi, trichomonads and Entamoeba histolytica. *Ann Trop Mede Parasitol 77, 13-26*.

Ramos H, Valdivieso E, Gamargo M & Dagger F (1996). Amphotericin B kills unicellular leishmanias by forming aqueous pores permeable to small cations and anions. *J Membr Biol* 152, 65-75.

Renslo A & McKerrow J (2006). Drug discovery and development for neglected parasitic diseases. *Nat Chem Biol* 2, 701–710.

Riniker S & Landrum G (2013). Open-source platform to benchmark fingerprints for ligand-based virtual screening. *J Cheminformatics* 5, 1–17.

Rimaroli C & Bruzzese T (1998) In vitro activity of a new polyene, SPA-S-843, against yeasts. *Antimicrob Agents Chemother* 42, 3012-3013..

Rimaroli C & Bruzzese T (2000). Overview of SPA-S-843 in vitro activity against filamentous fungi. *Chemotherapy* 46, 28–35.

Roberts CW, McLeod R, Rice DW, Ginger M, Chance ML & Goad JL (2003). Fatty acid and sterol metabolism: potential antimicrobial targets in apicomplexan and trypanosomatid parasitic protozoa. *Mol Biochem Parasitol* 126, 129–142.

Ritchie T & McLay I (2012). Should medicinal chemists do molecular modelling? *Drug Discov Today* 17, 534–537.

Rockett KA, Playfair J, Ashall F & Target G (1990). Inhibition of intraerythrocytic development of Plasmodium falciparum by proteinase inhibitors. *FEBS letters* 259, 257-259.

Rodgers J, Jones A, Gibaud S, Bradley B, McCabe C, Barrett MP, Gettinby G & Kennedy PG (2011). Melarsoprol cyclodextrin inclusion complexes as promising oral candidates for the treatment of human African trypanosomiasis. *PLoS Negl Trop Dis* 5, e1308.

Rogers D & Hahn M (2010). Extended-connectivity fingerprints. *J Chem Inf Model* 50, 742-754.

Rosenthal PJ, Lee GK & Smith RE (1993). Inhibition of a Plasmodium vinckei cysteine proteinase cures murine malaria. *J Clin Invest* 91, 1052-1056.

Rosenthal PJ, McKerrow JH & Rasnick D (1989). Plasmodium falciparum: inhibitors of lysosomal cysteine proteinases inhibit a trophozoite proteinase and block parasite development. *Mol Biochem Parasitol 35,* 177-183.

Rosenthal PJ, Olson JE, Lee GK, Palmer JT, Klaus JL & Rasnick D (1996). Antimalarial effects of vinyl sulfone cysteine proteinase inhibitors. *Antimicrob Agents Chemother* 40, 1600–1603.

Rossi A, Deveraux Q, Turk B & Sali A (2004). Comprehensive search for cysteine cathepsins in the human genome. *Biol Chem* 385, 363-372.

Roush W, Gwaltney S, Cheng J, Scheidt K, McKerrow J & Hansell E (1998). Vinyl Sulfonate Esters and Vinyl Sulfonamides: Potent, Irreversible Inhibitors of Cysteine Proteases. *J Am Chem Soc* 120, 10994–10995.

Roth HJ (2005). There is no such thing as "diversity"! *Curr Opin Chem Biol* 9, 293-295.

Roush WR, Cheng J, Knapp-Reed B, Alvarez-Hernandez A, McKerrow JH, Hansell E & Engel JC (2001. Potent second generation vinyl sulfonamide inhibitors of the trypanosomal cysteine protease cruzain. *Bioorg Med Chem Lett* 11, 2759–62.

Saha AK, Mukherjee T & Bhaduri A (1986). Mechanism of action of amphotericin B on Leishmania donovani promastigotes. *Mol Biochem Parasitol* 19, 195-200.

Sajid & McKerrow (2002). Cysteine proteases of parasitic organisms. *Mol Biochem Parasit* 120, 1–21.

Sanderson, Dogruel & Rodgers (2009). Pentamidine movement across the murine blood-brain and blood-cerebrospinal fluid barriers: effect of trypanosome infection, combination therapy, P-glycoprotein, and multidrug resistance-associated protein. *J Pharmacol Exp Ther* 329, 967-977.

Scott, Davidson, Moody, Grant, Felmingham, Scott, Olliaro & Bryceson (1992). Aminosidine (paromomycin) in the treatment of leishmaniasis imported into the United Kingdom. *Trans R Soc Trop Med Hyg* 86, 617–9.

Schumann Burkard G, Jutzi P & Roditi I (2011). Genome-wide RNAi screens in bloodstream form trypanosomes identify drug transporters. *Mol Biochem Parasitol* 175, 91–4.

Shapiro TA (1994). Mitochondrial topoisomerase II activity is essential for kinetoplast DNA minicircle segregation. *Mol Cell Biol* 14, 3660-3667.

Shapiro TA & Showalter AF (1994). In vivo inhibition of trypanosome mitochondrial topoisomerase II: effects on kinetoplast DNA maxicircles. *Mol Cell Biol* 14, 5891-5897.

Sheridan RP & Kearsley SK (2002). Why do we need so many chemical similarity search methods? *Drug Discov Today* 7, 903-911.

Sheskin (1965). Thalidomide in the treatment of lepra reactions. *Clin Pharmacol Ther* 6, 303–6.

Silva L, Coutinho A, Fedorov A & Prieto M (2006). Competitive binding of cholesterol and ergosterol to the polyene antibiotic nystatin. A fluorescence study. *Biophysical J* 90, 3625–3631.

Singer JA & Purcell WP (1967). Relationships among current quantitative structure-activity models. *J Med Chem* 10, 1000–1002.

Singh J, Petter R, Baillie T & Whitty A (2011). The resurgence of covalent drugs. *Nat Rev Drug Discov* 10, 307–317.

Sittampalam GS, Coussens NP, Brimacombe K, Grossman A, Arkin M, Auld D, Austin C, Baell J, Bejcek B, Chung TDYD, Dahlin JL, Devanaryan V, Foley TL, Glicksman M, Hall MD, Hass JV, Inglese J, Iversen PW, Kahl SD, Lal-Nag M, Li Z, McGee J, McManus O, Riss T, Trask OJ, Weidner JR, Xia M & Xu X (2004). Assay Guidance Manual. *Eli Lilly & Company and the National Center for Advancing Translational Sciences*.

Sjoerdsma, Golden, Schechter, Barlow & Santi (1984). Successful treatment of lethal protozoal infections with the ornithine decarboxylase inhibitor, alpha-difluoromethylornithine. *Trans Assoc Am Physicians* 97, 70–9.

Smith TK & Bütikofer P (2010). Lipid metabolism in Trypanosoma brucei. *Mol Biochem Parasitol* 172, 66–79.

De Souza W & Rodrigues JC (2009). Sterol Biosynthesis Pathway as Target for Anti-trypanosomatid Drugs. *Interdiscip Perspect Infect Dis* 2009, 642502.

Steverding D (2008). The history of African trypanosomiasis. *Parasites & vectors*.

Steverding D (2015). Evaluation of trypanocidal activity of combinations of anti-sleeping sickness drugs with cysteine protease inhibitors. *Exp Parasitol* 151-152, 2833.

Stich A, Abel P & Krishna S (2002). Human African trypanosomiasis. *BMJ* 325, 203–206.

Stijlemans B, Conrath K, Cortez-Retamozo V, Van Xong H, Wyns L, Senter P, Revets H, De Baetselier P, Muyldermans S & Magez S (2004) Efficient targeting of conserved cryptic epitopes of infectious agents by single domain antibodies. African trypanosomes as paradigm. *J Biol Chem* 279, 1256–1261.

Strippoli V, D'Auria FD, Simonetti G, Bruzzese T & Simonetti N (2000). Anticandidal activity of SPA-S-843, a new polyenic drug. *J Antimicrob Chemother* 45, 235–237.

Sundar S & Chakravarty J (2012). Recent advances in the diagnosis and treatment of kala-azar. Natl Med J India 25, 85-89.

Sun H (2008). Pharmacophore-based virtual screening. *Curr. Med. Chem.* 15, 1018–24.

Sun YN, No J.H, Lee GY, Li W, Yang SY, Yang G, Schmidt TJ, Kang JS & Kim YH (2016). Phenolic Constituents of Medicinal Plants with Activity against Trypanosoma brucei. *Molecules* 21, 480.

Sutterwala SS, Creswell CH, Sanyal S & Menon AK (2007). De novo sphingolipid synthesis is essential for viability, but not for transport of glycosylphosphatidylinositol-anchored proteins, in African trypanosomes. *Eukaryot Cell* 6, 454-464.

Sutterwala S, Hsu F, Sevova E, Schwartz K, Zhang K, Key P, Turk J, Beverley S & Bangs J (2008). Developmentally regulated sphingolipid synthesis in African trypanosomes. *Mol Microbiol* 70, 281–296.

Sykes ML & Avery VM (2009). Development of an Alamar Blue viability assay in 384-well format for high throughput whole cell screening of Trypanosoma brucei brucei bloodstream form strain 427. *Am J Trop Med Hyg* 81, 665–674.

Sykes ML, Baell JB, Kaiser M, Chatelain E, Moawad SR, Ganame D, Ioset J-RR & Avery VM (2012). Identification of compounds with anti-proliferative activity against Trypanosoma brucei brucei strain 427 by a whole cell viability based HTS campaign. *PLoS Negl Trop Dis* 6, e1896.

Thao NP, No JH, Luyen BTT, Yang G, Byun SY, Goo J, Kim KT, Cuong NX, Nam NH, Van Minh C, Schmidt TJ, Kang JS & Kim YH (2014). Secondary metabolites from Vietnamese marine invertebrates with activity against Trypanosoma brucei and T. cruzi. *Molecules* 19, 7869–80.

Todeschini R & Consonni V (2008) Handbook of molecular descriptors. Available at: http://books.google.com/books?hl=en&lr=&id=TCuHqbvgMbEC&oi=fnd&pg=PP2&dq=handbook+of+molecular+descriptors+todeschini&ots=jvyBAcALn9&sig=uz_7AOPlaleERv9u5GjlKn8_0-o.

Tonelli F, Lim KG, Loveridge C, Long J, Pitson SM, Tigyi G, Bittman R, Pyne S & Pyne NJ (2010), FTY720 and (S)-FTY720 vinylphosphonate inhibit sphingosine kinase 1 and promote its proteasomal degradation in human pulmonary artery smooth muscle, breast cancer and androgen-independent prostate cancer cells. *Cell Signal* 22, 1536–42.

Torreele E, Trunz BB, Tweats D & Kaiser M (2010). Fexinidazole–a new oral nitroimidazole drug candidate entering clinical development for the treatment of sleeping sickness. *PLoS Negl Trop Dis* 4(12):e923.

Troeberg L, Morty RE, Pike RN, Lonsdale-Eccles JD, Palmer JT, McKerrow JH & Coetzer TH (1999). Cysteine proteinase inhibitors kill cultured bloodstream forms of Trypanosoma brucei brucei. *Exp Parasitol* 91, 349–55.

Tuntland T, Ethell B, Kosaka T, Blasco F, Zang RX, Jain M, Gould T & Hoffmaster K (2014). Implementation of pharmacokinetic and pharmacodynamic strategies in early research phases of drug discovery and development at Novartis Institute of Biomedical Research. *Front Pharmacol* 5, 174.

Turk B, Bieth JG, Björk I, Dolenc I & Turk D (1995). Regulation of the activity of lysosomal cysteine proteinases by pH-induced inactivation and/or endogenous protein inhibitors, cystatins. *Biol Chem Hoppe Seyler* 376, 225-230.

Turk V, Turk B & Turk D (2001). Lysosomal cysteine proteases: facts and opportunities. *EMBO* 20, 4629-4633.

Turk B, Dolenc I, Turk V & Bieth JG (1993). Kinetics of the pH-induced inactivation of human cathepsin L. *Biochemistry* 32, 375–80.

Turk V, Stoka V, Vasiljeva O, Renko M, Sun T, Turk B & Turk D (2012). Cysteine cathepsins: from structure, function and regulation to new frontiers. *Biochimica et Biophysica Acta (BBA)-Proteins and Proteomics* 1824, 68–88.

Uchida Y, Tachikawa M, Obuchi W, Hoshi Y, Tomioka Y, Ohtsuki S & Terasaki T (2013). A study protocol for quantitative targeted absolute proteomics (QTAP) by LC-MS/MS: application for inter-strain differences in protein expression levels of transporters, receptors, claudin-5, and marker proteins at the blood-brain barrier in ddY, FVB, and C57BL/6J mice. *Fluids Barriers CNS* 10, 21.

Unciti-Broceta JD, Arias JL, Maceira J & Soriano M (2015). Specific cell targeting therapy bypasses drug resistance mechanisms in African trypanosomiasis. *PLoS Pathog* 11(6); e1004942.

Unknown (1959). JOINT WHO/FAO expert committee on zoonoses. *World Health Organ Tech Rep Ser* 58, 1–84.

Vedrenne C, Giroud C, Robinson DR, Besteiro S, Bosc C, Bringaud F & Baltz T (2002). Two related subpellicular cytoskeleton-associated proteins in Trypanosoma brucei stabilize microtubules. *Mol Biol Cell* 13, 1058–1070.

Vickerman K (1978). Antigenic variation in trypanosomes. *Nature* 273, 613-617.

Vincent IM, Creek D, Watson DG & Kamleh MA (2010). A molecular mechanism for eflornithine resistance in African trypanosomes. *PLoS Pathog* 6(11): e1001204.

Wasilewski MM, Lim KC & Phillips J (1996). Cysteine protease inhibitors block schistosome hemoglobin degradation in vitro and decrease worm burden and egg production in vivo. *Mol Biochem Parasitiol* 81, 179-189.

Watts KR, Ratnam J, Ang K-H, Tenney K, Compton JE, McKerrow J & Crews P (2010). Assessing the trypanocidal potential of natural and semi-synthetic diketopiperazines from two deep water marine-derived fungi. *Bioorg Med Chem* 18, 2566–2574.

Webster P & Shapiro SZ (1990). Trypanosoma brucei: a membrane-associated protein in coated endocytotic vesicles. *Exp Parasitol* 70, 154–63.

Welburn SC, Fèvre EM, Coleman PG & Odiit M (2001). Sleeping sickness: a tale of two diseases. *Trends Parasitol* 17, 19-24.

Weller RO, Kida S & Zhang ET (1992). Pathways of fluid drainage from the brain--morphological aspects and immunological significance in rat and man. *Brain pathology (Zurich, Switzerland)* 2, 277–84.

Te Welscher YM & Jones L (2010). Natamycin inhibits vacuole fusion at the priming phase via a specific interaction with ergosterol. *Antimicrob Agents Chemother* 54, 2618-2625.

Wheelis M (2002). Biotechnology and biochemical weapons. *Nonproliferation Rev* 9, 48–53.

Willstätter R & Bamann E (1929). Über die Proteasen der Magenschleimhaut. Erste Abhandlung über die Enzyme der Leukocyten. *Hoppe-Seyler´s Zeitschrift für physiologische CHemie* 180 , 127-143.

Wolber G & Langer T (2005). LigandScout: 3-D Pharmacophores Derived from Protein-Bound Ligands and Their Use as Virtual Screening Filters. *J Chem Inf Model* 45, 160–169.

Yamashita DS & Dodds RA (2000). Cathepsin K and the design of inhibitors of cathepsin K *Curr Pharm Des* 6, 1–24.

Zhang J & Ma PX (2013). Cyclodextrin-based supramolecular systems for drug delivery: recent progress and future perspective. *Adv Drug Deliv Rev* 65, 1215–33.

Zhang X-G, Li G-X, Zhao S-S, Xu F-L, Wang Y-H & Wang W (2014). A review of dihydroartemisinin as another gift from traditional Chinese medicine not only for malaria control but also for schistosomiasis control. J *Parasitol Res* 113, 1769–1773.

Zhang Y, Jiao Y, Liu H, Yuan H, Lu S, Ran T & Yao S (2013). An integrated virtual screening approach for VEGFR-2 inhibitors. *J Chem Inf Model* 53, 3163–3177.

Zhang YQ, Gamarra S, Garcia-Effron G & Park S (2010). Requirement for ergosterol in V-ATPase function underlies antifungal activity of azole drugs. *PLoS Pathog* 6(6): e1000939.